HYDRAULIC SORTING OF BED-SURFACE SEDIMENTS IN A SHALLOW LAKE

Victor O. Onyango

A Thesis
in
The Department
of
Civil Engineering

Presented in Partial Fulfilment of the Requirements
for the Degree of Master of Applied Science at
Concordia University
Montreal, Quebec, Canada

May 1992

National Library
of Canada

Acquisitions and
Bibliographic Services Branch

395 Wellington Street
Ottawa, Ontario
K1A 0N4

Bibliothèque nationale
du Canada

Direction des acquisitions et
des services bibliographiques

395, rue Wellington
Ottawa (Ontario)
K1A 0N4

Your file Votre référence

Our file Notre référence

ISBN 0-315-80970-1

Canada

HYDRAULIC SORTING OF BED-SURFACE SEDIMENTS IN A SHALLOW LAKE

By Victor O. Onyango

ABSTRACT

Hydraulic sorting of bed-surface sediments in a shallow lake is studied by examining the correlation between sediment characteristics and flow parameters. The examination is done using correlation plots of dimensionless variables commonly used in the study of sediment transport. The particle size distributions of bed-surface sediment samples are also analyzed. Median particle sizes of bed-surface sediment in the lake range from 0.1 microns to 2.5 mm.

The flow parameters, namely the shear velocities and water depths, are obtained by simulating the flow in the lake using a two-dimensional numerical model. The model is based on the MacCormack finite difference scheme. Turbulence stresses are computed using the depth-averaged k-ε model. These models are found to be capable of satisfactorily reproducing the flow in the lake.

Strong inter-dependence is found to exist amongst the three dimensionless variables considered, namely, the dimensionless particle size, the suspension parameter and the relative roughness.

ACKNOWLEDGEMENTS

During this work, I received financial support from the Kenya-Canada GTF II training program, for which I would like to thank the Canadian International Development Association (on behalf of the Canadian Government) and the Government of the Republic of Kenya. My employer, the Kenya Ports Authority, kindly granted me study leave to undertake this work.

I would like to express my gratitude to my Supervisor Dr. S. Sarraf for his guidance during my research and in the preparation of this thesis report, and to all my colleagues and professors who assisted me in various ways during my work. I would particularly like to thank Dr. S. Babarutsi, Messrs. R. Saade and G. Emissa and Mrs. X. Zhang.

The data used in this study was provided by several organizations, to whom I would like to express my appreciation; Canada's Inland Waters Research Institute, through Dr. N. Rukavina, provided the data on Lake St. Louis sediments; hydrometric and bathymetry data were provided by Hydro-Quebec; Canada's Inland Waters Directorate provided additional hydrometric data; The St. Lawrence Centre provided me with useful reports on previous studies of Lake St. Louis and Fisheries and Ocean Canada provided me with recent hydrographic survey maps of the lake.

Table of Contents

List of Figures

List of Figures (Cont'd)

List of Figures (Cont'd)

List of Figures (cont'd)

List of Tables

List of Tables (Cont'd)

Notation

The following symbols appearing in this thesis have the following meanings:

α = Coefficient in equation for reference shear stress;

a = Reference level above the bed;

A_{dm} = Area of Lake Des Deux Montangnes;

B = Width of movable bed;

β = Ratio of diffusion coefficients for sediment and momentum;

β_1 = Exponent in equation for reference shear stress;

$c_{1\varepsilon}$ = Empirical constant in k-ε model;

$c_{2\varepsilon}$ = Empirical constant in k-ε model;

c_a = Sediment concentration at reference level a above the bed;

c_ε = Empirical constant in k-ε model;

c_f = Bed friction coefficient;

c_k = Empirical constant in the k-e model;

c_μ = Empirical constant in k-ε model;

c_s = Sediment concentration;

c_y = Sediment concentration at level y above the bed;

d = Particle diameter or d_{50};

D_* = Dimensionless particle size $(((s-1)gd^3/v^2)^{1/3})$;

d_{50} = Median particle size, generally d_p = the p^{th} percentile size;

DC1 = Discharge condition 1 where average values are used;

DC2 = Discharge condition 2 where maximum values are used;

$\Delta\phi_{lim}$ = Maximum allowable difference in ϕ for convergence;

$\Delta\phi_{tn}$ = Difference in variable ϕ at convergence test number tn;

d_i = Mean particle diameter in size class i;

Δt = Time step;

Δ_{tx} = Partial time step used with L_x;

Δ_{ty} = Partial time step used with L_y;

Δx = Grid spacing in x-direction;

Δy = Grid spacing in y-direction;

E = Vector of conserved variables;

ε = Rate of dissipation of k;

e_r = Relative roughness (d_{50}/h);

ε_s = Diffusion coefficient for sediment;

F = Vector of fluxes of conserved variables in x -direction;

ϕ = General variable;

G = Vector of Fluxes of conserved variables in y-direction;

g = Acceleration due to gravity;

G_s = Volumetric sediment discharge;

h = Water depth;

h^0 = Initial value of h;

$h^{1/2}$ = Intermediate value of h;

h_{dm} = Water surface elevation in Lake Des Deux Montagnes;

h_{eq} = Equilibrium depth with regard to a particle on the bed;

h^P = Predicted value of h;

i = Grid reference for x-direction;

imax = Maximum value of i;

j = Grid reference for y-direction;

jmax = Maximum value of j;

k = Turbulent kinetic energy per unit mass of fluid;

κ = von Karman's constant;

ki = Number of iterations between successive convergence tests;

L = Global MacCormack discretization operator;

L_x = MacCormack discretization operator for x-direction terms;

L_y = MacCormack discretization operator for y-direction terms;

ν = Laminar kinematic viscosity;

n = Manning's coefficient;

Ni = Number of iterations;

ν_t = Turbulent kinematic viscosity coefficient;

p = Porosity of bed material;

$P_{\varepsilon v}$ = Additional source term for ε in the depth averaged k-ε model;

P_h = Energy production term due to mean velocity gradients;

P_{kv} = Additional source term for k in the depth averaged k-ε model;

θ = Dimensionless shear stress $(u*^2/((s-1)gd))$;

q = Water discharge per unit channel width;

Q_{car} = Ottawa river discharge at Carrilon;

θ_{cr} = Shield's Parameter;

Q_{dn} = Discharge of river du Nord;

Q_{dp} = Discharge of river de Prairies;

Q_{mi} = Discharge of river Mile Ile;

Q_{sa} = Discharge of St Anne channel;

Q_{va} = Discharge of Vaudreuil channel;

ρ = Water density;

Re_* = Particle Reynold's number (u_*d/ν);

Re_{*c} = Critical Particle Reynold's number ($u_{*c}d/\nu$);

ρ_s = Sediment particle density;

s = Specific gravity of sediment particle;

σ_e = Empirical constant in the k-ε model;

S_{fx} = Friction slope in x-direction;

S_{fy} = Friction slope in y-direction;

σ_g = Geometric standard deviation;

σ_k = Emprical constant in the k-ε model;

t = Time;

τ_{bx} = Bed shear stress component in x-direction;

τ_{by} = Bed shear stress component in y-direction;

tn = Convergence test number;

τ_{ri} = Reference shear stress ;

U = Unit discharge in x-direction (uh);

u = Depth averaged water velocity component in x-direction;

u_* = Shear velocity;

u_{*c} = Critical shear velocity;

U^0 = Initial value of U;

$U^{1/2}$ = Intermediate value of U;

u_{da} = Resultant depth averaged flow velocity;

U^p = Predicted value of U;

u_s = Resultant surface flow velocity;

V = Unit discharge in y-direction (vh);

v = Depth averaged water velocity component in y-direction;

V^0 = Initial value of V;

$V^{1/2}$ = Intermediate value of V;

V_P = Predicted value of V;;

ω = Particle fall velocity;

ω_s = Particle fall velocity in still water;

x = Horizontal coordinate direction;

y = Horizontal coordinate direction or vertical distance above bed;

y_w = Distance from the wall of the wall-nearest grid point;

z_b = Bed surface elevation;

Z_r = Rouse number ($\omega/\kappa\beta u*$); and

Z_{r*} = Suspension parameter ($\omega_s/u*$).

CHAPTER 1

INTRODUCTION

1.1 BACKGROUND

Hydraulic sorting is the selective entrainment, deposition and transport of sediment particles by flowing water, depending on their sizes, shapes and densities. In a natural water body, it causes spatial and temporal variation of sediment particle sizes.

In civil and environmental engineering applications, models for hydraulic sorting have mainly been used to predict bed level changes in rivers. Such changes usually take place after the construction of engineering works that tend to upset hydraulic equilibrium conditions. These works include dam constructions and dredging operations. Hydraulic sorting models can also be used to select open water disposal sites for dredged material and predict the deposition of toxic wastes in the aquatic environment.

The applicability of the presently available models for hydraulic sorting to hydro-environmental problems depends on the type of water body being considered and the type of sediments therein. In rivers, where the flow can be considered as one-dimensional and the sediment is coarse grained, it is possible to use sediment routing models to predict the spatial and temporal changes of bed material size. When the sediment routing models are used to determine scour

or deposition, hydraulic equilibrium conditions are considered achieved when no further changes occur in the characteristics of the bed material within the river reach considered. Unfortunately, these models incorporate some empirical sediment transport formula which tends to limit their applicability, since none of these formulae can presently be said to be universal.

When the flow is strongly two-dimensional, or when the sediment is fine grained, the existing routing models are not directly applicable. This is because, in the case of fine sediment, there are as yet no reliable sediment transport formulae that could be used in such models, even for unidirectional flows. In the case of two-dimensional flows, the movement of fine sediment by transverse diffusion is often significant and needs to be taken into account in addition to advective transport. Existing empirical formulae only account for the latter mode of sediment transport.

Attempts at analyzing the hydraulic sorting of fine sediment by solving the governing transport equations presently face two major difficulties. Firstly, the erosion and deposition terms cannot as yet be accurately quantified. The second difficulty, which is in fact common to the sediment transport problem as a whole, is that no generally applicable method has been found for expressing the coupled nature of the sediment/water flow in a tractable set of equations. In spite of these difficulties, solution of the governing equations, particularly their depth-averaged version, is the best method currently available for prediction of the movement of fine sediments by water.

The complexity of the study of hydraulic sorting by routing or solution of the governing transport equations greatly increases when both coarse and fine sediments occur in comparable proportions. This is due to the fact that no methods are available today for combining the results from the two different models that would be required, one for each type of sediment. Such situations are often encountered in estuaries and reservoirs.

Hydraulic sorting can, however, be studied without direct recourse to sediment transport analysis. An alternative approach is to relate the characteristics of sediment particles found in a water body with the parameters of the flow responsible for the state in which they exist. For example, large particles in a river bed may have been deposited during a certain flood event, or the height to which a particle is suspended may be related to the net upward turbulent fluid fluxes at that level. This more direct approach has mostly been used by geologists with some useful results. Under certain circumstances, it has even been possible to interpret the observed correlations in terms of established theories from fluid mechanics. Such correlations, when found to be of a universal nature, can form a foundation upon which more reliable sediment formulae could be based. This alternative approach was adopted in this work.

The movement of fine sediment in a water body with predominantly two-dimensional flow is of primary interest to the environmental engineer. Fine sediment acts as a prime medium for the transport of pollutants. This is due to their large surface area to volume ratios,

which enables the particles to adsorb a large amount of pollutants. Two-dimensional flows are characteristic of lakes, reservoirs and harbours, where, due to low water velocities, fine sediment also tends to settle. In the case of coastal waters, the settling of fine sediment is enhanced due to the presence of salts that encourage particle flocculation. It is in these water bodies that there is an urgent need to regulate the disposal of dredged material and wastes by selecting the appropriate disposal sites and methods. Also, a large amount of contaminated sediment is usually transported into these areas by in-flowing rivers, often causing severe pollution problems. At present, there is therefore a need to develop the ability to monitor and control the deposition of contaminated sediment in these depositional environments.

1.2 STUDY OBJECTIVE

The objective of this study is to investigate the relationship between the sizes of sediment particles found on the bed-surface of a natural water body and flow parameters responsible for their deposition. Attention is focused on an area where the flow is two-dimensional and whose bed material is predominantly fine.

1.3 THESIS OUTLINE

This thesis is divided into seven chapters, inclusive of this Introduction (Chapter 1).

The Literature Review is given in chapter 2. This review covers past work by researchers from various disciplines on analytical studies, field observations and experimental studies on hydraulic sorting. The review of analytical studies covers both theoretical and routing (numerical) models.

In chapter 3, the study methodology is presented. The overall strategy for the study is first outlined. This is followed by a description of a two-dimensional numerical flow model that was used in this study. Some modifications that were made to the model in order to make it applicable to the selected study area are also described. The final section of chapter 3 discusses the criteria that were used in selecting the particular site on which the study was carried out.

Chapter 4 presents in its first section a general description of the site. In sections 4.2 and 4.3, the hydrometric and sediment data are respectively presented and analyzed. Water temperature data is briefly discussed in section 4.4. The chapter concludes with a discussion on the bathymetry, space discretization and bed-roughness in section 4.5.

Chapter 5 presents the numerical simulation results. After general comments in section 5.1, some model tests and their results are discussed in section 5.2. These were tests on a turbulence model incorporated in the flow model and the assessment of the convergence behaviour of the numerical scheme used. A comparison

between the performance of the numerical flow model and a physical model that had previously been constructed for the same area under a different study is also given. Finally, section 5.3 presents the results of the simulation of the flow conditions used for hydraulic sorting correlations.

Chapter 6 presents the observed relationships between sediment properties and flow parameters. After preliminary remarks in section 6.1, the choice of dimensionless variables used for investigating the relationships is discussed in section 6.2. Correlation plots are presented in section 6.3 and discussed in section 6.4.

In chapter 7, the work and the results are summarized in section 7.1. Section 7.2 presents the conclusions made from the study and in section 7.3 recommendations for further work are made.

Data that was used in this work has been included as appendices. In appendix A, the sediment data is tabulated. The water temperature data is given in appendix B, while flow and other data used for the correlation plots is given in appendix C.

CHAPTER 2

LITERATURE REVIEW

2.1 GENERAL

In the past, hydraulic sorting has been studied by researchers from various disciplines. These have included engineers, geologists, sedimentologists, mineralogists and geographers. The broad interest in hydraulic sorting is due to the important applications of this phenomenon in these diverse fields, such as for example, the prediction of locations of heavy mineral deposits, prediction of changes in river profile with time and inference of past flood events from sedimentary deposits. Both analytical and experimental studies have been conducted. A review of analytical studies is presented in section 2.2, followed by reviews of field and experimental studies in section 2.3 and 2.4 respectively.

2.2 ANALYTICAL STUDIES

The analytical studies that have been conducted on hydraulic sorting have resulted in the construction of theoretical and routing models. Theoretical models are defined here as those that attempt to explain hydraulic sorting from basic principles. On the other hand, in routing models, hydraulic sorting is simulated in order to predict evolution of particle size distribution under given flow conditions. Theoretical

models are reviewed in subsection 2.2.1 and routing models in subsection 2.2.2

2.2.1 Theoretical Models

Amongst the earliest explanations offered for hydraulic sorting was that due to Rubey (Rubey 1933). After examining water laid sand stones from different sources, he postulated the principle of Hydraulic Equivalence. This states that particles of different densities and diameters are deposited together if they have the same fall velocity, or are in 'hydraulic equivalence'. This principle explained the reason why heavy minerals are usually present in the finer fractions of a water laid sandstone.

Since its inception, the principle of Hydraulic Equivalence has received considerable attention from researchers. This interest is partly because the principle can be used to estimate the proportion of light to heavy minerals in a water laid sandstone, given the composition of the sources of these minerals. However, it has often been found in practice that some water-laid deposits appear not to be in hydraulic equivalence and consequently attempts have been made to explain these deviations. One such attempt was made by Lowright et al (1972), who explained the deviations as being due to selective removal of the heavy mineral particles.

In another contribution, Lane (1938) explained the absence of fine silt and clay sized particles from the bottom of rivers that transport

all particle sizes, as being due to their low fall velocities. Lane noted the fall velocity is proportional to the square of the diameter below a diameter of 0.1 mm, but is only proportional to square root of the diameter for diameter above 0.3 mm. Considering that energy losses in a turbulent stream vary with the square of the flow velocity, the turbulence energy required to keep particles smaller than 0.1 mm in suspension decreases rapidly with decreasing diameter. Therefore, these materials are easily kept in suspension. For particles larger than 0.3 mm, the turbulence energy required to carry them in suspension varies in direct proportion to the diameter and hence the size found in the bed would change gradually above 0.3 mm size. The observation that bed material size is often in the range 0.1-0.3 mm compared well with many particle size distributions found in the hydraulic environments studied by Lane.

Inman (1949) used concepts from boundary layer theory to explain why grain sizes with mean diameters close to 0.18 mm are usually well sorted. Here, a measure of grain sorting is given by the ratio between the 75^{th} and the 25^{th} percentile diameters. He explained that for a bed made of uniform sizes, the bed material size of 0.18 mm represents the transition from a hydrodynamically smooth to a hydrodynamically rough bed. When the bed particles sizes are smaller in size, the boundary is smooth and the bed shear stress is shared out among many particles. When the bed particles are larger than this size, the boundary becomes hydraulically rough. In this case the particles project above the laminar sub-layer into the

turbulent flow and therefore experience greater forces due to form drag.

Inman defined the roughness velocity for a particle as the shear velocity when a bed composed of such particles changes from being smooth to rough. He calculated this shear velocity (u_*) from boundary layer theory as

$$u_* = \frac{3.5\nu}{d} \qquad (2.1)$$

where ν is the kinematic viscosity of the fluid and d the particle diameter.

Inman observed, as shown in fig. 2.1, that a spherical quartz grain with a diameter equal to 0.18 mm has a fall (settling) velocity equal to the roughness velocity. Larger particles have roughness velocities that are smaller than their fall velocities. The converse is true for smaller particles. He also noted that the threshold entrainment velocity, which can be obtained from Shield's diagram (see section 2.3 below), is equal to both the roughness and fall velocities for particles with a diameter equal to 0.18 mm. For larger particles, the threshold velocity is larger than the roughness velocities, but smaller than the fall velocities. For smaller particles, the threshold velocity is larger than the fall velocity, but smaller than the roughness velocity.

From the preceding observations, Inman concluded that a quartz particle with diameter 0.18 mm (fall velocity equals 2 cm/s) is the

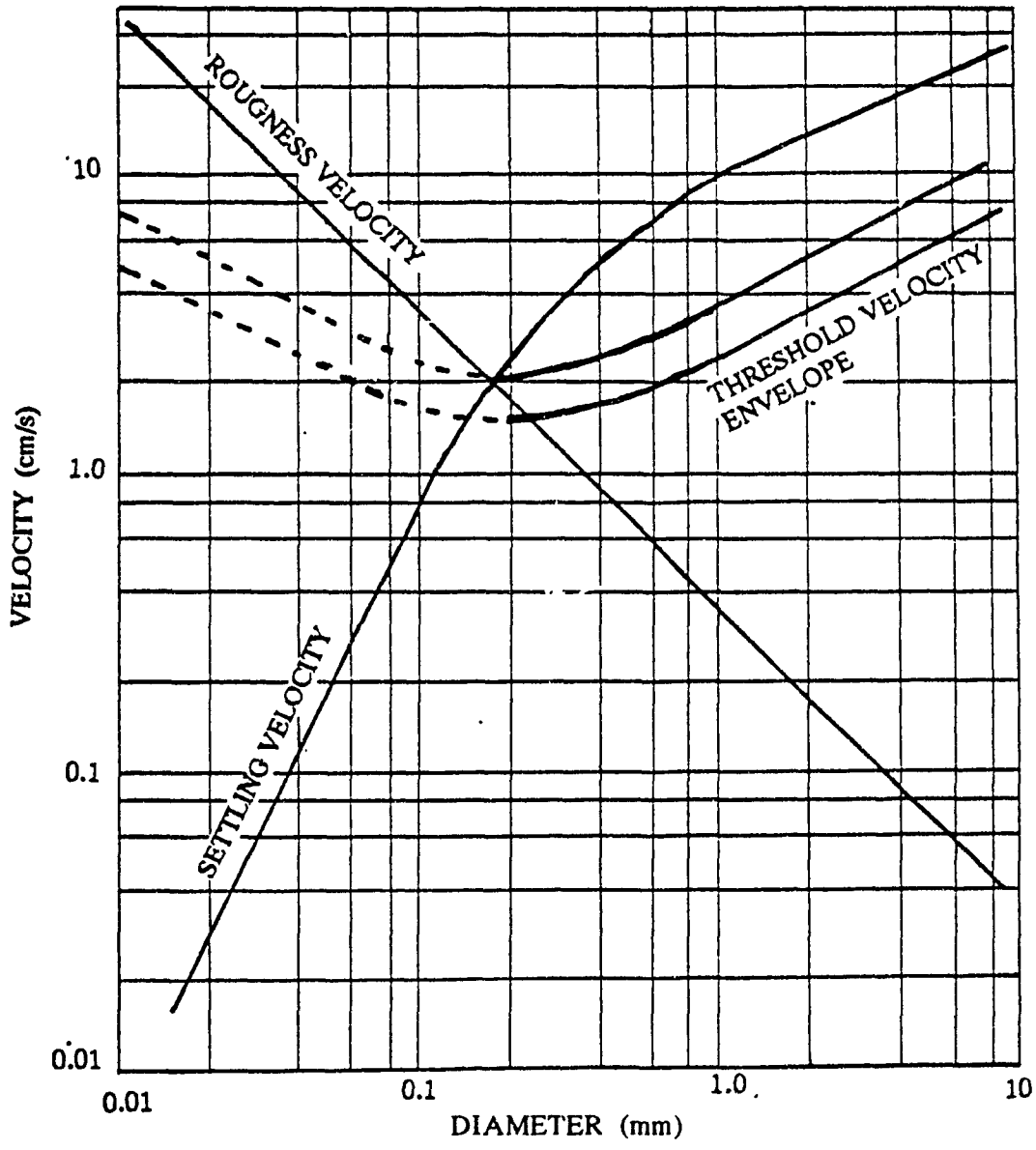

Fig. 2.1: Relation of Grain Size to Settling, Threshold and Roughness Velocities

most easily moved (it has the minimum threshold velocity). Since the value of the threshold velocity is numerically equal to both the roughness velocity and fall velocity, it can easily be transported either as bed load, suspended load or in saltation. For particles larger than 0.18 mm, since the threshold velocity is greater than the roughness velocity but less than the fall velocity, they are likely to be transported as bed load by rolling and sliding. The threshold velocity for particles smaller than 0.18 mm is larger than the fall velocity but smaller than the roughness velocity. If they are put into suspension, they are thus likely to be transported in suspension mode only. In later works, the coefficient appearing in equation 2.1 has generally been taken as 5.0 instead of 3.5 (Schlichting 1979, Henderson 1966). However, this does not significantly affect Inman's conclusions.

How particles smaller than 0.18 mm in diameter can be put into suspension is not clear. As had been demonstrated by Bagnold, it is very difficult to entrain such fine particles, due to their being submerged in the laminar sub-layer (Inman 1949, Raudkivi 1990). Inman (1949) suggested that a possible cause for the suspension of fine particles may be the formation of ripples. Another possible explanation is that in a turbulent flow, there are turbulent bursts that periodically penetrate even the laminar sub-layer (Raudkivi 1990).

Brush (1965) used the Rouse equation to explain the size/density distribution of water laid deposits consisting of different minerals.

The Rouse equation is a direct result of the integration of the Schmidt equation (Vanoni 1944). It expresses the basic idea that in a turbulent flow with suspended sediment, an equilibrium concentration profile exists when the downward flux of sediment due to gravity and the upward flux due to fluid turbulence are in balance. The Schmidt equation is

$$\omega c_s + \varepsilon_s \frac{dc_s}{dy} = 0 \tag{2.2}$$

where ω is the particle fall velocity, c_s is the sediment concentration, ε_s the diffusion coefficient for sediment and y the vertical coordinate. The Rouse equation is

$$\frac{c_y}{c_a} = \left\{\left(\frac{h-y}{y}\right)\left(\frac{a}{h-a}\right)\right\}^{\omega/\beta\kappa u_*} \tag{2.3}$$

where c_y is sediment concentration at level y and c_a that at a reference level a above the bed. κ is von Karman's constant (= 0.4), u_* the shear velocity, h the water depth and β the ratio between the fluid and sediment diffusion coefficients. A similar equation was independently derived by Ippen in 1934 (see Montes and Ippen 1973).

The Rouse equation is considered one of the most significant contributions to research on sediment transport (Kennedy 1983). However, a major difficulty in its use is the specification of the reference concentration c_a. This may require the use of empirical

formulae, such as the one proposed by van Rijn (1984 b). Another difficulty is the specification of β and consequently the variation of ε_s with distance from the boundary. Vanoni (1944) used Prandtl's mixing length theory to determine the diffusion coefficient for fluid momentum and assumed a value of unity for β. A recent contribution in this area has been made by Celik and Rodi (1991). They derived a relation for the reference concentration by considering the transport equation for the turbulence kinetic energy.

Brush (1965) postulated that in a suspension of mixed sizes and densities, equation 2.3 could be applied to individual classes of fall velocities. With a known bed material composition, he was able to predict the particle size distribution of suspended sediment in a laboratory flume. Similar studies were conducted by Sengupta (Sengupta 1975, 1979).

2.2.2 Sediment Routing Models

An approach favoured by civil engineers for predicting the response of fluvial environments to man induced changes is the use of sediment routing models. These models have been developed mainly in the last two decades, during which, models of varying complexities have been constructed. Routing models, which use numerical solution procedures, have a very clear advantage when compared to, say, physical hydraulic models. This is due to their ability to make long term predictions. In some routing models, time steps of up to 30

days can be used in the computations, thereby making it possible to model many years of river response.

As mentioned in the preceding chapter, routing methods were not used in this study. There are, nevertheless, some concepts embodied in these models that are relevant to this study. These are concepts on the armour layer development, the existence of a mixed (active) layer as distinct from the parent bed material layer and the response time scales for bed material evolution. For this reason, these models have been included in this review.

The routing models basically solve the conservation equations for individual sediment size fractions and water mass. In many of the models available today, the sediment phase is considered independently of the water phase. In all the models, empirical sediment transport formulae are used to compute the sediment discharge and in some, backwater curve computations are used to determine water surface profiles. Most of the models are constructed for analyzing one-dimensional flows.

Amongst the many one-dimensional sediment routing models available today are those of Thomas and Prasuhn (1977), Deigaard (1980), Holly and Karim (1986), Rahuel et al (1989), van Niekerk et al (1992) and Correia et al (1992). Two dimensional sediment routing has been attempted by Lopez S. (1978) and Yang et al (1988).

The model of Thomas and Prasuhn (1977) uses the sediment conservation equation

$$B\frac{\partial z_b}{\partial t} + \frac{\partial G_s}{\partial x} = 0 \qquad (2.4)$$

where G_s = volumetric sediment discharge, t = time, x = distance along the channel, B = width of movable bed and z_b = elevation of movable bed.

For computing the sediment discharge G_s, Einstein's bed load formula may be used, but the model allows for use of other appropriate formulae. The hydraulic parameters required for input in the sediment transport equation are determined by using backwater curve computations. These parameters include water depth, bottom shear stress and flow velocity.

When scour is expected, the existing bed material size distribution is required as input. Formation of armour layer is considered by determining a depth, known, as equilibrium depth, at which sediment of a given diameter will remain stationary on the bed. Consideration of the Manning-Strickler equation and Einsten's equation for flow intensity gives this depth as

$$h_{eq} = \left(\frac{q}{10.21 d^{1/3}}\right)^{6/7} \qquad (2.5)$$

for quartz particles in a rectangular channel. In this equation, h_{eq} is the equilibrium depth, q the water discharge per unit width and d the grain diameter. Equation 2.5 is not dimensionally homogeneous and though not explicitly stated by Thomas and Prasuhn (1977), it appears that the variables are in English Units (lb-ft-S).

An active layer is defined as the layer between the equilibrium depth and the channel bottom. When all the material in this layer is removed, the channel bottom becomes armoured. Each time a new discharge is analyzed, the armour layer is tested for stability.

In the models of Deigaard (1980) and Holly and Karim (1986), equation 2.4 is modified to account for bed porosity. The modified equation is

$$(1\text{-}p)B\frac{\partial z_b}{\partial t} + \frac{\partial G_s}{\partial x} = 0 \qquad (2.6)$$

where p is the bed material porosity.

In the model of Deigaard (1980), the assumption that the river bed profile has an exponential decrease in slope is used as an initial condition. It is also assumed that at each section (into which the river reach under consideration has been subdivided), the incoming sediment is instantaneously mixed with the bed sediment in a mixed layer. The depth of the mixed layer is set equal to the dune heights. The dune heights are estimated at 15% of the water depth. The water

surface slope is set equal to the bed slope. The porosity is assumed to have a constant value of 0.35. Bed load sediment discharge is computed using Engelund and Fredsoe formula, which is assumed to apply to each sediment size fraction of the bed material. Suspended load is calculated using a model based on the Rouse equation. For each time step, sediment conservation equation is solved together with a conservation equation for each size fraction in the whole river section under consideration. Exchange between bed material on original bed and the mixed layer is allowed for by considering the upward movement of the interface between the mixed layer and the bed.

Deigaard (1980) demonstrated that the river profile changes very slowly as compared to the size gradation changes. He did this by showing that two disparate time scales exist for global and individual fraction sediment mass conservation.

In the model of Holly and Karim (1986) a sediment transport formula based on regression analysis of a large amount of field and laboratory data is used. The model is otherwise similar to that of Thomas and Prasuhn (1977), but introduces some improvements. For example, the effect of bed forms on armouring is included. The bed is divided into two layers, the mixed layer at the top and the parent bed material layer below. The mixed layer is similar to that of Deigaard (1980), but is taken as half the bed form height. The latter is calculated using a more involved expression that takes into account the bed shear stress and water depth.

The aforementioned models use sediment transport equations that were developed for equilibrium transport conditions. The model of Rahuel et al (1989) is slightly different from that of Holly and Karim (1986), in that the response of sediment discharge to changing flow conditions is incorporated through a loading law. Also, the model can be used for simulating bed evolution under unsteady discharge conditions. Bed load discharge is computed using Meyer-Peter Muller formula, which is assumed to be applicable to individual size fractions. Sheltering of smaller particles by larger ones is accounted for through a hiding factor.

The model of van Niekerk et al (1992), introduces a new method of calculating bed load transport rates. The method takes into account the temporal fluctuation of bed shear stresses due to turbulence. The bed load formula is specifically derived for transport of individual size fractions.

Correia et al (1992), have used a fully coupled approach in constructing their model. In this approach, the mass and momentum conservation equations for both the sediment and water phase are written in a fully coupled form. Many methods for computing both the friction terms in the momentum conservation equation and evaluating the sediment discharge are given. The computation of friction losses is coupled with the bed configuration. The model predicts the type of bed forms present under different flow and bed material conditions.

The quasi two-dimensional model of Lopez S. (1978) was developed to predict sedimentation in reservoirs. In this model, one dimensional flow analysis is first used to determine the discharge and water depth at each section. The reservoir is then divided into sub- channels, with jet theory being used to analyze flow in areas where flow separation can occur. Sediment is routed by individual size fraction. An empirical power relationship is used to compute sediment discharge as a function of flow velocity. Interchange of water and suspended sediment between the sub-channels is accounted for by considering continuity equation for each sub channel separately.

Another quasi-two dimensional model is that of Yang et al (1988). In this model, backwater curve computations are made for surface water profile. The channel is then sub-divided into stream tubes for sediment routing analysis. Armour layer development is considered and the flow width is allowed to vary. Bed and Bed material evolution are modelled using the concepts of mixed layer as for the one dimensional models. The active (mixed) layer thickness is taken as a multiple of the geometric mean size of the largest size class used.

2.3 FIELD AND EXPERIMENTAL STUDIES

2.3.1 Field Studies

The earliest field studies on hydraulic sorting appears to have been carried out by Steinberg in 1875 (Deigaard 1980, Rana et al 1973).

Steinberg found that on the Rhine, the maximum bed particle size decreased exponentially in the downstream direction. This downstream size decrease has been observed in many rivers all over the world (Deigaard 1980). Although this decrease in size was at first attributed to abrasion, i.e. particle size reduction by collision impact, rubbing and grinding, it was later realized through experiments that abrasion accounted for only a small percentage of the size reduction observed in nature. A more satisfactory explanation has since been found in the phenomena of hydraulic sorting (Deigaard 1980, Rana et al 1973).

At the sources of sediments derived by erosion and weathering, theory indicates that the size distribution of a sediment sample would be log-normal. This is because, as shown by Kolmogorov, if a block is randomly divided and subdivided, the resulting size distribution would be log-normal (Deigaard 1980). When the sediment is transported by water, this initial size distribution is likely be altered due to both hydraulic sorting and abrasion effects. Investigation into this phenomena by Visher (1969), indicated that sediment deposits as found in the hydraulic environment consist of a mixture of several (up to 4) log-normally distributed sub-populations. Each sub-population reflects a different mode of transport. Under normal circumstances, there should be three of these sub-populations. The various sub-populations can be identified by making a log-probability plot of the size distribution. The first sub-population is composed of the material transported as bed load by "traction" i.e rolling or sliding, the second sub-population is

transported by saltation and the third by suspension. A fourth sub-population arises in the case of beach deposits, in which the saltation population shows a break. It was proposed by Visher (1969) and experimentally confirmed by Kolmer (1973) that this saltation break is due to the different transport characteristics of the swash and backwash motions of water waves on the beach.

Visher (1969) observed that the sizes at which the sub-populations showed breaks between and the sorting within each sub-population, were dependent upon the characteristic of the depositing current. In the case of populations with three sub-populations, Visher (1969) noted that the two breaks occur near diameters that can be given a simple hydraulic interpretation. The break between suspension and saltation sub-population occurs near a diameter of 0.1 mm, while that between saltation and traction sub-population occurred near a diameter of 0.25 mm as would be expected from the analysis of Lane (1938). Visher's analysis used about 1,200 samples from different depositional environments in the Gulf coast and Atlantic of the United States of America.

When an unknown particle size distribution is needed as input in solving a problem, as is the case in some sediment routing analyses, engineers often make the assumption that the entire population is log-normally distributed. Garde (1973), from analysis of previously published data noted that the size distribution of the entire population of a sediment sample was rarely log-normal. He observed that for river samples, the three sub-populations proposed by Visher

(1969) were usually present. He however noted that as much as 40% of the data showed log-normal distribution in the range between 15^{th} and 84^{th} percentile size.

Garde (1972) also analyzed the standard deviation of the particle size distributions. He found that the geometric standard deviation (σ_g) of the samples increased with the median diameter in the form

$$\sigma_g = 2.4\, d_{50}^{0.34}, \quad d_{50} \geq 0.2\text{mm} \tag{2.7}$$

where

$$\sigma_g = \frac{d_{84.1}}{d_{50}} = \frac{d_{50}}{d_{15.9}} \tag{2.8 a}$$

for log normally distributed populations. Otherwise it may be approximated from

$$\sigma_g = \frac{1}{2}\left(\frac{d_{84.1}}{d_{50}} + \frac{d_{50}}{d_{15.9}}\right) \tag{2.8 b}$$

where $d_{15.9}$, d_{50}, $d_{84.1}$ are sediment sizes such that 15.9%, 50% and 84.1% of material by weight are finer than these sizes respectively. The median size (d_{50}) is measured in mm in equation 2.7. Garde proposed that the standard deviation would remain at a constant value of 1.4 for sediment finer than 0.2 mm.

Middleton (1976) was able to predict the shear velocity prevailing at the time of deposition of a sediment sample. He used the criteria that for suspension to occur, the particle fall velocity must be less or just equal to shear velocity. He postulated that the fall velocity of the particle size marking the break between the traction and saltation sub-populations, was equal to the shear velocity at the time of deposition. Middleton's analysis compared well with field observations for river deposits.

Two issues on the break analysis are not yet fully resolved. These are whether a distinct saltation sub-population exists separate from the traction sub-population and whether the sub-populations are truncated or overlapping (see Bridge 1981). Both of these affect the accuracy with which the break diameter can be determined.

2.3.2 Experimental Studies

Probably the most intensively studied aspect of hydraulic sorting is the entrainment of sediment particles. These studies led to the construction of the classical Shield's diagram, which has formed the basis of many sediment transport formulae.

In the Shield's diagram, the dimensionless shear stress at the incipience of motion of a particle is plotted against the particle Reynold's number. The dimensionless shear stress is also referred to as Shield's parameter or Shield's entrainment function (θ_{cr}). It is

given by the equation

$$\theta_{cr} = \frac{u_{*c}^2}{(s-1)\,gd} \tag{2.9}$$

and the critical particle Reynold's number (Re^*_c) at which the motion just begins is given by the equation

$$Re^*_c = \frac{u_{*c}\,d}{\nu} \tag{2.10}$$

where u_{*c} = critical shear velocity, s = specific gravity of the particles, g = acceleration due to gravity, d = particle diameter and ν = kinematic viscosity of water.

Shield's diagram was originally developed by Shield in 1936 from experimental studies. It has since been extended by many researchers (Graf, 1984).

For convenience of use, Shield's diagram has been expressed analytically in at least two different ways. The expressions given by van Rijn (1984 a) are:

$$\theta_{cr} = 0.24\, D_*^{-1}; \quad D_* \leq 4 \tag{2.11a}$$

$$\theta_{cr} = 0.14\, D_*^{-0.64}; \quad 4 < D_* \leq 10 \tag{2.11b}$$

$$\theta_{cr} = 0.04\, D_*^{-0.1}; \quad 10 < D_* \leq 20 \tag{2.11c}$$

$$\theta_{cr} = 0.013\, D_*^{0.29}; \quad 20 < D_* \leq 150 \tag{2.11d}$$

$$\theta_{cr} = 0.055\,; \quad D_* > 150 \tag{2.11e}$$

where D_* is the dimensionless particle size given by

$$D_* = \left\{ \frac{(s-1)\, g\, d^3}{\nu^2} \right\}^{1/3} \tag{2.12}$$

The second relationship, given in Raudkivi (1990) is

$$D_* = 2.15\, Re_*; \quad Re_* < 1 \tag{2.13a}$$

$$D_* = 2.5\, Re_*^{4/5}; \quad 1 \leq Re_* < 10 \tag{2.13b}$$

$$D_* = 2.5\, Re_*^{3/8}; \quad Re_* > 10 \tag{2.13c}$$

For fine sediments, with $Re_{*c} < 1$, and subject to some cohesion, the following relationship is given in Raudkivi (1990)

$$D_* = Re_{*c}^2 \tag{2.14}$$

In the past, Shield's diagram has been used for evaluating critical shear stresses for both uniform and graded sediments, it is however, strictly speaking, only applicable to the former. In the laboratory studies by Wilcock and Southard (1988), a reference shear stress analogous to the Shield's critical shear stress, is defined as the shear stress at which a small reference bed load for each size fraction of the bed material can be detected. The reference shear stress concept has also been used in the works of Komar (1987), Ferguson et al (1989) and Parker (1990). This reference shear stress has been found to be related to the median particle size in the form

$$\tau_{ri} = \alpha \left(\frac{d_i}{d_{50}} \right)^{\beta_1} \qquad (2.15)$$

where τ_{ri} is the reference shear stress for size class i, d_i the mean diameter of size class i, α and β_1 are constants (Wilcock and Southard 1988).

Another mechanism of sorting that affects bed sediment is sorting by shear. This was experimentally demonstrated by Bagnold (Bagnold 1954, Slingerland 1984). Bagnold showed that when a dense dispersion of solids in a newtonian fluid is subjected to shear, the larger particles tend to move to the zones of lesser shear stress. This phenomena is important in beds where ripples or dunes are present. It explains the tangential grading of many sedimentary deposits (Brush 1965).

The overall effect of the various modes of hydraulic sorting can be seen by comparing the transport rates of particles of different sizes (Slingerland 1984). This is referred to as transport sorting and subsumes all other modes of hydraulic sorting, like suspension sorting, entrainment sorting and shear sorting. The transport rate and the relevant parameters influencing it have been subjects of laboratory studies. The transport rate or transport velocity of a particle is measured as the longitudinal distance traversed by the particle per unit time. The time used for computing it is, therefore, inclusive of any intermittent rest periods in the particle motion.

Meland and Norman (1969) found that the transport velocity of a single particle was influenced by water velocity, particle interactions, bed surface stability, particle characteristics, bed roughness and bed forms. Bed surface stability was defined as the resistance due to particle re-arrangement and displacement in the bed surface by weight and impact, as well as secondary turbulence caused by the particle. The effect of bed roughness on particle transport velocity was also studied by Steidtmann (1982). He found that this effect depends primarily on the ratio between the particle size and the roughness elements. In both the studies of Meland and Norman (1969) and Steidtmann (1982), only qualitative results were given.

Hydraulic sorting of fine sediments appears not to have been investigated in as much detail as coarse sediments. Fine sediment tends to behave differently from coarse sediment because of cohesion. Cohesive forces depend not only on the mineralogical composition of the sediment particles, but also on the chemical properties of the ambient fluid. The relatively recent experimental studies on the transport of fine sediments by water have mainly been intended for determining the rates of erosion and deposition. Erosion rates have been experimentally studied by Ariathurai and Arunalandan (1978), Thorn and Parsons (1980), Parchure and Mehta (1981) and Kamphius and Hall (1983). Deposition rates have been studied by Mehta and Partheniades (1975). A review of the state of the art in fine sediment transport can be found in Mehta et al (1989 a and b) and Raudkivi (1990).

In the studies carried out on erosion and deposition of fine sediments, the bed shear stress features prominently in almost all the formulae proposed. However, the particle diameter does not appear to have been considered. The exception may be the study by Thorn and Parsons (1980), where the consideration of the sediment bulk density incorporates the particle size distribution implicitly.

For the study of hydraulic sorting, particle size distribution is of major importance and must therefore be included. Furthermore, most sediments occur as a mixture of both coarse and fine particles.

CHAPTER 3

STUDY METHODOLOGY

3.1 OUTLINE OF METHODOLOGY

In this study, an existing numerical model was used to compute flow parameters in a natural water body. These flow parameters were then correlated with the characteristics of the sediment found on the bed-surface of the water body considered.

The basic flow parameters considered in the correlations were the shear velocity and the water depth. The sediment characteristics considered were the median particle size and its fall velocity.

A description of the numerical model and some modifications that were made to it are given in sections 3.2 and 3.3 respectively. Section 3.4 discusses the criteria that were used for selecting the study site.

3.2 DESCRIPTION OF THE NUMERICAL MODEL

3.2.1 Model History

The computer code used in this work was developed by the Hydraulic Computations Group (HCG) at the civil engineering department of Concordia University, between the periods 1986-90. It

has been used primarily as a research tool by this group, who has applied it to both field and laboratory cases (Plouffe 1987, Sarraf and Saade 1990, Saade, 1990, Sarraf and Zhang 1991, Zhang 1992).

The code comprises several utility models, including a two-dimensional flow model, a turbulence model, a heat transfer model and an ice cover melting model. These models are implemented as independent subroutines to allow for a diversity of applications.

For this study, only the two-dimensional flow and the turbulence models were of interest. These are described more fully in sub-sections 3.2.2 and 3.2.3 respectively.

3.2.2 The Two-dimensional Flow Model

The two-dimensional flow model solves the depth averaged flow equations using the explicit finite difference MacCormack scheme on dense uniform rectangular computational grids. An enhancement of the original MacCormack scheme due to Garcia (Garcia 1983, Garcia and Kahawita 1986), in which the sequence of applying the MacCormack split time operators was symmetrized, is incorporated in the model.

The depth averaged flow equations when both Coriolis and wind effects are neglected are (see for example, Flokstra 1976):

$$\frac{\partial h}{\partial t} + \frac{\partial (uh)}{\partial x} + \frac{\partial (vh)}{\partial y} = 0 \qquad (3.1\ a)$$

$$\frac{\partial (uh)}{\partial t} + \frac{\partial (u^2 h)}{\partial x} + \frac{\partial (uvh)}{\partial y} = -\rho g h \frac{\partial}{\partial x}(h+z_b) + \frac{\partial}{\partial x}(2h\nu_t \frac{\partial u}{\partial x}) + \frac{\partial}{\partial y}(h\nu_t \frac{\partial u}{\partial y}) + \frac{\partial}{\partial y}(h\nu_t \frac{\partial v}{\partial x}) - \frac{\tau_{bx}}{\rho} \qquad (3.1\ b)$$

$$\frac{\partial (vh)}{\partial t} + \frac{\partial (uvh)}{\partial x} + \frac{\partial (v^2 h)}{\partial y} = -\rho g h \frac{\partial}{\partial y}(h+z_b) + \frac{\partial}{\partial x}(h\nu_t \frac{\partial v}{\partial x}) + \frac{\partial}{\partial y}(2h\nu_t \frac{\partial v}{\partial y}) + \frac{\partial}{\partial x}(h\nu_t \frac{\partial u}{\partial y}) - \frac{\tau_{by}}{\rho} \qquad (3.1\ c)$$

where t is time, x,y the horizontal cartesian coordinates, u,v the depth averaged velocity components along x and y directions respectively, h the water depth, g the acceleration due to gravity, ρ the water density, z_b the bed elevation, ν_t the kinematic turbulent viscosity coefficient and τ_{bx} , τ_{by} the bed shear stresses per unit area along x and y directions respectively.

Equation 3.1a expresses the conservation of mass while equations 3.1b and 3.1c express the conservation of linear momentum along x and y directions respectively.

The bed shear stress terms are computed using the Manning equation as follows:

$$\frac{\tau_{bx}}{\rho g h} = S_{fx} = -\frac{n^2 u \sqrt{(u^2 + v^2)}}{h^{4/3}} \qquad (3.2\ a)$$

$$\frac{\tau_{by}}{\rho g h} = S_{fy} = -\frac{n^2 v \sqrt{(u^2 + v^2)}}{h^{4/3}} \qquad (3.2\ b)$$

where n is Manning's coefficient, and S_{fx}, S_{fy} the friction slopes in the x and y directions respectively.

To simplify notation, it is desirable to cast the depth averaged equations in vector conservation form. This can be achieved by defining the vector E of conserved variables, the vector F of fluxes of the conserved variables in the x direction, and the vector G of fluxes of the conserved variables in the y direction. These are given below.

$$E = \begin{bmatrix} h \\ uh \\ vh \end{bmatrix}$$

$$F = \begin{bmatrix} uh \\ u^2h + \frac{gh^2}{2} + z_b - 2\nu_t\frac{\partial u}{\partial x} + \int s_{fx}\,dx \\ uvh - \nu_t(\frac{\partial u}{\partial y} + \frac{\partial v}{\partial x}) \end{bmatrix} \quad G = \begin{bmatrix} vh \\ uvh - \nu_t(\frac{\partial u}{\partial y} + \frac{\partial v}{\partial x}) \\ v^2h + \frac{gh^2}{2} + z_b - 2\nu_t\frac{\partial v}{\partial y} + \int s_{fy}\,dy \end{bmatrix}$$

The depth averaged flow equations can then be written as

$$\frac{\partial E}{\partial t} + \frac{\partial F}{\partial x} + \frac{\partial G}{\partial y} = 0 \qquad (3.1d)$$

The primary variables used in the HCG code for the elements of the vector E are the unit discharges U = uh, V = vh and the water depth h.

The MacCormack scheme discretizes the flow equations using the following time splitting procedure. The overall time step Δt is split into two time steps Δt_x and Δt_y. Two discretization operators L_x and L_y are used. Operator L_x is applied to equation 3.1d but the flux vector G is assumed absent (G=0), while the operator L_y is applied to the same equation but neglecting the flux vector F (F=0). Each operator discretizes the appropriately modified equation 3.1d in two steps, namely a predictor and corrector step. In the predictor step of the L_x operator, in which the solution is advanced from time t_0 to $t_0+\Delta t_x$, the space derivatives are computed using backward differences. The values of U, V and h obtained from the predictor step, U^p, V^p, h^p and those prevailing at time t_0, i.e. U^0, V^0, h^0 are averaged to give values $U^{1/2}$, $V^{1/2}$, and $h^{1/2}$ at an intermediate time $t_0+\Delta t_x/2$. In the corrector step, the solution is advanced from the intermediate time $t_0+\Delta t_x/2$ to the time $t_0+\Delta t_x$. In this step, forward differencing is used to compute the derivatives, but the fluxes are computed using the values U^p, V^p, and h^p obtained during the predictor step. The time derivatives are computed using forward differencing in both steps. The operator L_y is applied in a similar manner, but over a time step Δt_y. A detailed description of the MacCormack scheme can be found in MacCormack (1969), Baldwin et al (1975) and Garcia (1983).

In order to improve the accuracy of the MacCormack scheme, the partial time steps Δt_x, Δt_y are split further. The symmetrized sequence of applying these split operators proposed by Garcia (1983) is:

$$L(\Delta t) = \{L_x(\Delta t_x/2)L_y(\Delta t_y/2)\ L_x(\Delta t_x/2)L_y(\Delta t_y/2)\}\ .$$

in which $L(\Delta t)$ may be interpreted as the global MacCormack discretization operator. In the original scheme, MacCormack (1969) used the sequence

$$L(\Delta t) = \{L_x(\Delta t_x/2)\ L_y(\Delta t_y)L_x(\Delta t_x/2)\},$$

which has a directional preference because the L_y operator is applied only once while the L_x operator is applied twice.

The stability criteria for the enhanced MacCormack scheme is (Garcia 1983)

$$\Delta t \leq \max\left\{\frac{2\Delta x}{u+\sqrt{gh}}\ ;\ \frac{2\Delta y}{v+\sqrt{gh}}\right\} \tag{3.3}$$

The enhanced scheme allows the use of up to twice the maximum time step of the original MacCormack scheme. Both the enhanced and the original scheme have second order accuracies in space and time.

Boundary conditions are specified in a manner consistent with the recommendations of Abraham et al (1981). These are required at inlets, walls and at one outlet in the case of sub-critical flows. At the inlets, unit discharges are specified. The water surface elevation is specified at the outlet for sub-critical flows and the inlet for super-critical flows. At solid walls, a non-slip condition is approximated.

This approximation is achieved by defining fictitious points outside the computation domain. At these points the flow velocity components are assigned values which are equal in magnitude but opposite in direction to those at the corresponding point in the domain. Details of the flow boundary condition specification can be found in Garcia (1983) and Saade (1990).

Additional, mainly computational, boundary conditions specified in the model are zero gradients of U, V and h both at the inlets and outlets. The specification of zero gradient for h at the outlet also serves to prevent wave reflections.

With regard to Computational Hydraulics, the discretization technique used in this model has two major attributes. The first attribute can be appreciated by considering that in the flow described by the depth averaged equations, transport by diffusion is often much smaller than that by convection, thereby giving the system of equations a near hyperbolic character. Indeed, the widely used de-Saint Venant's equations for shallow water flow are similar to the depth averaged equations, except that the diffusive terms are omitted in the former, thereby making them purely hyperbolic (see for example Abbot 1979). The suitability of the MacCormack scheme for hyperbolic type flows is due to its structure, which is similar to those of the Lax-Wendroff family of algorithms. These algorithms have been found to be particularly suitable for solving hyperbolic partial differential equations (Lapidus and Pinder 1982, Hirsch 1990, Baldwin et al 1975). In fact, in the one dimensional linear case, the

MacCormack scheme reduces to the Lax-Wendroff scheme (see for example, Garcia-Navaro and Saviron 1992). The second attribute, is that though not a strict one, it approximates the control volume methods due to the manner in which it discretizes the flux terms (Baldwin et al 1975). The property of flux conservation is desirable because the flow equations being discretized are themselves flux conservation equations. Detailed discussion on flux conserving schemes can be found in Patankar (1980).

It should be emphasized that the flux conservation property of the MacCormack scheme is only approximate and gets worse as transport by diffusion becomes appreciable. The scheme is therefore not suitable for modelling the transport of scalar quantities such as heat, species concentration and turbulent kinetic energy, unless the manner in which the f .xes are computed is modified. Flux conservation using the basic scheme is best when the Courant number is close to unity (Baldwin et al 1975). For the depth averaged equations, this number is given by $(u+\sqrt{gh})\Delta t/\Delta x$ in the x-direction and $(v+\sqrt{gh})\Delta t/\Delta y$ in the y-direction.

The flow model obtains steady state solutions by solving the full unsteady equations, beginning from guessed initial values. This procedure offers a convenient way of carrying out the required iterations (Roache 1976).

3.2.3 Model Inputs

In addition to the inlet and outlet boundary conditions, the flow model requires as input, the bathymetry, initial conditions, Manning's coefficient and turbulent viscosity coefficient.

The bathymetry input consists of an array of river bed elevations, supplemented by boundary codes that identify the location of exits, inlets and walls.

In order to start the computations, initial values for U, V and surface water elevation need to be specified at all points in the computation domain. In the absence of better information, the values of U and V may all be set to zero, while the surface water elevation may be set to a constant equal to the downstream water elevation.

The value of Manning's coefficient depends on the area being modelled. The best value for this coefficient may have to be obtained through computational experiments. Typical values for various cases are given in standard texts such as Chow (1959) and Henderson (1966). When the area being modelled has a bed consisting of gravel of known size distribution, the Manning-Strickler equation (Henderson 1966) may be used.

If the intention is only to model the flow velocities and depth, the turbulent viscosity coefficient may be set to some reasonable constant value. This is because the variables U, V, and h are not

significantly influenced by the coefficient if its magnitude is within a reasonable limit. In cases where the streamlines are known to be more or less straight (far-field) the viscous terms may be omitted since their contribution is usually insignificant (Rodi 1984). However, in order to correctly model recirculating flows, these terms should be included and their magnitudes correctly specified. This is also the case when modelling the transport of a scalar quantity, such as heat or turbulent kinetic energy. In simulations where the viscous terms are omitted, the HCG flow model does not impose the no-slip boundary condition on the velocity component parallel to walls.

In applications where an accurate specification of the turbulent viscosity coefficient is deemed necessary, a turbulence model is required. The option of using such a model is available in the HCG code. The particular turbulence model available in the code is described in the next sub-section.

3.2.4 The Turbulence Model

The turbulence model incorporated in the HCG code is the depth averaged k-ε model developed by Rastogi and Rodi (Rastogi and Rodi 1978, Rodi 1984). In this model the depth averaged kinematic turbulent viscosity coefficient is computed from the equation

$$\nu_t = c_\mu \frac{k^2}{\varepsilon} \tag{3.4}$$

in which k is the depth averaged turbulent kinetic energy per unit mass of fluid and ε its rate of dissipation. c_μ is an empirical constant taken as 0.09.

In order to compute k and ε, their transport equations are solved. For unsteady flows, these equations can be written in the following general form (see for example Chapman 1982):

$$\frac{\partial(kh)}{\partial t} + \frac{\partial(uhk)}{\partial x} + \frac{\partial(vhk)}{\partial y} = \frac{\partial}{\partial x}\left(h\frac{\nu_t}{\sigma_k}\frac{\partial k}{\partial x}\right) + \frac{\partial}{\partial y}\left(h\frac{\nu_t}{\sigma_k}\frac{\partial k}{\partial y}\right) + hP_h + hP_{kv} - \varepsilon h \quad (3.5a)$$

$$\frac{\partial(\varepsilon h)}{\partial t} + \frac{\partial(uh\varepsilon)}{\partial x} + \frac{\partial(vh\varepsilon)}{\partial y} = \frac{\partial}{\partial x}\left(h\frac{\nu_t}{\sigma_\varepsilon}\frac{\partial \varepsilon}{\partial x}\right) + \frac{\partial}{\partial y}\left(h\frac{\nu_t}{\sigma_\varepsilon}\frac{\partial \varepsilon}{\partial y}\right) + hc_{1\varepsilon}\frac{\varepsilon}{k}P_h + hP_{\varepsilon v} - hc_{2\varepsilon}\frac{\varepsilon^2}{k} \quad (3.5b)$$

where

$$P_h = \nu_t\left[2\left(\frac{\partial u}{\partial x}\right)^2 + 2\left(\frac{\partial v}{\partial y}\right)^2 + \left(\frac{\partial u}{\partial y} + \frac{\partial v}{\partial x}\right)^2\right], \quad P_{kv} = c_k\frac{u_*^3}{h}, \quad P_{\varepsilon v} = c_\varepsilon\frac{u_*^4}{h^2}$$

Equations 3.5a and b are the transport equations for k and ε respectively. These equations were adapted from the standard k-ε model for three dimensional flow analysis. In this adaptation, Rastogi and Rodi (1978) added the terms P_{kv} and $P_{\varepsilon v}$ to the standard k-ε model to account for the production of turbulence energy by bottom friction. The source term P_h accounts for the production of turbulence energy due the interaction of turbulent stresses with mean flow gradients.

In the expressions for P_{kv} and $P_{\varepsilon v}$, u_* is the shear velocity. The empirical constants c_k and c_ε are related to c_f as follows

$$c_k = \frac{1}{\sqrt{c_f}} \; ; \; c_\varepsilon = 3.6\frac{c_{2\varepsilon}}{c_f^{3/4}}\sqrt{c_\mu}$$

where c_f is the friction coefficient.

In the derivation of these empirical coefficients, Rastogi and Rodi (1978) used Laufer's empirical formula for turbulent viscosity. This formula is

$$\nu_t = \frac{u_* h}{13} \tag{3.6}$$

The empirical constants included in the depth averaged k-ε model were taken directly from the standard k-ε model of Launder and Spalding (1974). The constants are: $c_{1\varepsilon}$ =1.44, $c_{2\varepsilon}$ =1.92, σ_k=1.0, and σ_ε =1.3.

The shear velocity is calculated using the formula

$$u_* = \sqrt{c_f(u^2 + v^2)} \tag{3.7}$$

In the case of hydraulically rough boundaries, the friction coefficient c_f is related to Manning's coefficient as follows (Rastogi and Rodi 1978):

$$c_f = \frac{n^2 g}{h^{1/3}} \tag{3.8}$$

In natural water bodies, the boundaries are usually hydraulically rough. This is due to the fact that even when the bed sediment is fine and smaller than the thickness of the laminar sub-layer, the presence of bed irregularities in the form of ripples always makes the boundary hydraulically rough.

In the HCG code, the transport equations for k and ε are discretized using the second upwind differencing method (Roache 1976) for first order space derivatives, the central differencing method for second order space derivatives and forward differencing for the time derivatives. The formulation is an explicit one, in which all the space derivatives and the source/sink terms are evaluated at time = t when advancing the solution to time $t+\Delta t$. Like the MacCormack scheme, the second upwind scheme has a second order accuracy in space and is used with a fully dense grid. It is only of first order accuracy in time. However, the contribution of the unsteady term becomes negligible as the steady state solution is approached.

Other schemes, such as the power-law scheme and the exponential scheme (Patankar 1980), could be used in preference to the upwind scheme for general fluid flow computations. However, when these schemes are applied to large scale external flows, they usually reduce to an equivalent of the upwind scheme due to the large grid Peclet numbers. The large Peclet numbers result primarily from the large grid sizes that must be used in order to make the computations economically viable.

The boundary conditions used for modelling k and ε are zero gradients for both quantities at inlets and outlet. At solid walls, use is made of the wall function method developed by Launder and Spalding (1974) to take account of the finite rate of turbulence energy dissipation in the laminar sub-layer. In applying the wall function method, the gradients of the velocity components parallel to the wall are set to zero as suggested by Chapman (1982).

The initial values of k and ε need to be chosen carefully in order to ensure convergence. These are best obtained through computational experiments for each case of application. A detailed description of the k-ε model as implemented in the HCG code can be found in Saade (1990).

3.3 MODIFICATIONS TO THE CODE

The following modifications were made to the HCG code in order to make it suitable for use in this study

3.3.1 Number of inlets

The original code allowed for two inlets, the main river inlet and a side effluent discharge inlet. The number of inlets was generalized to allow the modelling of lakes which have several in-flowing rivers. The generalization was fairly simple because of the use in the HCG code of a sub-routine for identifying various types of boundaries. In the modified code, when an inlet point is identified, the values of the

unit discharges U and V are assigned their boundary values. These remain unchanged throughout the simulation time when modelling steady state conditions.

It would have been desirable to extend this generalization to the number of outlets as well. However it is not as yet clear what boundary conditions need to be specified in the case of more than one outlet.

3.3.2 Boundary Conditions for k-ε model

The boundary conditions for k-ε model were reviewed. For all inlet points, the values of both k and ε need to be specified as is the case for all scalar variables (Patankar 1980). This specification improves the convergence behavior of the code. The actual values of k and ε specified at the inlets do not have much influence on the solution in the interior domain (Rodi 1984), but these must nevertheless be reasonable.

The boundary conditions for k and ε at solid walls were modified to k = 0 and ε = 0 in preference to the theoretically superior wall function method. The reason for this modification was that proper application of the wall function method requires that the distance from the wall, y_w, of wall nearest grid point be within the range given by the following equation (Rastogi and Rodi 1978):

$$30 \leq \frac{y_w u_*}{\nu} \leq 100 \qquad (3.9)$$

where ν is the laminar kinematic viscosity coefficient. It is difficult to satisfy this condition when modelling the flow in water bodies with irregular boundaries. When the actual distance exceeds the upper limit given by equation 3.9, the value of ε obtained from the model becomes small as compared to that of k, thereby giving an unreasonably high value of the turbulent viscosity coefficient. The alternative boundary conditions implemented here have been suggested by Hirsch (1990), who also suggested the setting of zero gradients for ε at the walls as another alternative. At this point, it is necessary to remark that the most accurate boundary condition for k at the walls is $k = 0$, since both the time mean and fluctuating components vanish here (Rodi 1984). It is the specification of ε at the wall that poses a problem.

3.3.3 Convergence Testing

A subroutine for testing the convergence of iterations was added to the code. This subroutine checks the convergence of iterations using two methods. In the first method, convergence of overall mass conservation in the computation domain is checked by comparing the mass outflow with the sum of the mass inflows. The difference between these two is required to be small, and to remain so for many time steps, before the iterations can be considered to have converged. The second method used was that of maximum differences (Roache 1976). In this method the maximum difference in the computed values of any of the variables between successive test periods is required to be within a set tolerance. The test periods

are set at sufficiently large number of iteration time steps apart. This requirement can be expressed for any variable ϕ as:

$$\Delta\phi_{tn} = \max \left| \phi^{Ni} - \phi^{Ni+ki} \right|_{i=1,imax;\ j=1,jmax} \leq \Delta\phi_{lim} \qquad (3.10)$$

where $\Delta\phi_{tn}$ is the computed difference in test number tn, $\Delta\phi_{lim}$ is the desired limit, i and j are the grid references in x and y directions respectively and i_{max}, j_{max} their maximum values, Ni is the the number of iterations carried out before test tn and ki the number of iterations between test intervals.

The most rigorous convergence test available today is the method of residuals, in which the computed variables are substituted back in the discretized equations to see how well these are satisfied. The resulting errors, known as residuals, should ideally be equal to the machine zero when the iterations have converged. However, this technique was not used in this work because the predictor-corrector sequence in the MacCormack scheme generates more than one discretization equation for each variable.

3.3.4 Empirical Viscosity Formula

A subroutine for computing turbulent viscosity using equation 3.6 was also added to the model. By changing the denominator in this equation, several empirical formulae such as those given in Fischer et al. (1979) can be used. As pointed out by Rodi (1984), the turbulent viscosity coefficient, given by the k-ε model does not include the

effects of shear flow dispersion. Some of the empirical eddy viscosity formulae are derived from field measurements in which the effects of shear flow dispersion and turbulent diffusion cannot be separately identified. Such coefficients must, therefore, be representative of both processes.

The advantage of incorporating the empirical formula option is that preliminary tests for a particular application may indicate both that the turbulence model and the empirical formula give similar results. In such situations, the empirical formula can be used instead of the turbulence model with great saving in computation time.

3.4 CHOICE OF STUDY SITE

3.4.1 Selection Criteria

The main considerations in the selection of the study site were the availability of reliable data on bed sediments, hydrometry and bathymetry. In addition, the site had to be sufficiently large to allow discernable spatial differences in the composition of bed sediments. The selection had also to be consistent with the stated objective of investigating areas whose beds consist predominantly of fine sediments.

For practical reasons, the selection of the site was made with due regard to the limitations inherent in the presently available two-dimensional depth-averaged flow model and the turbulence model.

The flow model cannot be applied to areas with strong density stratification or small aspect ratios and such areas were consequently not considered. In such areas, the hydrostatic pressure distribution assumption, which is central to the derivation of the depth-averaged flow equations, is not satisfied.

Another limitation of the flow model is that, since the influence of sediment on the flow is not accounted for, the model is only valid for flows where the suspended sediment concentration by volume is less than about 10%. When the sediment concentration is within this limit, less than 3% of the total flow energy is required to keep the sediment in suspension, which justifies neglecting the influence of the suspended sediment on the flow field (Celik and Rodi 1991). The converse is, however, not the case and an accurate determination of suspended sediment transport needs a fully coupled formulation as was pointed out in section 1.1 of chapter 1 and in the Literature review.

With regard to the k-ε model, there is the inherent assumption that the eddy viscosity is isotropic. Its application is therefore limited to areas where this assumption is valid, such as thin shear flows and recirculating flows where normal and shear stresses are small compared to the inertial and pressure gradient terms (Rodi 1984).

3.4.2 Chosen Site

Preliminary enquiries on local lakes and rivers revealed that lake St. Louis (also referred to as Lac St. Louis) on the St. Lawrence river, in Canada, was a feasible site for the study. Previous studies carried out on this lake had indicated that it contains a large amount of fine sediment on its bed and has strongly two-dimensional flow with recirculating regions (Champoux and Sloterdjik 1989, Boivin et al 1982). Records on hydrometric data were available (Environment Canada 1986 a) and a sediment survey had been carried out (Rukavina 1986). The flow in the lake is a shallow one, with aspect ratios of the order of 2000. In addition, the discharge is regulated at a nearly constant value. The flow regulation is important for this study because it eliminates the need to consider in detail which discharge condition is best related to the bed material composition.

Although adequate field data that could be used for model calibration could not be found at the time of this study, the previous study by Boivin et al (1982) involved the construction of a physical model, the results of which were available and could be compared with the results of the numerical model.

In view of the above considerations, lake St. Louis was chosen for this study. A description of this lake together with a summary of the data relevant to this study are presented in the next chapter.

CHAPTER 4

SITE DATA ANALYSIS

4.1 GENERAL SITE DESCRIPTION

Lake St. Louis is located to the south-west of Montreal island, in the province of Quebec, Canada. It has a surface area of approximately 148 km^2, with a lengthwise span of about 16 km and a maximum breadth of about 10 km. The maximum water depth in the lake is about 20 m and the average depth is 4m. The location of the lake is shown in fig. 4.1.

Two major rivers discharge through Lake St. Louis. These are Ottawa river and St. Lawrence river. Of these, St. Lawrence river, with its source at the Great Lakes, is the dominant one, carrying nearly 90% of the total discharge through the lake. The total discharge is normally about 10,000 m^3/s or 864 million m^3/day. This large through-flow gives the lake an average detention time of only 4 hours.

The flow from Ottawa river enters Lake St. Louis via Lac Des Deux Montagnes (Lake of two mountains). These two lakes are connected by Vaudreuil and St. Anne channels. At low discharges, St. Anne channel tends to carry less flow than Vaudreuil, but these channels carry approximately the same quantity of water at moderate to high

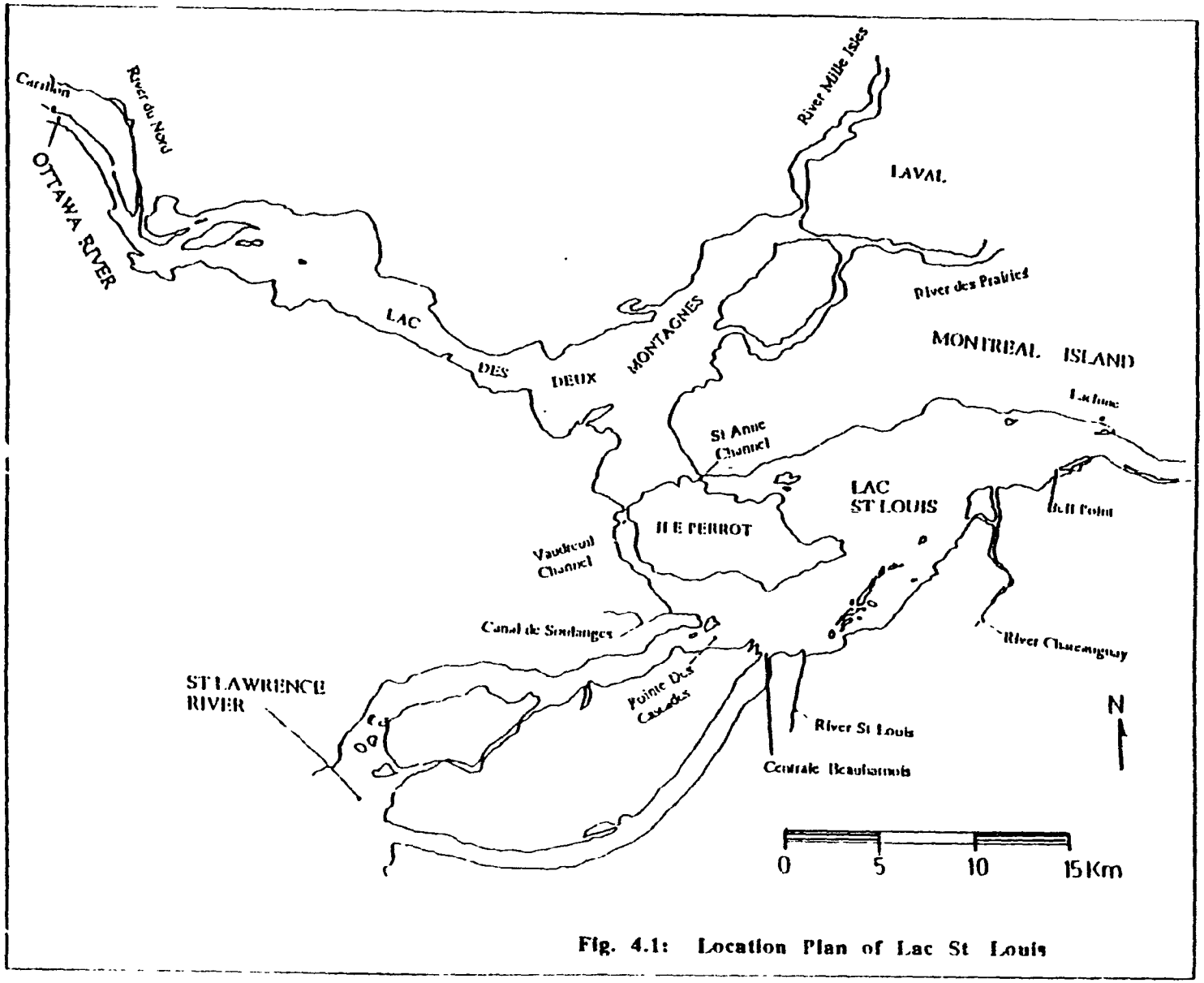

Fig. 4.1: Location Plan of Lac St Louis

discharges. Together, they divert slightly more than one half of the Ottawa river discharge into Lake St. Louis.

The flow from St. Lawrence river enters Lake St. Louis at two locations. These are Pointe Des Cascades and Centrale Beauharnois. At the latter location the discharge is over 80% of the St. Lawrence river flow, and contributes over 70% of the total inflow into Lake St. Louis. It is therefore the most significant inlet in terms of water discharge.

Apart from Ottawa and St. Lawrence river in-flows, there are some minor in-flows from rivers Chateauguay and St. Louis and canal de Soulanges, just beside Pointe Des Cascades. River Chateauguay, the largest of these minor inlets, has a maximum discharge of the order of 100 m^3/s and a minimum one of the order of 10 m^3/s.

The discharges from rivers Chateauguay and St. Louis have been neglected in this study because they are not only minimal but also irregular. But the discharge from canal de Soulanges, which is normally constant at 74 m^3/s, has been included as part of the discharge through Pointe Des Cascades in the flow simulations.

Due to its importance for generation of hydroelectric power and as a waterway between the Atlantic ocean and the Great lakes, the entire St. Lawrence river is regulated by several dams and locks. The Ottawa river is also regulated. This regulation makes the lake more suitable for this study, since the discharges do not have large fluctuations.

In the next section, the hydrometric data is presented and analyzed. This is followed by the presentation and analysis of the bed-surface sediment data in section 4.3. The water temperature data is discussed briefly in section 4.4. The chapter concludes with a discussion on bathymetry, space discretization and bed-roughness in section 4.5.

4.2 HYDROMETRIC DATA

Several hydrometric stations have been established around Lake St. Louis by Environment Canada. The flow records are published annually by the Inland Waters Directorate, Canada, in their publication "Surface Water Data: Quebec". Records for some of the stations are not listed in this publication, but are obtainable on request from the Quebec regional office of Environment Canada. The hydroelectric power Company, Hydro-Quebec, also maintains records of flow into Lake St. Louis.

The hydrometric data most relevant to this study are those for the periods just before a sediment survey, undertaken between 17th June and 28th July, 1985.

During winter, particularly from December until March, the lake is usually ice-covered. In this period, the movement of sediment is considerably reduced (Stichling 1974, Lau and Krishnappan 1984). Once the freeze-up period ends, the sediment size distribution on the bed is likely to respond to the increased spring discharge. It was

therefore decided to consider the flow between 1st April 1985 to 16th June 1985.

When the discharge in a water body fluctuates, it has been proposed that there is a 'dominant' discharge which the bed sediment characteristics are most likely to be related to. Middleton (1976) and Deigaard (1980) suggested that this should be the maximum annual discharge. However, in the case of Lake St. Louis, the total discharge had little variation during the period of interest because of the flow regulation. For example, the main inlet at Centrale Beauharnois discharged 7,168.5 m^3/s on the average, with a minimum of 6,640 m^3/s and a maximum of 7,640 m^3/s. The total discharge through the lake was 10,061.7 m^3/s on the average, had a minimum of 8,999 m^3/s and a maximum of 11,197 m^3/s. The standard deviation was 609 m^3/s, which was only 6% of the mean discharge. On the other hand, the flows through Vaudreuil and St. Anne channels had large variations. For example, the discharge through Vaudreuil had mean value of 663 m^3/s, but varied from a minimum of only 239 m^3/s to a maximum of 1410 m^3/s. The standard deviation was 339 m^3/s, which is over 50% of the mean discharge.

The discharges through Centrale Beauharnois, Pointe Des Cascades and Vaudreuil are gauged. The first two are gauged by Hydro-Quebec and the last one by Environment Canada. The data was made available for this study by these organizations (Hydro-Quebec; Personal Communication, Environment Canada; Personal Communication).

The discharge through St. Anne channel is not gauged, but can be deduced from the difference in water surface elevations between Lake St. Louis and Lac Des Deux Montagnes. Although charts are available for this purpose, they showed low sensitivity in the discharge range considered.

In this study, the discharge through St. Anne channel was computed by applying a control volume analysis to Lac Des Deux Montagnes (see fig. 4.1). This lake has two major in-flowing rivers; the Ottawa river and river du Nord. Out-flows from the lake are through rivers Mille Iles and de Prairies and Vaudreuil and St. Anne channels. The out-flow through de Prairies and Mille Iles and inflow from Ottawa and du Nord are gauged and the data was made available by Hydro-Quebec (Hydro-Quebec, Personal Communication).

The mass conservation equation for the control volume is

$$A_{dm}\frac{dh_{dm}}{dt} = (Q_{car} + Q_{dn}) - (Q_{dp} + Q_{mi}) - (Q_{sa} + Q_{va}) \qquad (4.1)$$

where A_{dm}, h_{dm} are respectively the surface area and water elevation of Lac Des Deux Montagnes. Q_{car} is the Ottawa river discharge measured at Carillon gauging station, Q_{dn} the inflow from river du Nord, Q_{dp}, Q_{mi}, Q_{sa} and Q_{va} the out-flows through river de Prairies, river Mille Iles, St. Anne channel and Vaudreuil channel respectively and t is time.

The water elevation in Lac Des Deux Montagnes is measured at a point near Vaudreuil. The data is published in the surface water data publication (Environment Canada 1986 a). Due to friction losses, this surface elevation cannot be taken to be representative of the average surface elevation of the entire control volume. However, the interest was not on its absolute value, but rather on its change with time, which should be approximately the same (in an average sense) in all parts of the lake. The water elevations at this station are plotted in fig 4.2 for the period 1st April to 30th June, 1985.

The area of the control volume was estimated at 160 km^2 from the hydrometric station map published by Environment Canada (Environment Canada 1986 b). The derivatives of surface elevation with respect to time were computed using forward differences of average daily elevations.

The discharges into Lake St. Louis during the period 1st April to 30th June, 1985 are plotted in figure 4.3. The discharges shown for (Pointe Des) Cascades in figure 4.3 do not include the constant value of 74 m^3/s for canal de Soulange.

The water surface elevations used for the downstream boundary condition in the flow model (see chapter 3) were those prevailing at Lachine. These were obtained from the surface water data

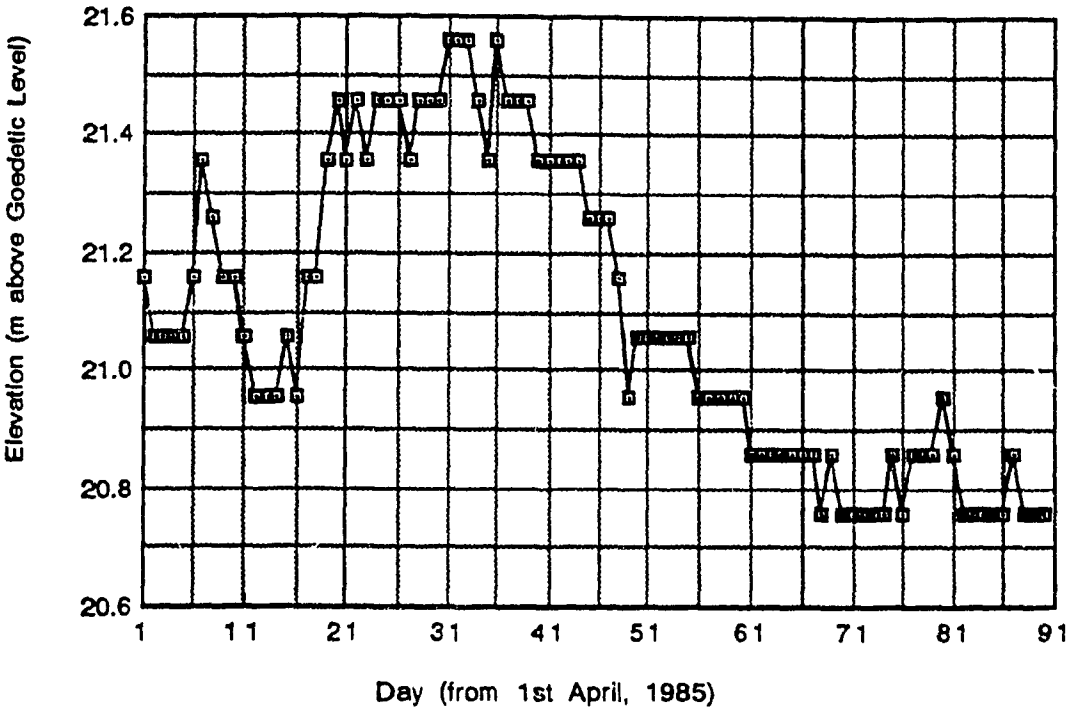

Fig 4.2: Water levels on Lac Des Deux Montagnes

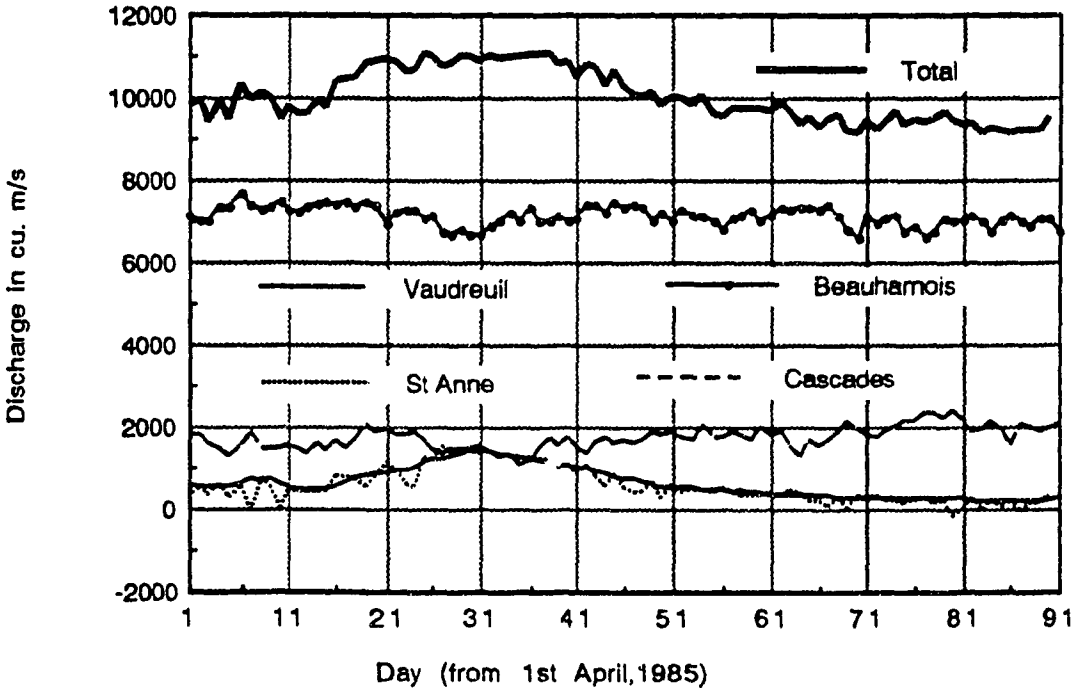

Fig 4.3: Discharges into Lac St. Louis

publication (Environment Canada 1986 a). They are plotted in figure 4.4. (In this work, surface water elevations have been referred to the reference level used by Canada's Geodesic Services. This reference level is hereafter referred to as Canadian Geodetic Reference Level or simply as Geodetic level.)

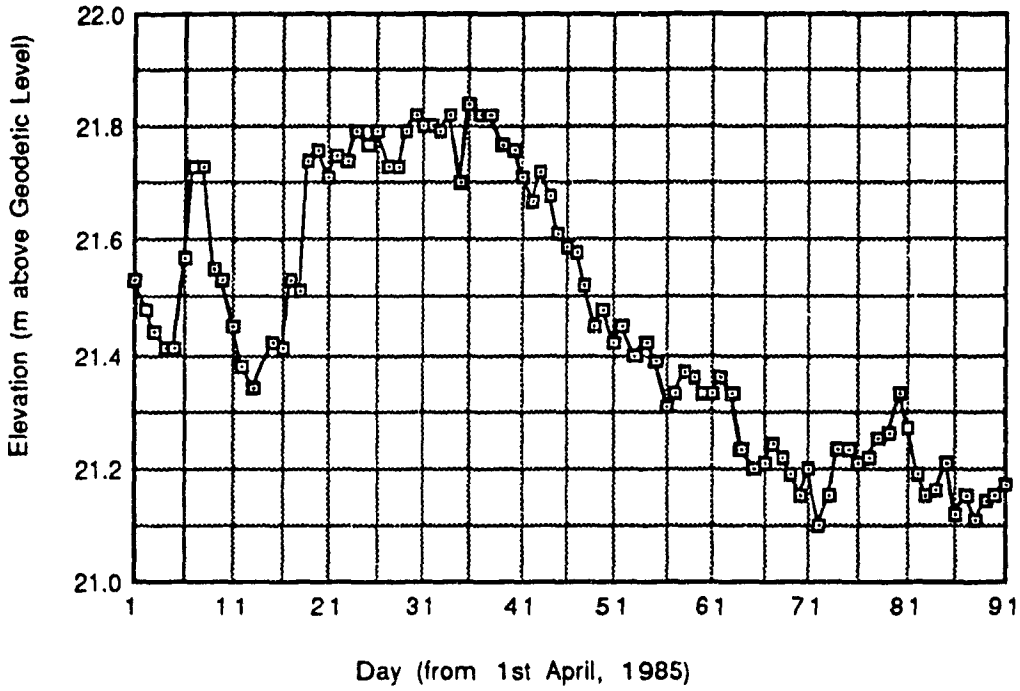

Fig 4.4: Water levels at Lachine

Two discharge conditions were considered. These were the overall Lake St. Louis average (DC1) and the Ottawa river maximum discharge conditions (DC2). The Lake St. Louis average discharge condition (DC1) was obtained by time averaging each in-flow between the period 1st April to 16th June, 1985. The maximum Ottawa river discharge occurred on 1st May. It also corresponds with the maximum total discharge into Lake St. Louis. The maximum St.

Lawrence river discharge does not occur at the same time as that of Ottawa river, and could be have been considered as a third discharge condition. It is, however, of less significance, because the fluctuations are small compared to the mean value. The maximum Ottawa river discharge is significant in two respects. Firstly, it induces stronger currents in some parts of Lake St. Louis than those prevailing under the overall average discharge condition. Secondly, it is considered to carry a fairly large amount of sediments. This latter observation is evident from the fact that the Ottawa river water is usually more turbid as compared to the St. Lawrence river water. The two waters do not mix well and appear to take separate routes through Lake St. Louis (Boivin et al 1982).

The flow data for the two discharge conditions, DC1 and DC2 that were simulated are shown on table 4.1. In this table, the discharge at Pointe Des Cascades includes 74 m^3/s from canal de Soulanges. The Lachine water elevation corresponding to the two discharge conditions are 21.59 and 21.88 metres (above the Canadian Geodetic reference level) for discharge conditions DC1 and DC2 respectively. The downstream orientation of the in-flows are given as bearings in table 4.1. The outflow is in an easterly direction

Table 4.1 Modeled Discharge Conditions

	Beauharnois	Cascades	Vaudreuil	St. Anne
DC1(m^3/s)	7147	1659	663	587
DC2(m^3/s)	6640	1613	1410	1337
BEARING	34°	110°	125°	90°

4.3 SEDIMENT DATA

4.3.1 Sediment Survey

As part of a pollution study of Lake St. Louis undertaken by Environment Canada (Champoux et al 1989), a well coordinated bottom sediment survey was carried out. The survey was carried out by a team from Canada's Inland Waters Research Institute, between 17th June, and 28th July, 1985 (Rukavina 1986).

The sediment survey involved the collection of bed-surface sediment samples on a spatial grid of 1 km. The samples were collected using a Double-Shipeck sampler. Accurate determination of the sampling locations was achieved by using an electronic positioning system. The sampling locations are shown in fig 4.5.

A total of 139 samples were collected. The difference between this number and the number of stations is due to the fact that some stations had beds made of rock or organic material. These were

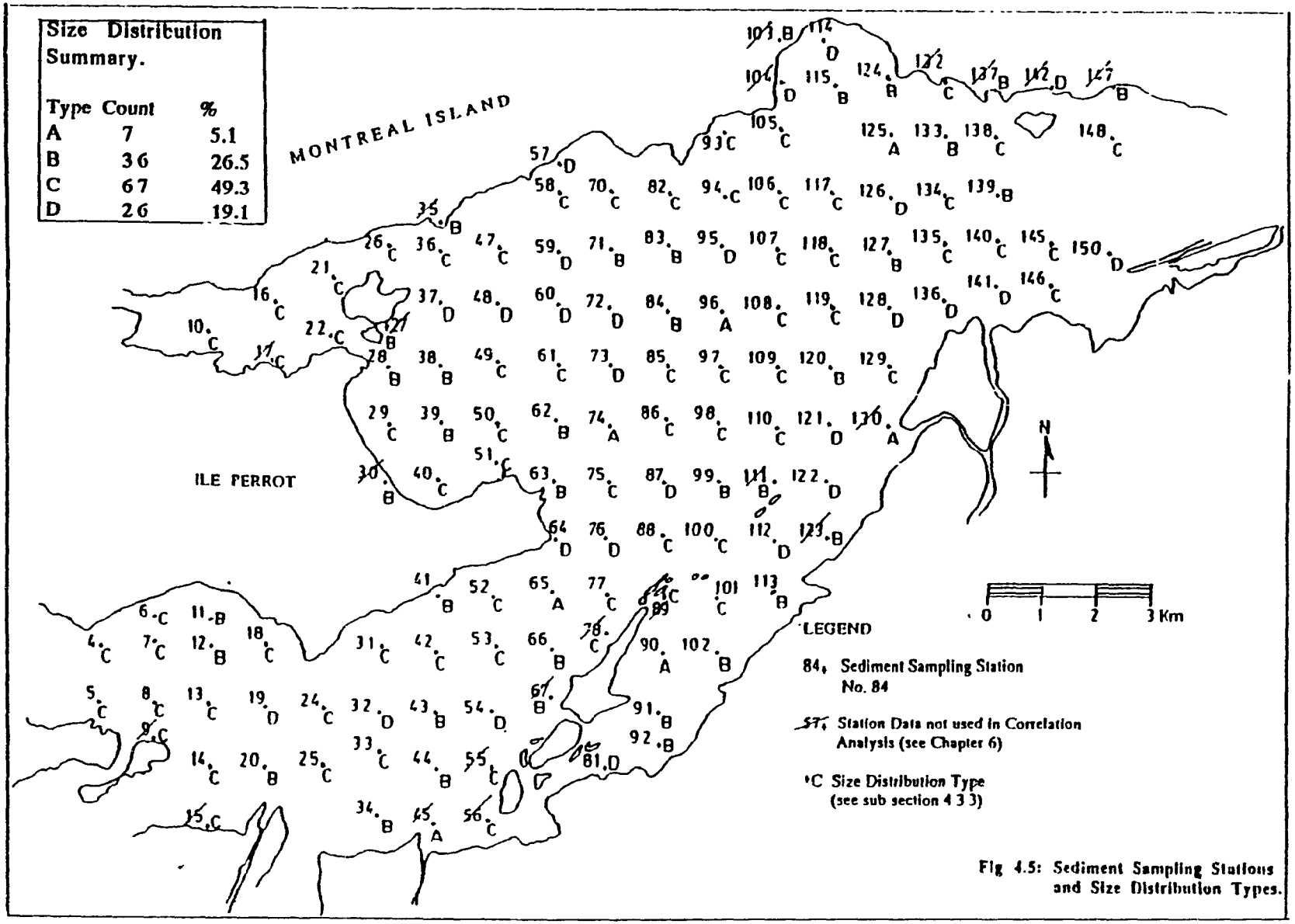

Fig 4.5: Sediment Sampling Stations and Size Distribution Types.

either not sampled or not considered in the subsequent sediment size analysis. Stations 1 to 3 inclusive were located further upstream on Vaudreuil Channel and are not shown in fig. 4.5.

From each sample, a sub-sample comprising the top 3 cm was taken using a 5 cm by 5 cm box sampler. The sub-sample was used for granulometric analysis, in which a combined sieve, sedigraph and settling tube procedure was used. The analysis was carried out in the range of -3.5 to 9 phi units, at intervals of half phi (phi = $-\log_2 d$, where d is the particle size in mm). The sediment size data is tabulated in appendix A.

The median particle size (d_{50}) varied from 0.1 microns to 2.5 mm with an average of 0.213 mm and standard deviation of 0.321 mm. The spatial distribution of the median particle sizes is shown in fig. 4.6. The percentage content of clay sized material (less than 4 microns in size) varied from 0% to 74.6%. The percentage of fine sediments, taken to include silt and clay (less than 0.0625 mm in size), varied from 0 to 100%.

Due to the high percentage of clay sized material present in many samples, the samples size distribution was occasionally not sufficiently resolved to allow direct interpolation of d_{50} from the data. In such cases, the median size was obtained by extrapolation on log-probability plots. This extrapolation was also used in many instances for the determination of the 16^{th} percentile size.

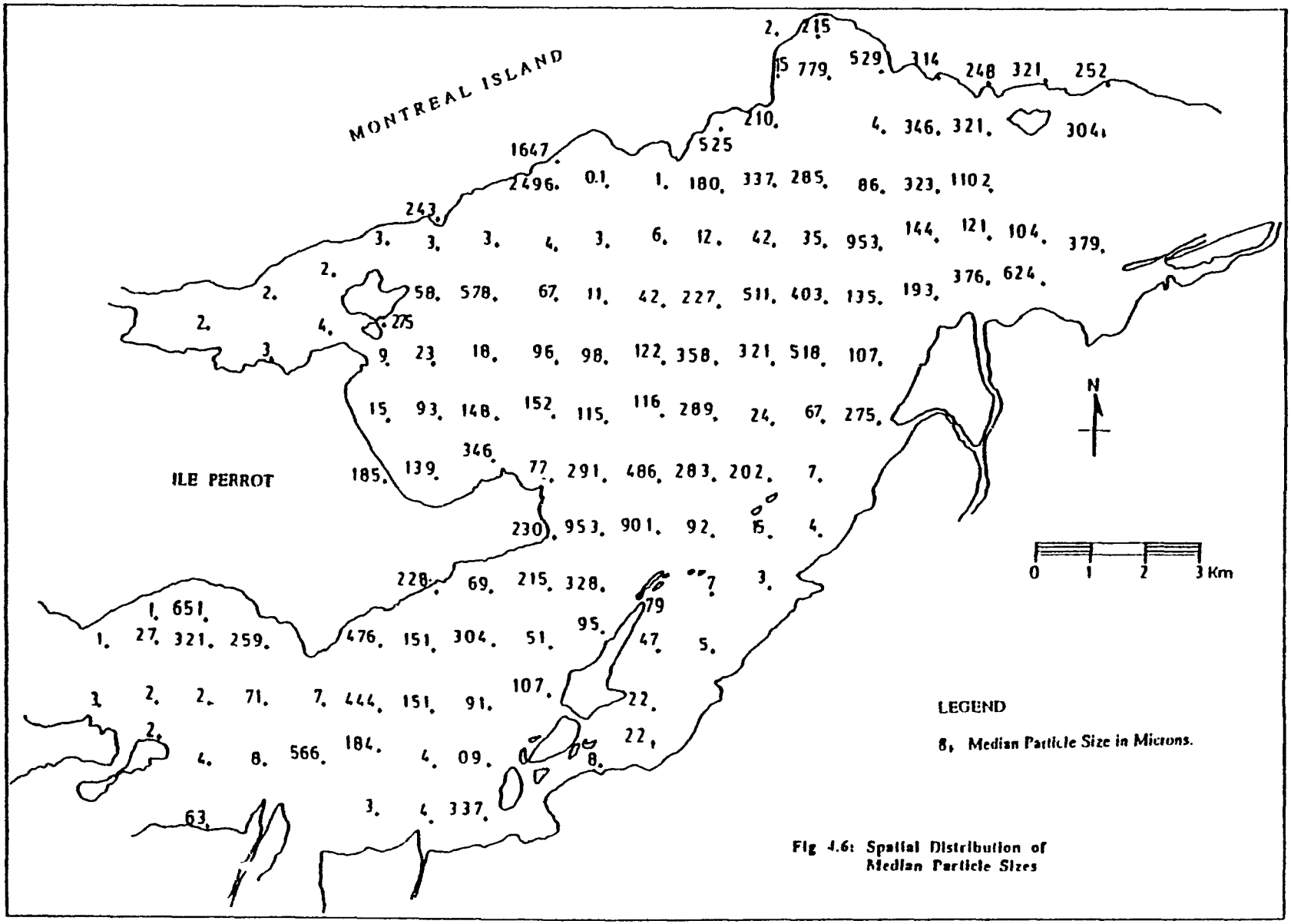

Fig 4.6: Spatial Distribution of Median Particle Sizes

4.3.2 Characteristic Particle size

In this study, the particle size that is representative of the sediment sample has been taken as the median size (d_{50}). In the past, there has been considerable controversy on the choice of the particle size that characterizes the sediment sample (see, for example, discussion by Stelzcer 1984). However, the present trend in sediment transport research is to use d_{50}. This trend is reflected in modern sediment transport formulae of van Rijn (1984 a and b) , Parker (1990) and Yang (1984) amongst many others, and in the theoretical studies of Lyn (1986).

4.3.3 Break Size Analysis

A limited investigation was carried out to determine whether the bed-surface sediment samples could be resolved into distinct sub-populations as discussed in chapter two. The cumulative percentage coarser than each sieve size was transformed to its equivalent on the normal probability scale and plotted against the size on the phi scale (log-probability plot).

It was observed from the log-probability plots that the sub-populations were generally present. However, some of the sub-populations appeared to be more attributable to the sediment sources rather than hydraulic sorting. This could be due to the relatively short distances that the sediments from the various inlets had travelled within the lake. In most samples, a clearly distinct

suspension sub-population with a break around 4 phi was present. It was mainly the coarser particles that tended to show sub-populations that could not be attributed to hydraulic sorting.

The results of the break analysis are summarized in figures 4.5 and 4.7. Samples were classified into four categories. In category A were the samples whose entire size distributions were approximately log normal. Category B contained samples which showed two distinct sub-populations with a break point. In ..egory C were the samples that showed three sub-population with two break points. Samples which showed disjointed or more than three sub-populations were classified into category D. The category of each sample is shown against the sampling stations in fig. 4.5. The typical size distribution for each of the categories is given in figures 4.7a to d

4.3.4 Analysis of the Standard Deviation

A complete description of the sediment particle size distribution requires the standard deviation, the skewness and kurtosis in addition to the median size. The significance of skewness and kurtosis in sediment transport has not been fully understood, although they are important from the geologists point of view (Garde 1972). On the other hand, the standard deviation, which is a measure of the spread of particle sizes, is important, particularly in hydraulic sorting studies, since it influences the development of the armour layer (Little and Mayer 1976) and the size of bed forms (Simons and Richardson 1961).

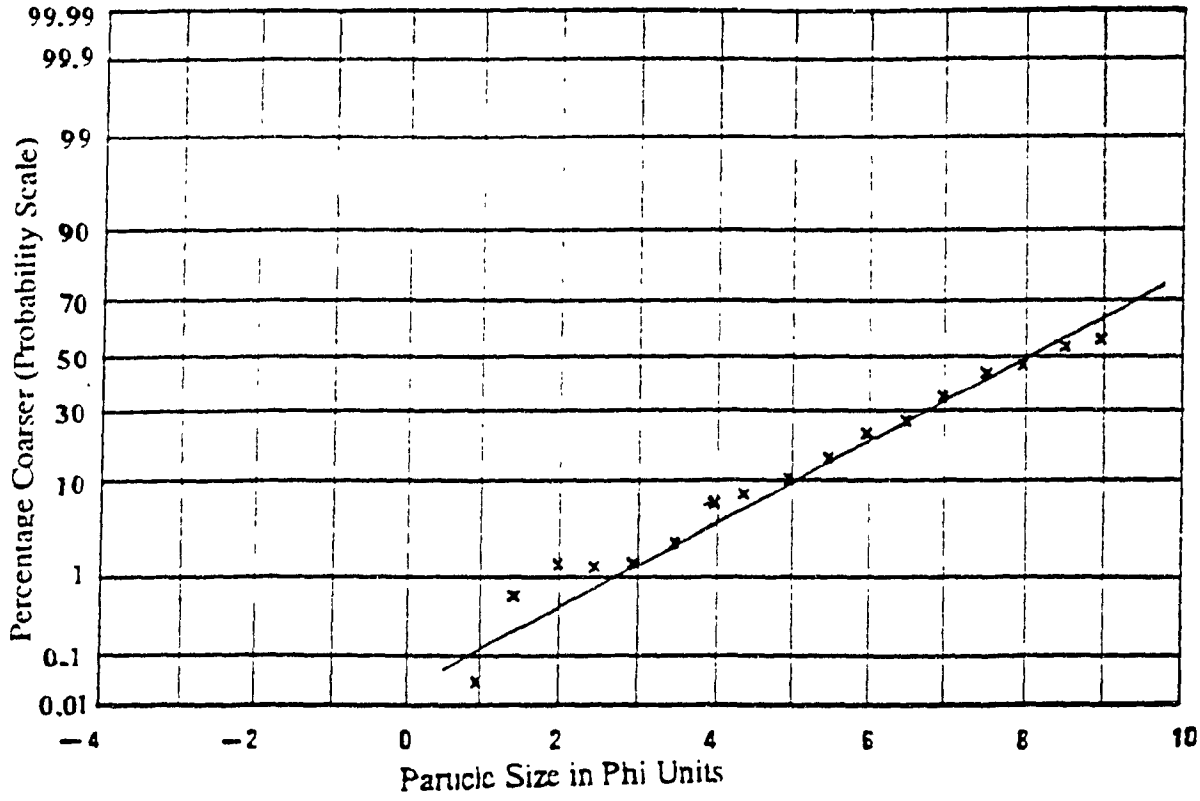

Fig. 4.7a: Typical Size Distribution Type A, from Station No. 45

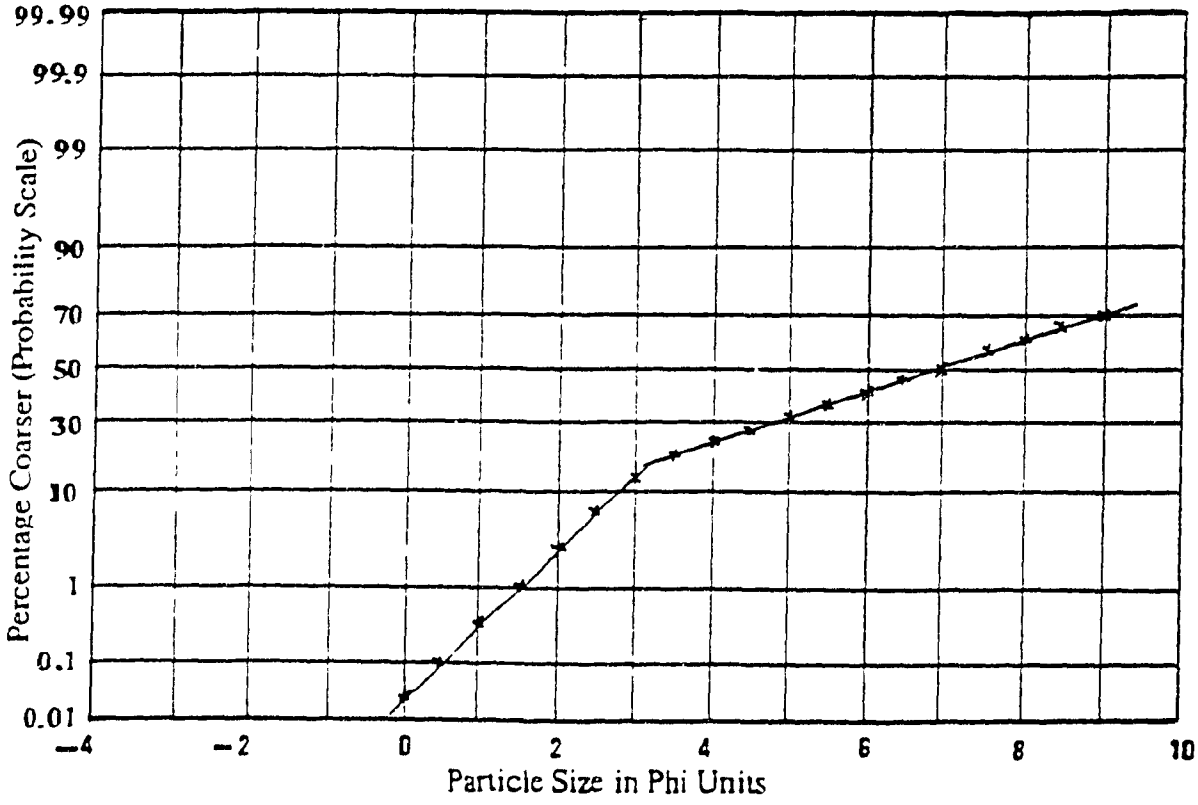

Fig. 4.7b: Typical Size Distribution Type B, from Station No. 20

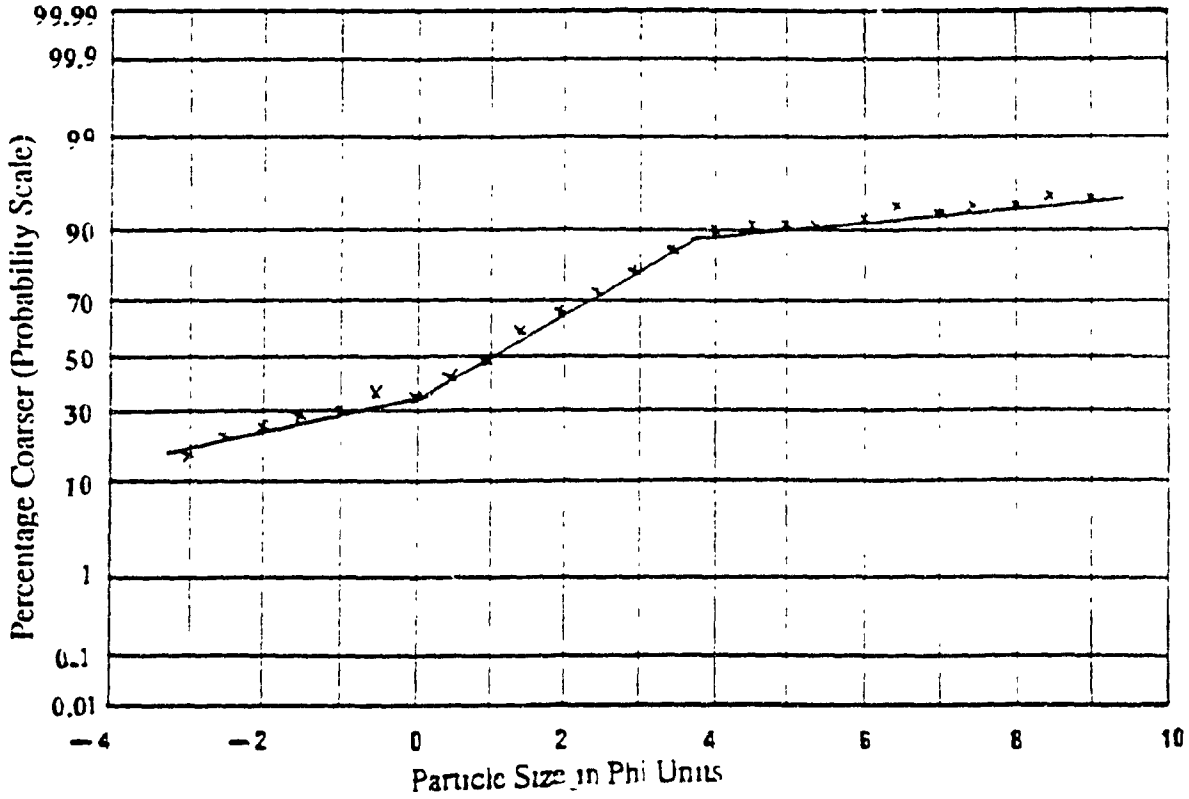

Fig. 4.7c: Typical Size Distribution Type C, from Station No. 31

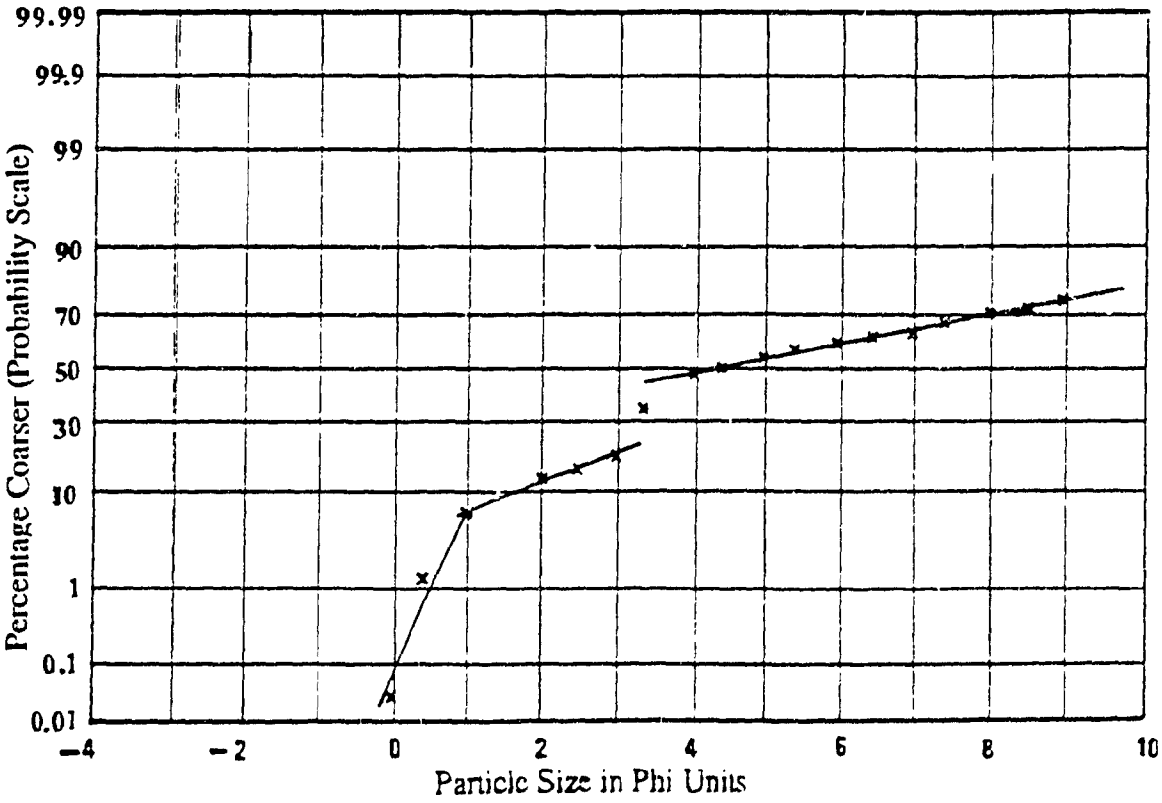

Fig. 4.7d: Typical Size Distribution Type D, from Station no. 37

If the particle size distribution is log-normal, then it is completely specified by it median size and geometric standard deviation. In sediment sorting analysis, log-normality of particle size distribution is often taken as an approximation (Rana et al 1973, Thomas and Prasuhn 1977, Deigaard 1980). In this study, this approximation was examined by plotting the ratio d_{84}/d_{50} against d_{50}/d_{16}. The plot is shown in fig 4.8. When the particle size distribution is log-normal, these two ratios should be equal. It can be seen from fig. 4.8 that many points plot on or near the line of perfect agreement. However, there is considerable scatter, with a tendency for d_{50}/d_{16} to be larger than d_{84}/d_{50}. In terms of size sorting, this implies that the bed load sub-population is usually better sorted (smaller size spread) than the suspension sub-population.

The variation of the standard deviation with the median size was also examined. Use was made of equation 2.8b to estimate the geometric standard deviation, which was then plotted against the median size. The plot is shown in fig 4.9. The amount of scatter in this figure is considerable. Therefore, no quantitative interpretations of the relationship were attempted. However, the following qualitative observations were made: Firstly, there is considerable cluster in the median diameter range of 0.2-0.3 mm. More significantly, these show the lowest standard deviation, which is consistent with the analysis of Inman (1949). The value of the standard deviation is about 1.4, which is equal to that given by the analysis of Garde (1972) for particles smaller than 0.2 mm. Secondly,

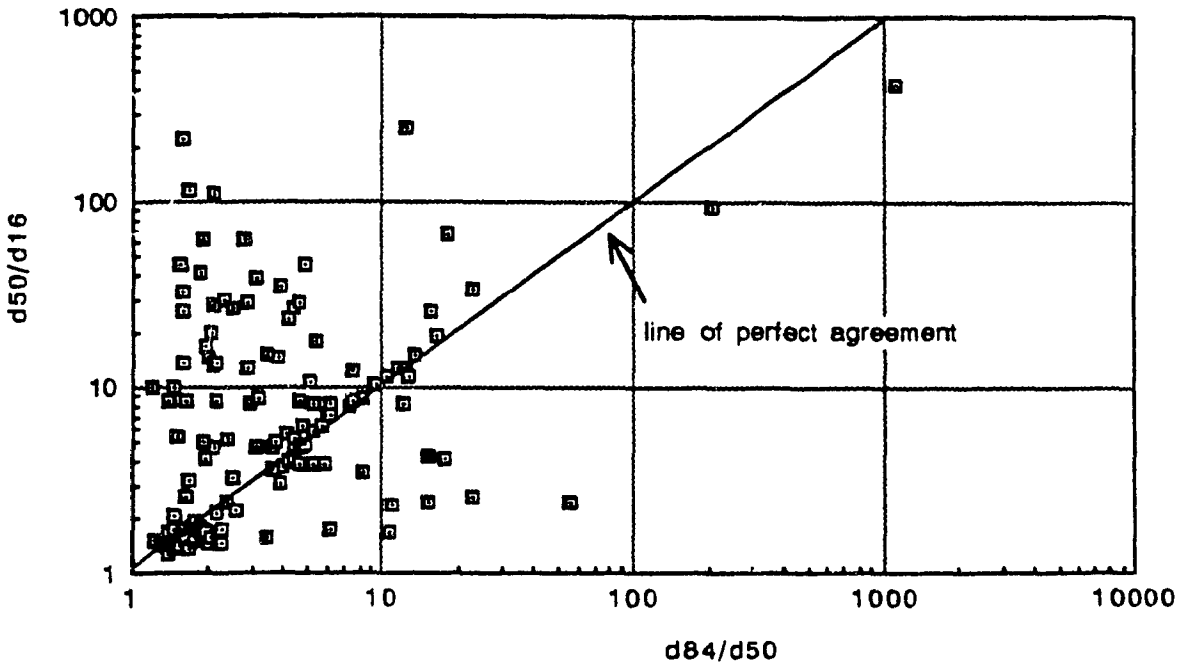

Fig 4.8: Plot of (d50/d16) vs (d84/d50)

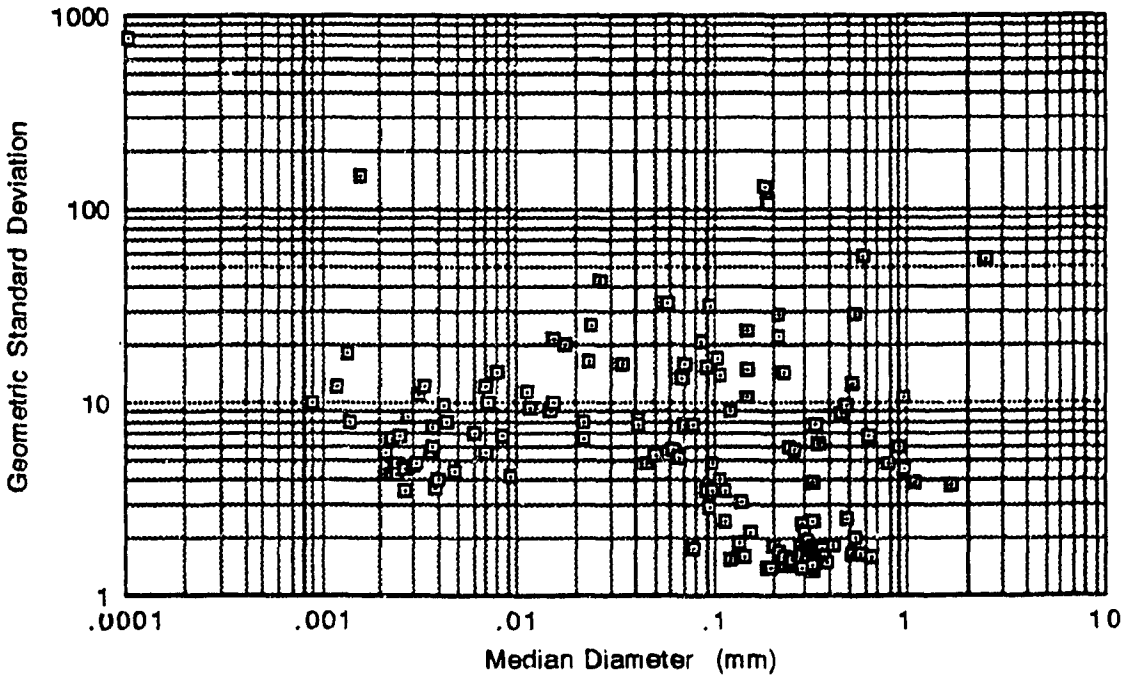

Fig 4.9: Plot of Geometric Standard Deviation vs Median Diameter.

by comparing figures 4.8 and 4.9 it is seen that the sediment samples with diameters in this range also have an approximate log-normal distribution (they plot as a bunch of points in both figures). Thirdly, the sediment samples with median diameter in the range 0.002 mm to 0.004 mm show a cluster similar to that shown by those in the size range 0.2-0.3 mm, but have a higher standard deviation of approximately 5. They also have log-normally distributed particle sizes as can be seen from fig 4.8.

Perhaps a clearer illustration of the last two points above can be seen in fig 4.10, where the ratio $(d_{84}/d_{50})/(d_{50}/d_{16})$ has been plotted against the median grain size. This ratio should be unity for sediment samples that have log-normal particle size distribution in the range of 16th to 84th percentile size. Fig 4.10 shows that this ratio decreases from unity to about 0.1 in the size range 0.04 to 0.1 mm and then increase rapidly to unity between the size range 0.1 to 0.2 mm. Beyond 0.3 mm, it exceeds unity. Therefore, in the median size range 0.04 to 0.2 mm, the suspension sub-population is always better sorted than the traction sub-population whereas the converse is almost the case for median sizes greater than 0.3 mm.

It can be seen from fig 4.10 that the accuracy of the log-normal distribution assumption depends on the median size of the sediment sample under consideration. Since many river deposits have median sizes in the range 0.02-0.03 mm (medium sand), it appears from the above, and from the work of Garde (1972), that the assumption of a log-normal particle size distribution with a standard deviation of 1.4

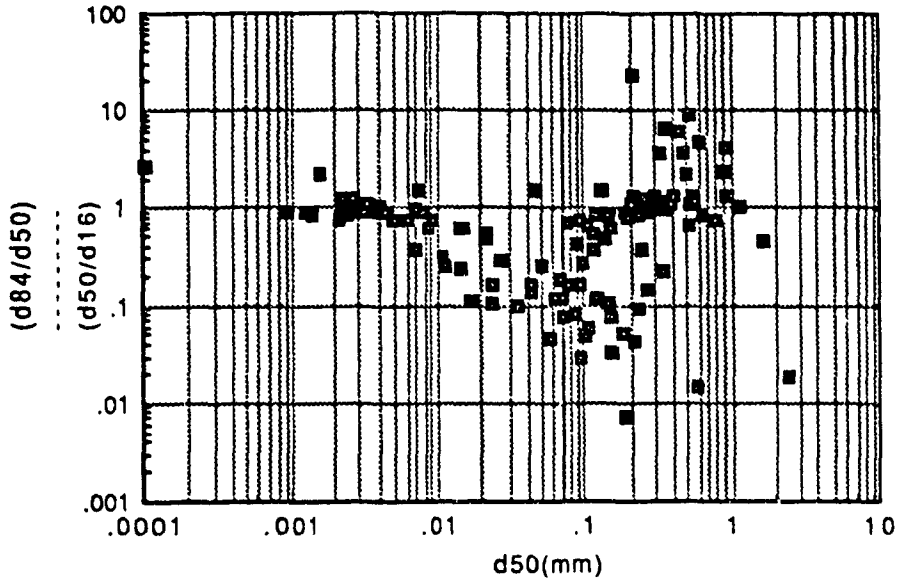

Fig 4.10: Plot to show log-normality in the range of 16th to 84th percentiles

is reasonable for many river deposits. However, it is also apparent that the standard deviation does not remain constant at 1.4 below the size 0.2 mm but decreases as already noted. There is need for further data from different sources to confirm the observed constancy of the standard deviation in the size range 0.002 to 0.004 mm.

4.4 WATER TEMPERATURE

In conjunction with the sediment survey, water temperatures at 0.1 metre below the water surface and 1 metre above the river bed were measured at each sediment sampling location. The results, which have been taken from the report by Champoux and Sloterdjik (1988), are given in Appendix B. The temperature data shows that there was no significant thermal stratification in the lake.

These temperature data cannot, however, be taken as representative of the spatial temperature distribution in the lake, since they were taken on different days and different hours of the day. As such they could not be used for numerical model calibration purposes.

4.5 BATHYMETRY, SPACE DISCRETIZATION AND BED ROUGHNESS

4.5.1 Bathymetry

The bathymetry data for Lake St. Louis was made available for this study by Hydro-Quebec (Hydro-Quebec, Personal Communication). The data compared well with a recent hydrographic survey of Lake St. Louis carried out by Fisheries and Ocean Canada (Kielland 1985). This survey was carried out at the same time as the sediment survey discussed in section 4.3.

The bathymetry is shown in fig 4.11. The bed elevations are shown in metres and have been referred to the Canadian Geodetic level.
The lake is characterized by a gently sloping bed and a deep channel, about 1 km wide. The channel is oriented in a north-easterly direction and extends from Centrale Beauharnois to Pointe Bell. Part of this channel is used as a maritime waterway (the St. Lawrence Seaway). On both sides of the channel, the water depth is shallow and has a near constant value of about 4 meters (for water surface elevation of 22 m). In these shallow areas, there are several small islands.

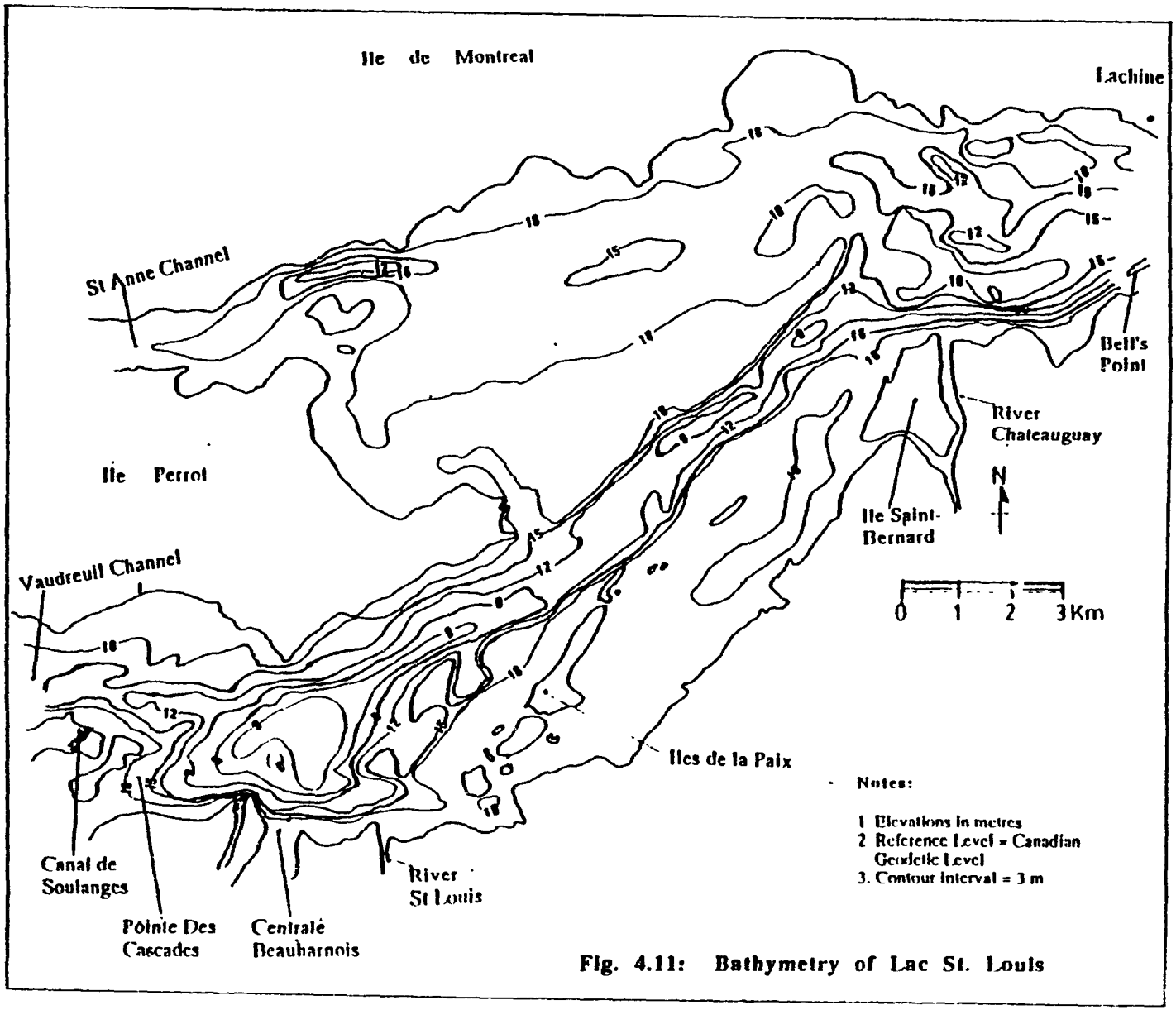

Fig. 4.11: Bathymetry of Lac St. Louis

An area just in front of Centrale Beauharnois is deeply scoured with a water depth of about 20 metres. This scour is probably due to the very high water velocities in this region.

4.5.2 Space Discretization

The lake was discretized using a uniform mesh with grid sizes $\Delta x = \Delta y = 228.6$ metres (750 feet). The x-coordinate direction had an easterly orientation. This grid system had previously been used for other studies by Hydro-Quebec (Carballada and Nguyen 1982), but the numerical scheme they employed was different from the one used in this study.

The grid system resulted in an overall number of 91 grids in the x-direction and 67 grids in the y-direction. These include the fictitious grids required for the specification of boundary conditions and calculation of space derivatives at boundary points lying on the extremities of the computation domain. The discretization gave a total of 2,635 wet grid points out of which 403 were boundary points. The number of dry grid points was 3,462. Even though this number is large, it posed no major problem because the HCG code economizes on the simulation time by considering only the wet grid points.

4.5.3 Bed Roughness

In previous studies of Lake St. Louis, the value of the Manning's coefficient has been found to lie between 0.025 and 0.035 with an average value of 0.03 (Boivin et al 1982). The average value of 0.03 was used in this work.

CHAPTER 5

HYDRAULIC COMPUTATION TESTS AND RESULTS

5.1 GENERAL

In order to assess the suitability of the numerical model described in chapter 3 for modelling the flow in Lake St. Louis, some tests were conducted. The first test involved checking the convergence behaviour of the numerical model. Secondly, the numerical model results were compared with those of a physical model. Finally, results from the k-ε model were compared with those expected for wall shear flows. These tests and their results are discussed in section 5.2

Final model results for discharge conditions DC1 and DC2 are presented in section 5.3

5.2 MODEL TESTS

5.2.1 Convergence Tests

Convergence of iterations were tested using the new sub-routine described in sub-section 3.3.3 of chapter 3.

In general it was found that the MacCormack scheme was stable for time steps up to 30 seconds for the space discretization discussed in

Chapter 4 and discharge condition DC2. However the overall mass conservation was better for time steps giving Courant numbers near unity as had already been pointed out by Baldwin et al (1975). A time step of 20 seconds was found to give good mass conservation. Smaller time steps led to mass loss (outflow < inflow) while larger ones resulted in mass gains.

The k-ε model posed major stability problems. The upwind scheme that was used for discretizing the governing equations converges in general for Courant numbers less than unity. However, this general rule, though necessary, is not sufficient to ensure the convergence of the k-ε model. An additional constraint is that neither k nor ε should become negative during simulation. One reported remedy for the instability in the k-ε model is the clipping technique, whereby the signs of k and ε are checked and simply reversed should they become negative (Simonin et al 1989). Another reported remedy is the use of $\sqrt{k}$ and $\sqrt{\varepsilon}$ as the basic variables in the transport equations (Finnie and Jeppson 1991).

In this work, it was found that instability could be avoided if small enough time steps were used. For the space-discretization used and flow condition DC2, simulations with a time step of 2 seconds or less were stable. In order to use this time step, it was necessary to carry out ten iterations in the k-ε sub-routine for each iteration of the flow model.

The results of the overall mass conservation test are shown in figure 5.1, where the percentage mass difference (inflow - outflow) is plotted against the simulated time. In order to present mass losses on a log scale, a constant of 10 has been added to all the results to avoid negative figures. It is seen from this figure that the mass difference attained a perfect steady state simulated time t= 30,000 seconds or 1,500 iterations of the flow model. The final mass difference was only -0.4% (gain) which was considered satisfactory. This difference remained unchanged for the remainder of the test period which covered a simulated time of 200,000 seconds or 10,000 iterations of the flow model.

In the maximum difference test, the number of flow model iterations considered before performing a test was 51. The test results are shown in figures 5.2 to 5. 6 inclusive for h, u, v, k and ε. It can be seen that the differences, which should be zero in the ideal steady state case, drop off quite rapidly at the beginning of the simulations, but the rates of decrease slow down as the number of iterations increase. Convergence to a near-steady difference was achieved at simulation times of t= 50,000 seconds for h, t = 80,000 seconds for u and v and t = 60,000 seconds for k and ε. The maximum differences were of the order 10^{-5} m for h, 10^{-5} m/s for u and v, 10^{-7} m^2/s^2 for k and 10^{-8} m^2/s^3 for ε. Unlike the perfect steady state shown by the mass conservation test, there were always some oscillations in the maximum differences. However, the final differences were quite small, thereby showing good overall convergence.

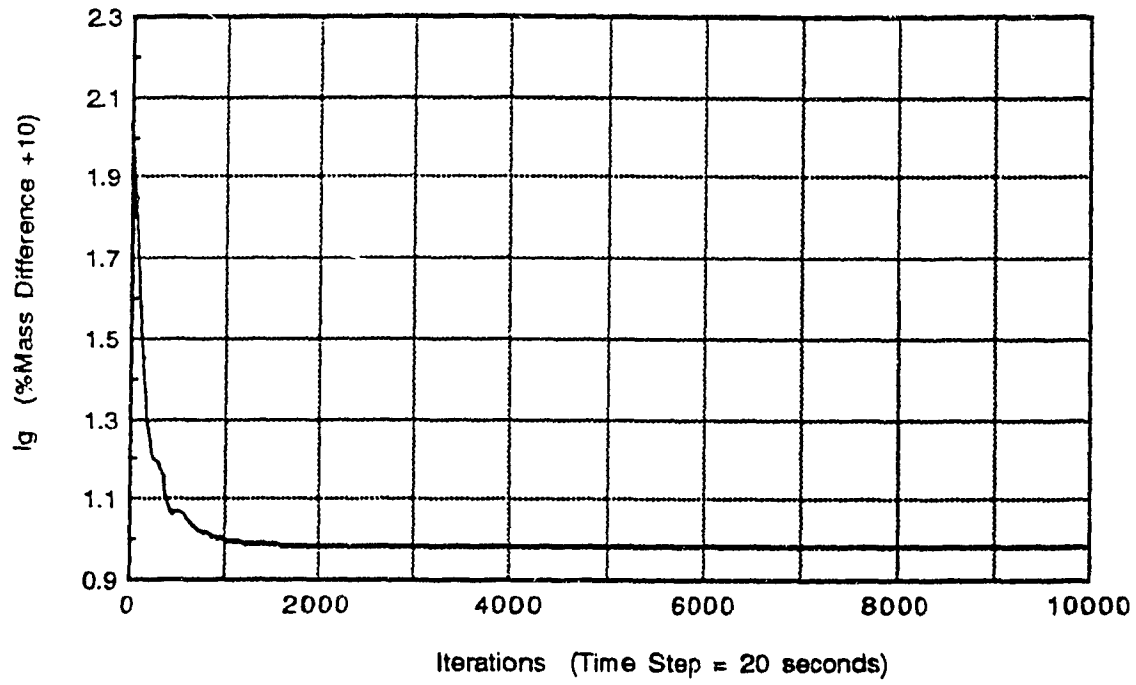

Fig 5.1: Results of Mass Conservation Test

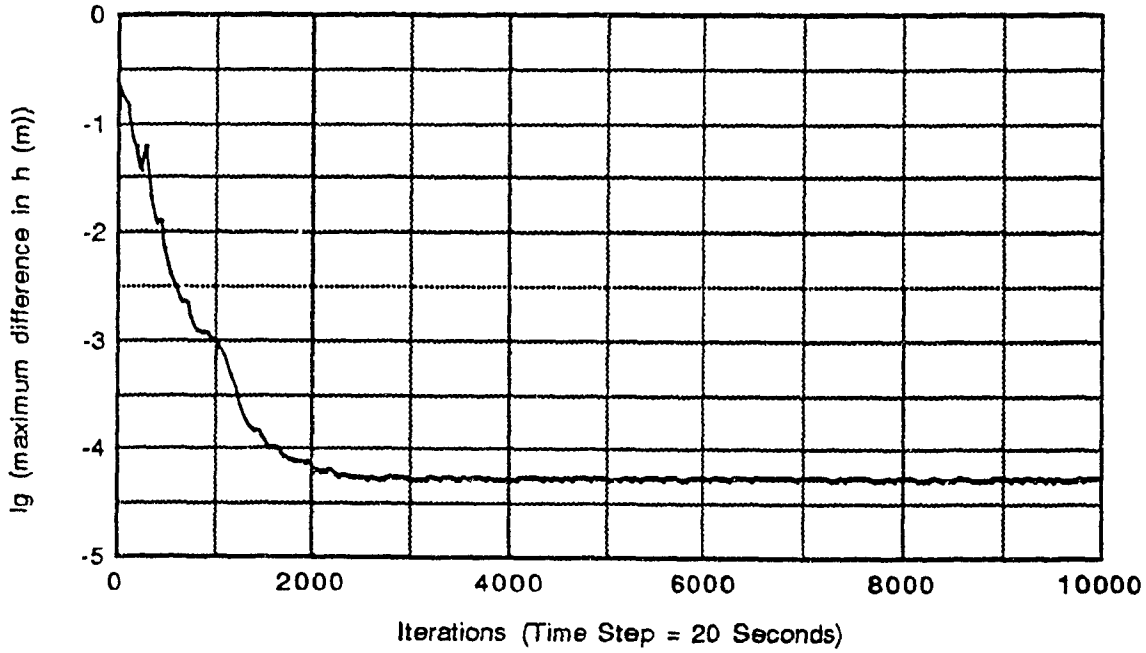

Fig 5.2: Results of Maximum Difference Test on Depths

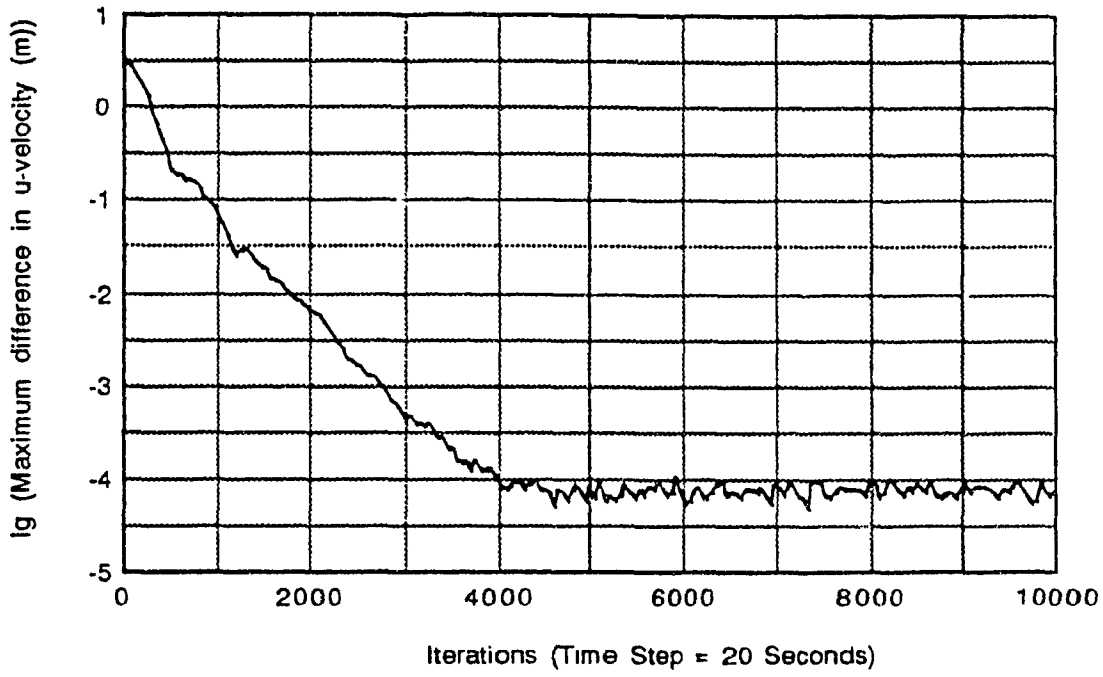

Fig 5.3: Results of Maximum Difference Test on u-velocity component.

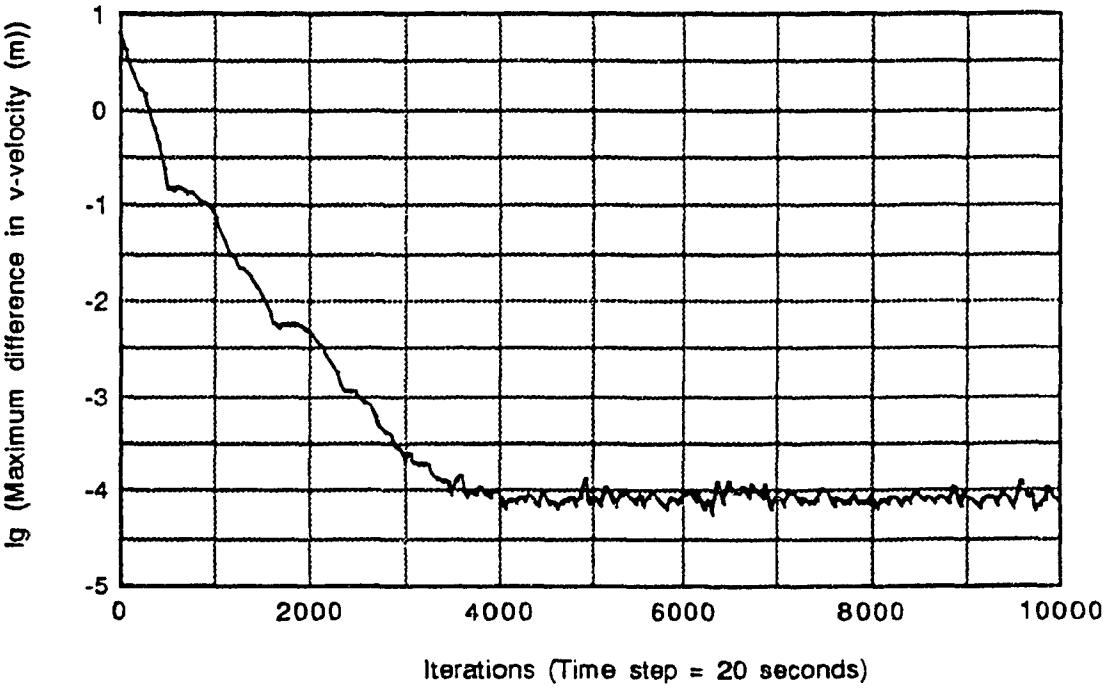

Fig 5.4: Results of Maximum Difference Test on v-velocity component

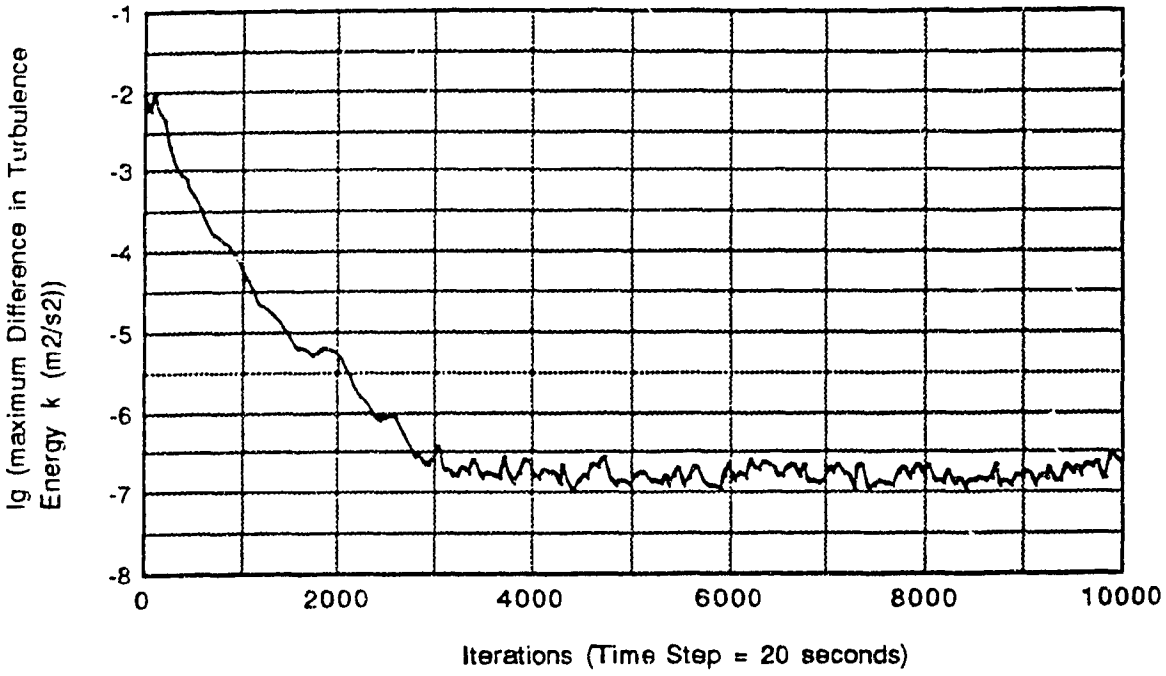

Fig 5.5: Results of Maximum Difference Test on Turbulence Energy.

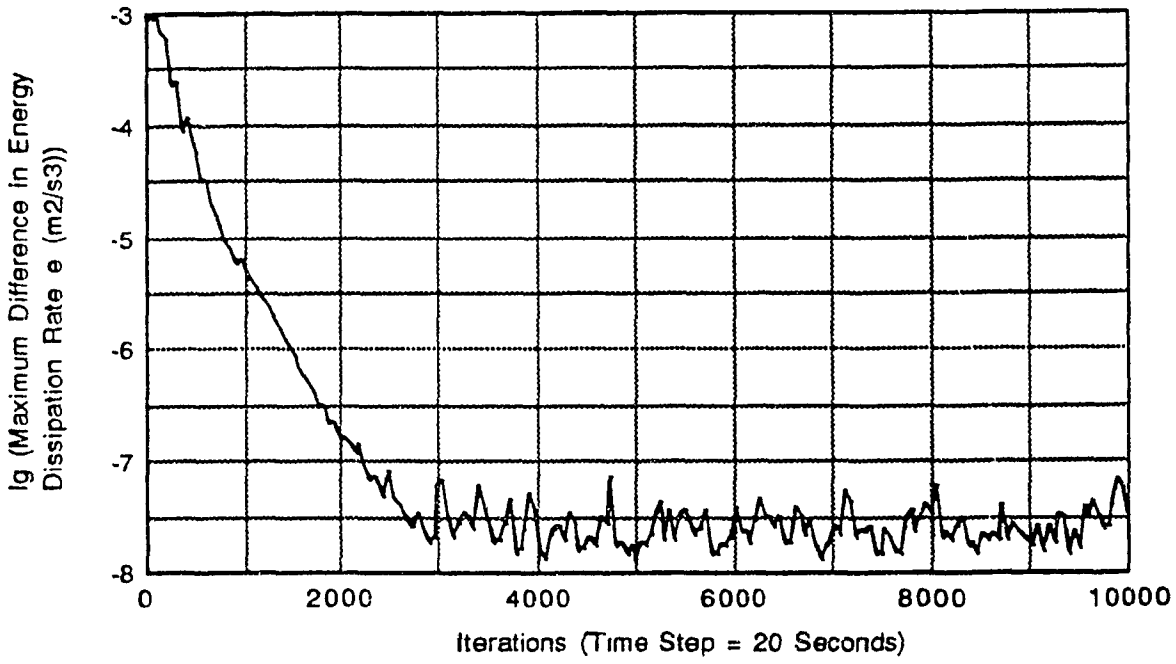

Fig 5.6: Results of Maximum Difference Test on Turbulence Energy Dissipation Rate.

From the convergence tests, it can be concluded that, for this model, the mass conservation test is a less rigorous test for convergence as compared to the method of maximum differences. Mass conservation test is nevertheless an essential part of the simulation since it can be used to select the appropriate time step.

5.2.2 Comparison of Numerical and Physical Models

Where possible, it is always desirable to compare the results of a numerical model with actual field data. This comparison should ideally be carried out in two stages. In the first stage, known as the calibration stage, the field data is used to adjust the empirical coefficients embodied in the numerical model until a satisfactory agreement is reached between observed and computed values of each modelled variable. These coefficients are typically the Manning's n coefficient and the empirical constants used for computing the eddy viscosity coefficient. In the second stage, known as validation, the calibrated model is used to predict the modelled variables for a different flow condition without altering the empirical coefficients obtained during the calibration process (Abraham et al 1981). Of course, this is not valid if the coefficients are known to vary with the flow. In such a case the known variation should be used to explain observed differences. In practice, the ideal calibration/verification procedure is usually implemented only for very large projects where there are sufficient resources for the often expensive field data collection.

Data that could be used for calibration/verification could not be found for Lake St Louis. However, in a previous study for this lake, the flow was modelled using a physical model (Boivin et al 1982). The physical model had been verified against a limited amount of field measurements.

The physical model was constructed at the Lasalle Hydraulics Laboratory, in Montreal, Canada. It had a horizontal scale of 1:550 and a vertical scale of 1:150. The prototype average value of Manning's n of 0.03 (see chapter 4) was used to size the model bed roughness elements. Further details on the physical model can be found in Boivin et al (1982).

The set of discharges that were modelled is shown in Fig 5.7. This discharge condition is herein referred to as DC3. The downstream water surface elevation at Pointe Bell was set at 21.2 m above Canadian Geodetic level.

In the physical model, surface velocities were measured by recording the movement of floats using a video camera. The prototype surface velocities predicted by the model are shown in fig. 5.7. Fig. 5.8 shows the velocity vector plot from the numerical for discharge condition DC3, while fig. 5.9 shows the predicted surface water elevations. The plots in figures 5.7 and 5.8 can be seen to be in reasonable qualitative agreement in the prediction of the flow pattern. It can for instance be seen that both models predict two recirculation zones in front of Centrale Beauharnois.

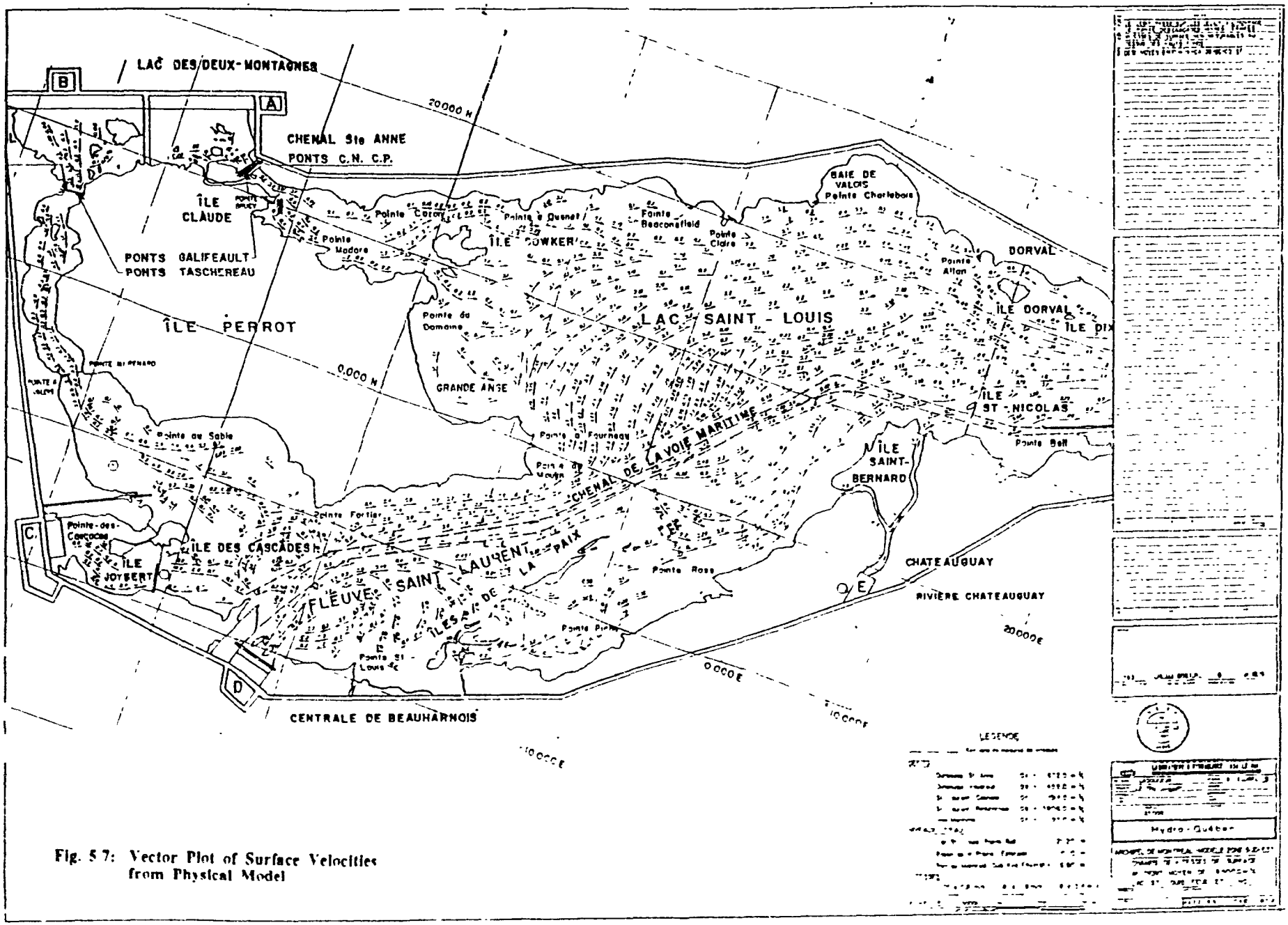

Fig. 5.7: Vector Plot of Surface Velocities from Physical Model

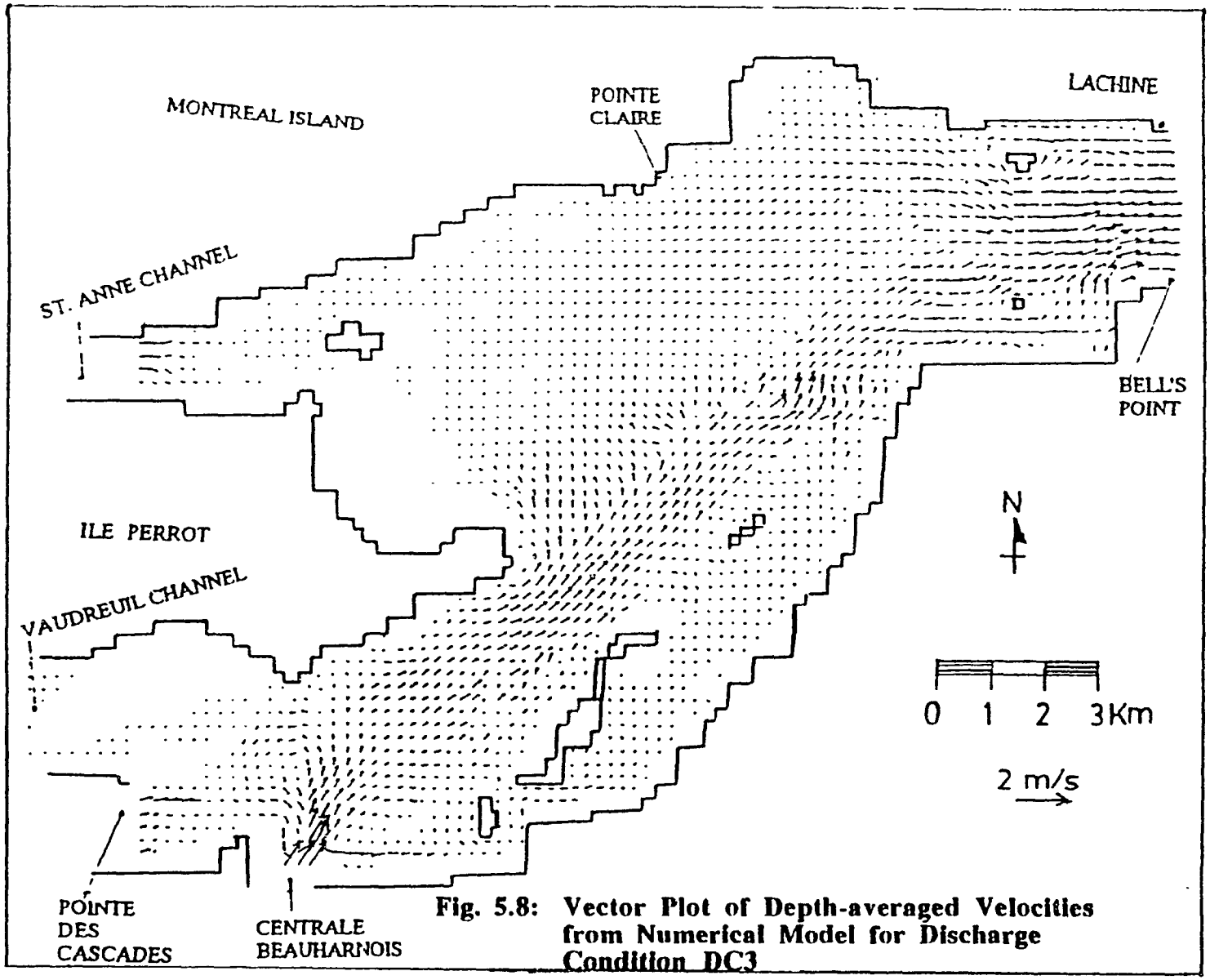

Fig. 5.8: Vector Plot of Depth-averaged Velocities from Numerical Model for Discharge Condition DC3

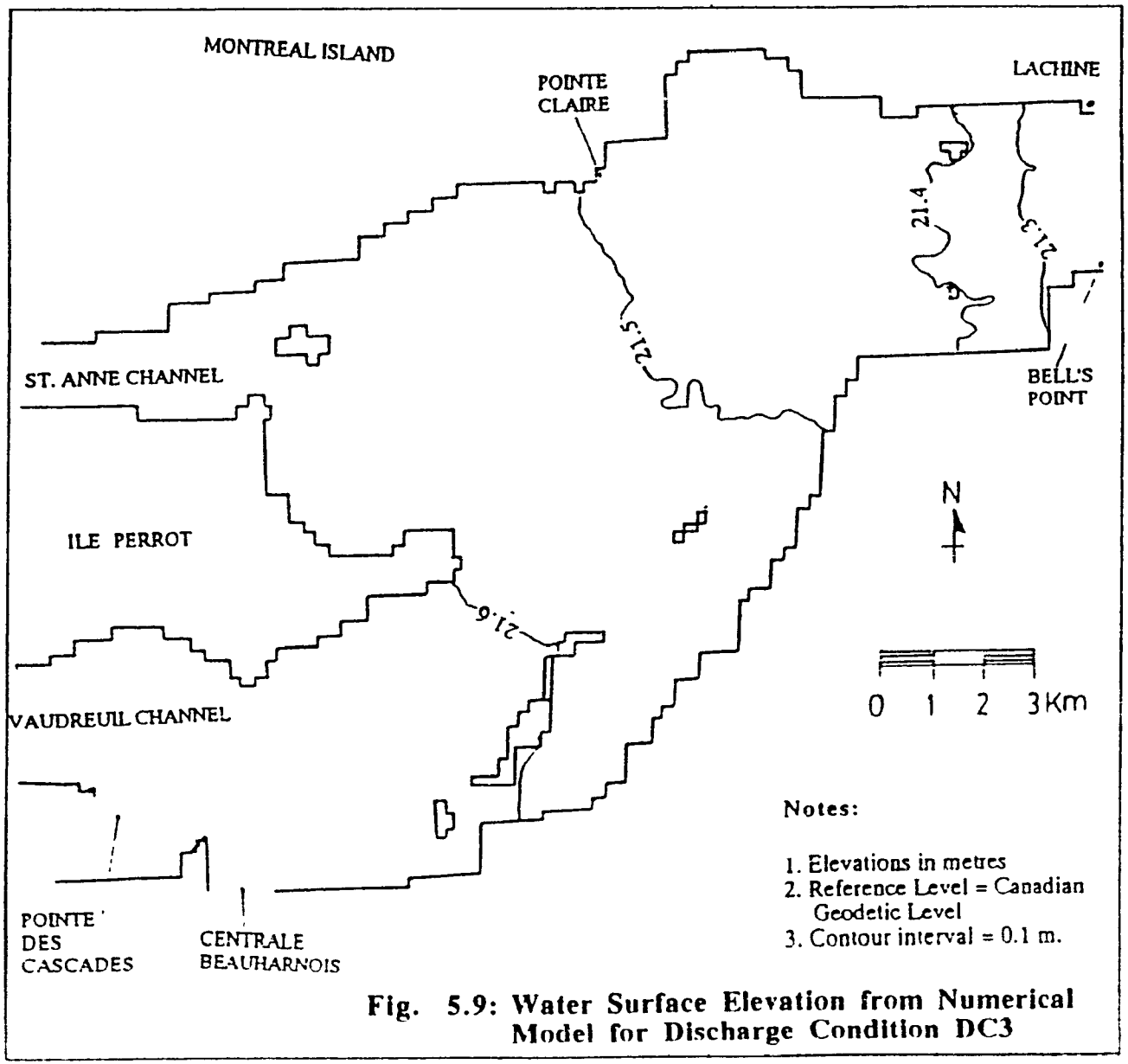

Fig. 5.9: Water Surface Elevation from Numerical Model for Discharge Condition DC3

It is seen in figure 5.8 that there are some velocity vectors near Pointe Bell that are not parallel to the boundary, giving an impression of what is usually referred to as a numerical leak. This is thought to be the result of the model trying to reproduce a small recirculation zone, but with an insufficient number of grids. This recirculation zone was absent from the physical model probably because it was run with the maritime channel open as opposed to the numerical model for which it was closed (see subsection 3.3.1 of chapter 3).

The numerical model predicted a head loss of 0.3 m between Pointe Bell and Pointe Claire and a head loss of 0.13 m between Pointe Claire and Centrale Beauharnois (elevation at Centrale Beauharnois was 21.63 m). According to Boivin et al, the head loss in the prototype between Pointe Bell and Pointe Clair is 0.1 m. The difference between this and the numerical model result of 0.3 m was attributed to the fact that the numerical model was run with the maritime channel closed. This view is reinforced by the fact that the head loss in the Prototype between Pointe Claire and Centrale Beauharnois is 0.1 m (Boivin et al 1982). This compares well with the numerical model result of 0.13 m. It should be remarked that in terms of the computation of the flow depth, the differences are insignificant, being typically of the order of 1%.

Use of a lower Manning's coefficient of 0.02 instead of 0.03 predicted a head loss of 0.25 m between Centrale Beauharnois and Pointe Bell, which agrees better with the 0.2 m loss measured in the prototype

when the maritime channel is open. However, as will be seen later, the agreement between the physical and numerical model velocities became worse as compared to the agreement obtained using the original value of 0.3. This further confirmed that the higher head loss predicted by the numerical model between Pointe Claire and Pointe Bell was due to simulation with the maritime channel closed.

As to the quantitative comparison of the magnitudes of the velocities, it should first be mentioned that both models predict that the maximum velocity occurs just in front of Centrale Beauharnois inlet. The physical model gives a surface velocity of 2.1 m/s. The numerical model predicts a depth averaged velocity of 1.763 m/s with water depth of 12 metres, which gives a surface velocity of 1.9 m/s. The agreement is therefore good. The surface velocity was computed by assuming a logarithmic velocity variation. This gives (Fischer et al 1979):

$$u_s = u_{da} + \frac{u*}{\kappa} \qquad (5.1)$$

where u_s is the surface velocity, u_{da} is the depth averaged velocity, $u*$ is the shear velocity and κ the von Karman's constant.

Further comparison of the velocity magnitudes was made using every fourth grid point in each direction. For each considered grid point, the velocity from the physical model was either interpolated or read off as the case required. The surface velocity computed by

the numerical model is plotted against that obtained from the physical model in fig 5.10. A bar chart of the differences as percentages of the physical model velocities is shown in figure 5.11a. It can be seen that tnere is considerable scatter in fig 5.10. The scatter about the line of best agreement is seen to be worse for low velocities. This may be due to the difficulty of measuring low velocities accurately in the physical model.

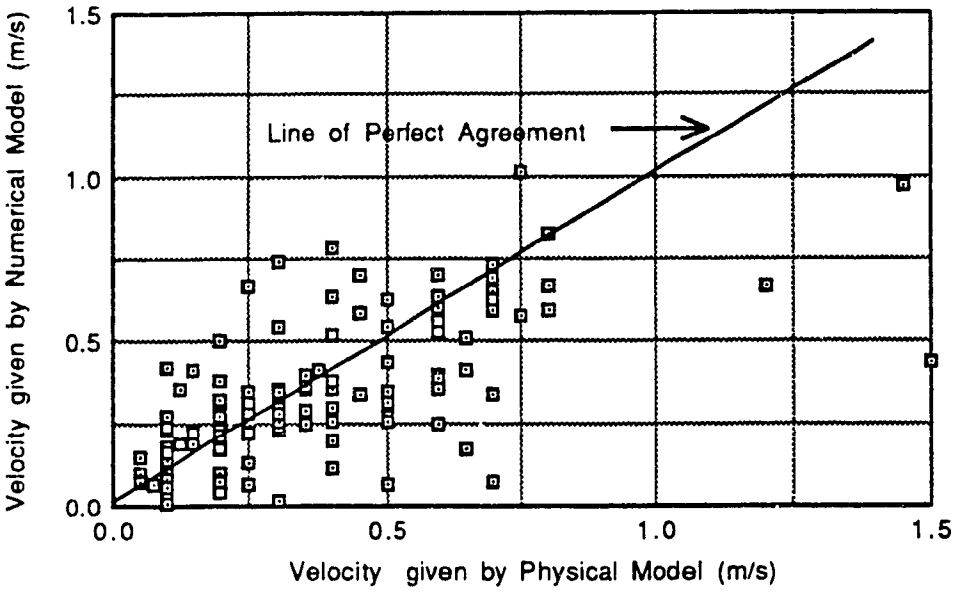

Fig 5.10: Comparison of Velocity Magnitudes given by Physical and Numerical Models

The relative differences plotted in fig 5.11a appear to follow the normal error curve, which can be interpreted to mean that errors in either model were not systematic.

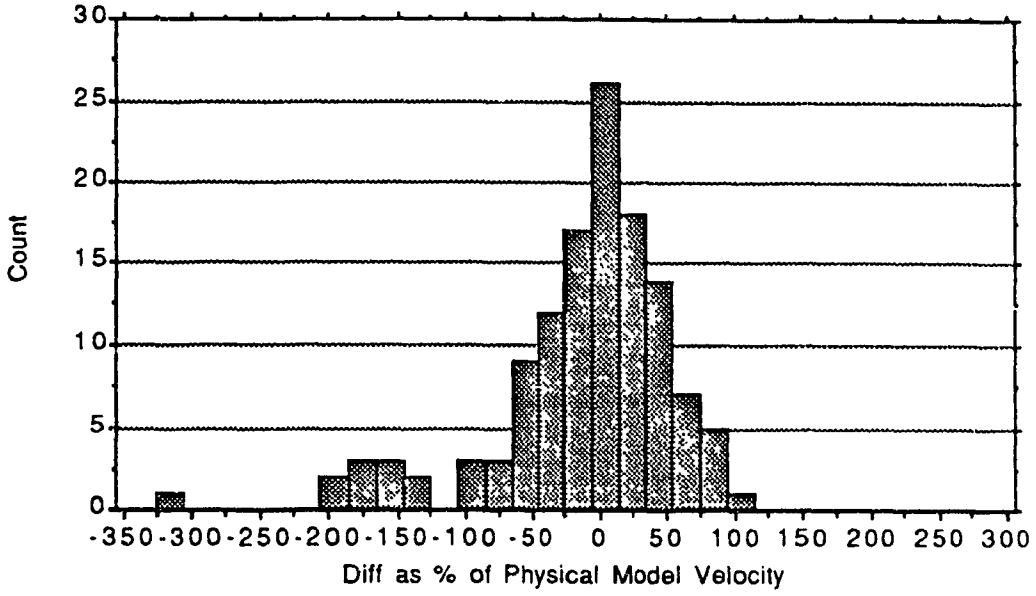

Fig 5.11a: Bar Chart of Velocity Differences as % of Physical Model Velocities for n = 0.03

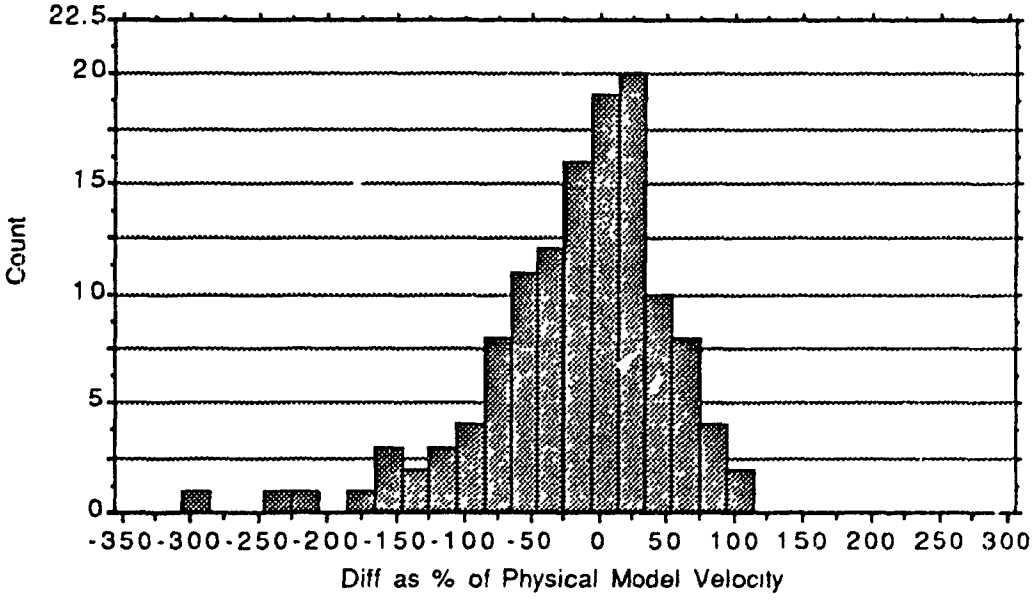

Fig 5.11b: Bar Chart of Velocity Differences as % of Physical Model Velocities for n = 0.02

As was mentioned earlier, use of a Manning coefficient of 0.02 gave poorer agreement between the physical and numerical model velocities. This can be seen in fig 5.11b. The modal value is seen to be skewed to the right and the count for the modal value is less than that given by fig 5.11a.

In a numerical model, errors arise from discretization of space and governing equations and rounding off in arithmetical operations. On the other hand, errors in a physical model arise from accuracy of measurements, scale effects and accuracy in the reproduction of the bathymetry. Boivin et al (1982) quoted an accuracy of 15% for the physical model velocity results as compared to flow in the prototype. Since neither of these models can be said to be perfect, the main purpose of this comparison was to show that even when approaches to flow simulation are as far apart as numerical and physical modelling, it is possible to obtain results which do not substantially differ. Under such circumstances, it may then be reasonable to suppose that the numerical/physical model results are representative of the prototype condition.

5.2.3 Assessment of k-ε Model Results

Even though the turbulence kinetic energy (k) plays a key role in sediment transport, it rarely appears explicitly in sediment transport formulae. In its place, the shear velocity (u_*) is normally used. The existence of a direct relationship between k and u_* is well known in the case of Shear flows. In such flows, the other property required to

describe flow turbulence, namely the turbulence length scale, can be taken as proportional to the flow depth (Fischer et al 1979). In such cases, the knowledge of the shear velocity and water depth should enable the computation of the turbulent viscosity coefficient. Because of the large aspect ratios in most parts of Lake St Louis, the results of the turbulence model were examined for consistency with those expected for thin shear flows.

In the examination of the results, a plot was made for u* vs k. Also the turbulent viscosity coefficient computed by the k-ε model was compared with that given by Laufer's empirical formula (equation 3.6). These plots are shown in figures 5.12 and 5.13a. In both plots, every third interior grid point in each direction was used.

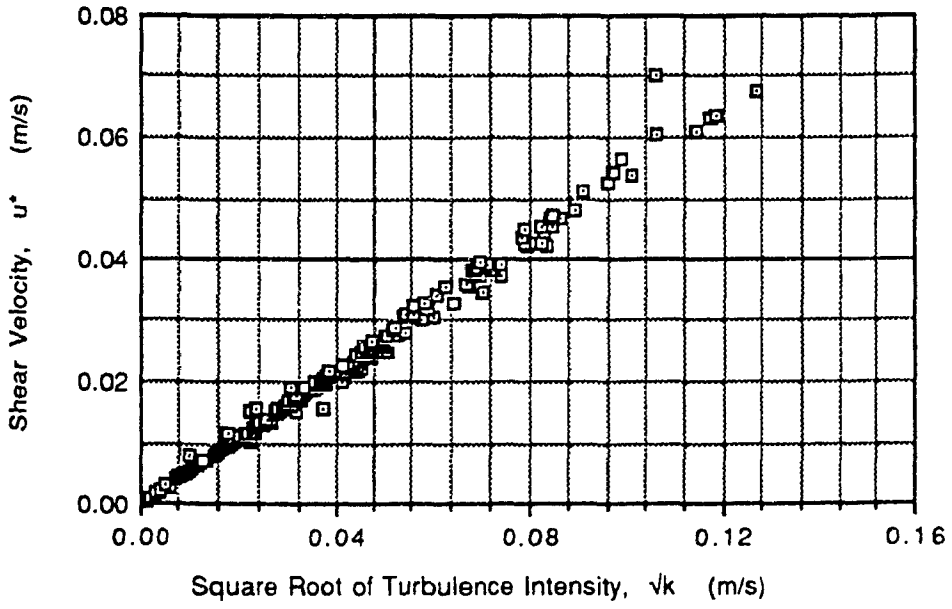

Fig 5.12: Plot of Shear Velocity vs Square Root of Turbulence Energy

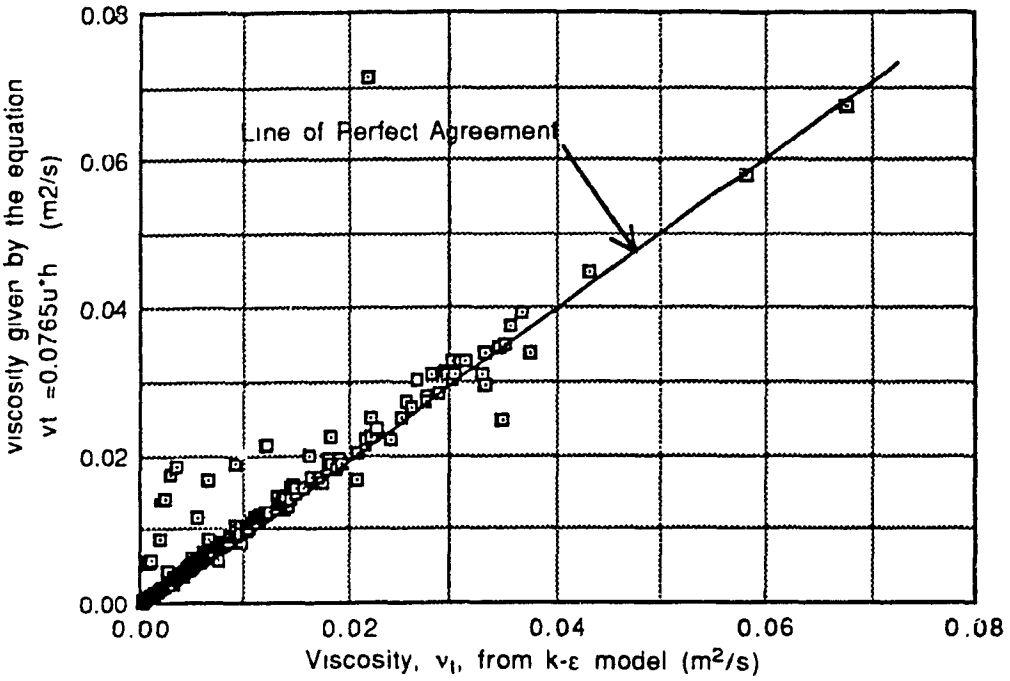

Fig 5.13a: Comparison of viscosity computed using k-ε Model with Laufer's formula for the same Simulation

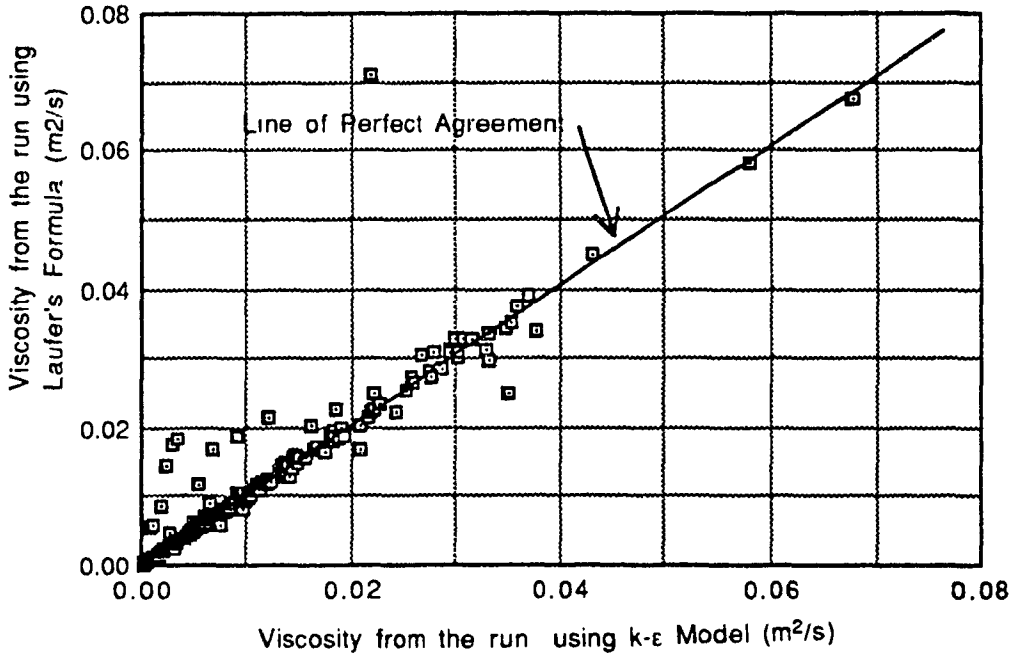

fig 5.13b: Comparison of viscosity computed using Laufer's formula and k-ε model in two separate runs.

It is seen from figure 5.12 that there exists a very strong correlation between u* and k. Linear regression of log u* on log k gave an r-squared value of 0.994 and predicted the following relationship between u* and k:

$$u* = 0.55\sqrt{k} \qquad (5.2)$$

.

From figure 5.13a it can be seen that the turbulent viscosity coefficient was predicted quite well using Laufer's empirical formula, except at few points. Even for the points where the agreement was not exact, the empirical equation gave a viscosity coefficient that was of the same order of magnitude as that from the k-ε model.

From these tests, two conclusions were made with regard to the flow in lake St. Louis. Firstly, the shear velocity ($u*$) is a good measure of the turbulent intensity (k) and could be used in its place in the hydraulic sorting investigations. Secondly, the flow in the lake could be modelled with almost similar accuracy if Laufer's empirical equation (equation 3.6) was used to calculate the ν_t.

The second conclusion above was verified by running the flow model using Laufer's equation to compute ν_t. The values of ν_t computed in this run was compared with those obtained previously from the k-ε model. The results are plotted in figure 5.13b, which can be seen to be very similar to figure 5.13a. Differences in the values of ν_t computed using the two methods were pronounced in the vicinity of

islands and at the sides of the deep channel in the lake. Grid points at which relative differences (expressed as percentages of the viscosity obtained from the k-ε model) exceeded 20% are shown in fig 5.14.

The difference in magnitudes of velocity and water depths computed using the two runs were insignificant. For example, at the grid point giving the worst agreement in velocity, the run with k-ε model gave a velocity of 0.1279 m/s, while that using Laufer's formula gave a velocity of 0.1336 m/s. The worst agreement for water depth occurred at a grid point where the run using the k-ε model gave a depth of 13.076 m as compared to 13.074 m obtained using Laufer's formula. These grid points were both in the recirculation zone near Centrale Beauharnois. It should be emphasized here that these small differences between the computed variables are due to the fact that the influence of viscosity on the flow field is usually small, as was pointed out in Chapter 3. The differences may have been more pronounced if the transport of a scalar quantity had been modelled instead. For this reason, the conclusion regarding the applicability of Laufer's formula is only applicable to modelling the flow field and is not to be generalized.

The results of these comparisons also served a second and perhaps more important purpose from the point of view of numerical modelling. Because well known relationships were reproduced with high accuracy, it could be argued that numerical errors were not of such magnitude as to obscure the actual results. This is often a major source of concern in numerical modeling, since it is difficult to

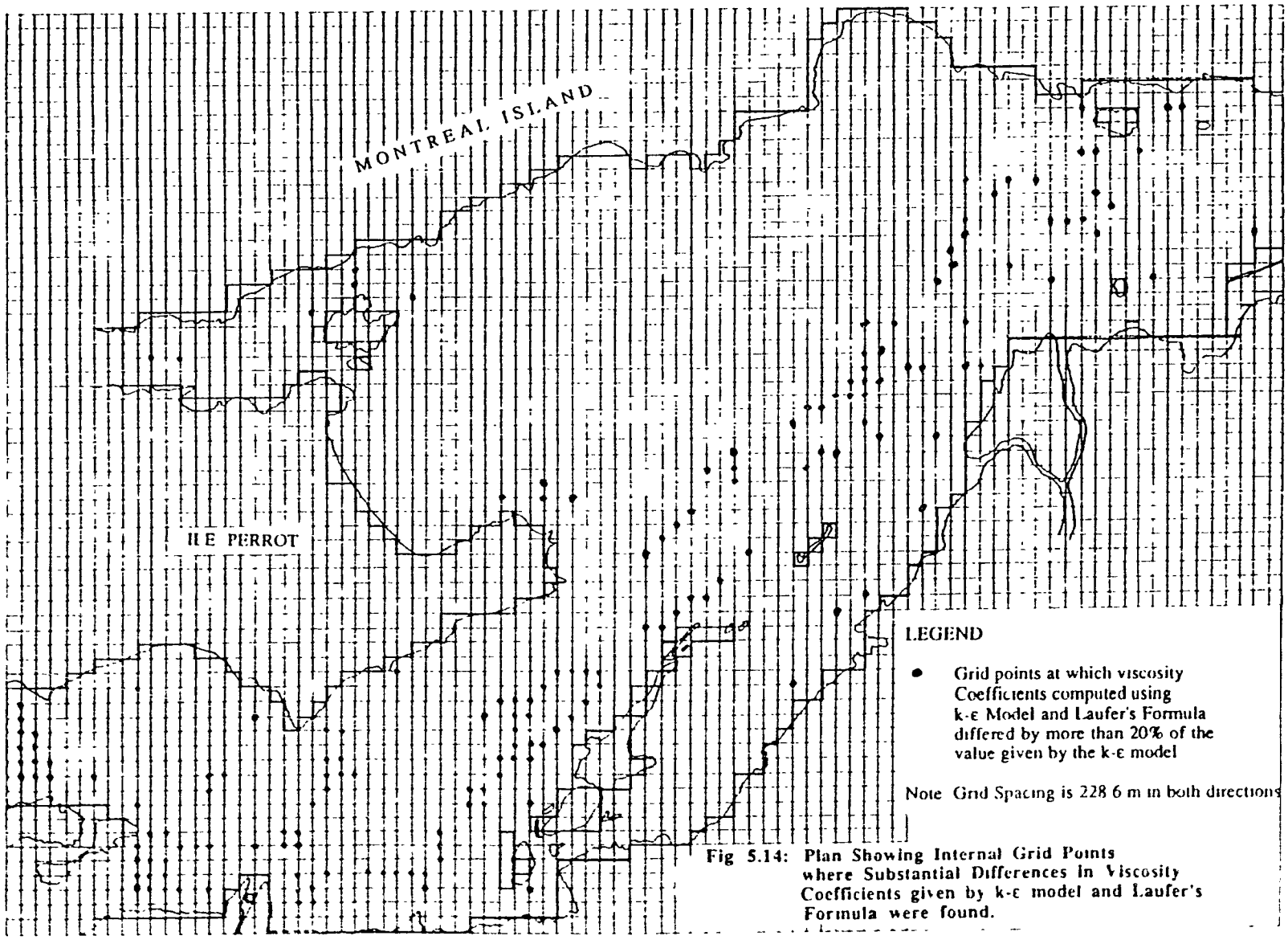

Fig 5.14: Plan Showing Internal Grid Points where Substantial Differences In Viscosity Coefficients given by k-ε model and Laufer's Formula were found.

theoretically estimate the errors incurred during the computations. These tests therefore complemented the comparison between the physical and numerical model in establishing the reliability of the model.

5.3 MODEL RESULTS

The numerical simulation results for discharge condition DC1 are plotted in figures 5.15 and 5.16. In figure 5.15 the velocity vector field is plotted, while figure 5.16 gives a plot of the surface water elevation. Similar plots for discharge condition DC2 are given in figure 5.17 (velocity vectors) and 5.18 (surface elevation). The shear velocities and water depths at the sediment sampling stations are tabulated in Table C1 of appendix C. Shear velocities were computed using equation 3.7.

In the above simulations, the k-ε model was used to compute eddy viscosity coefficients. The time steps used for both simulations were 20 seconds for the flow model and 2 seconds for the k-ε model. Each simulation took about 4 hours of cpu time on Concordia University's Vax 6000 model 510 mainframe computer (VAX 2). The mass difference at convergence for DC1 was -0.85% (gain) and the maximum difference tests results were of the same order of magnitude as those given in section 5.2 for DC2.

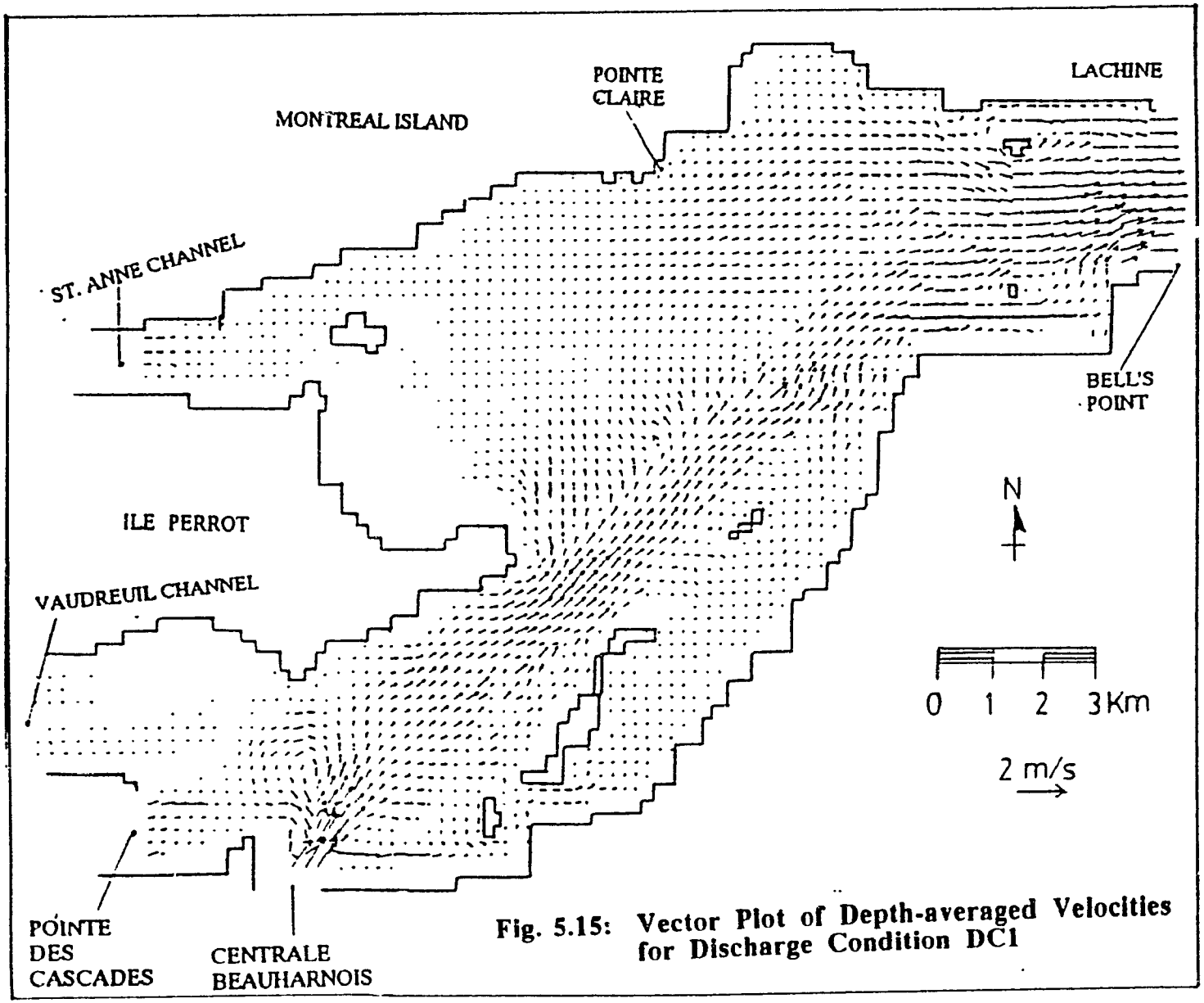

Fig. 5.15: Vector Plot of Depth-averaged Velocities for Discharge Condition DC1

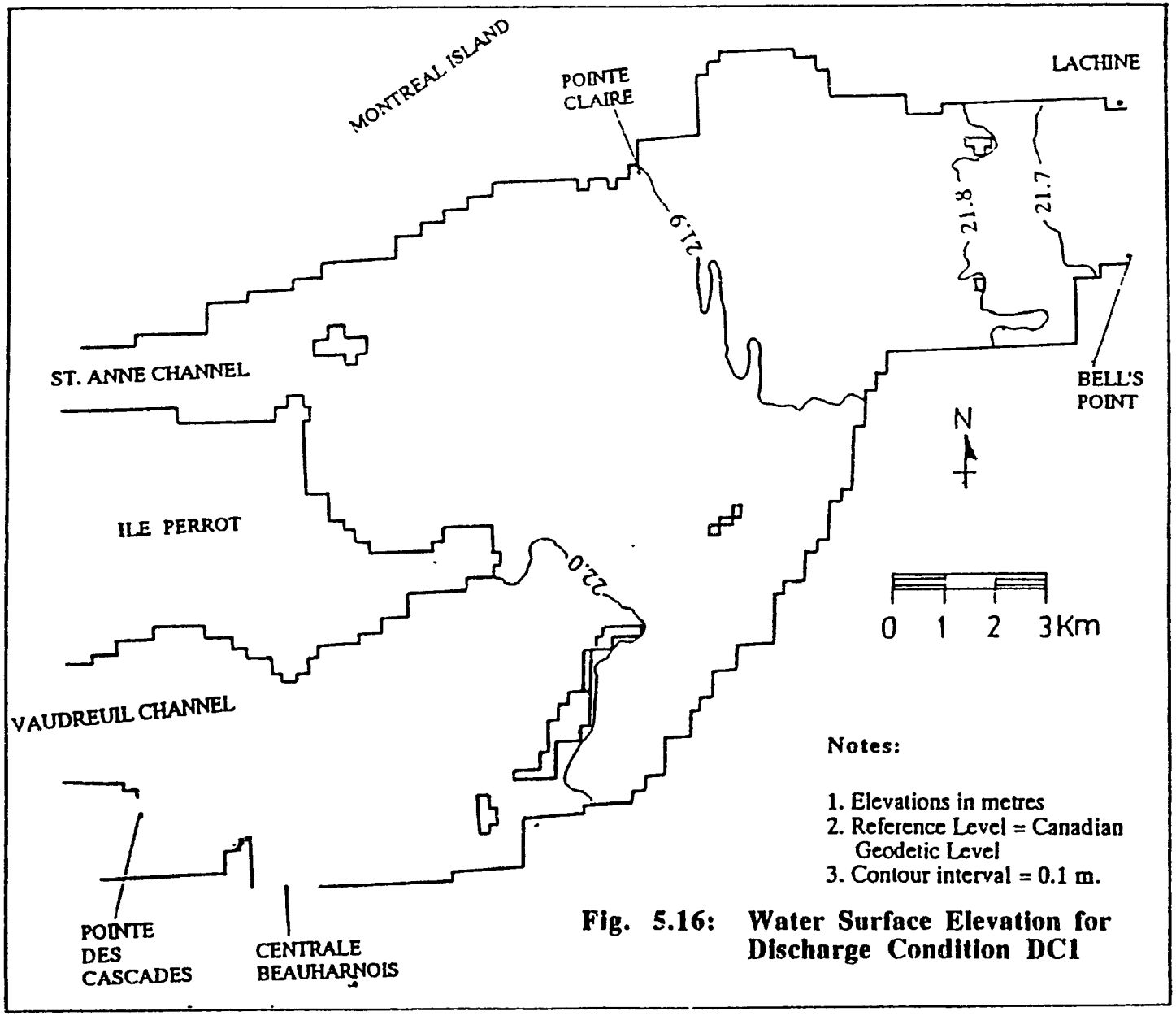

Fig. 5.16: Water Surface Elevation for Discharge Condition DC1

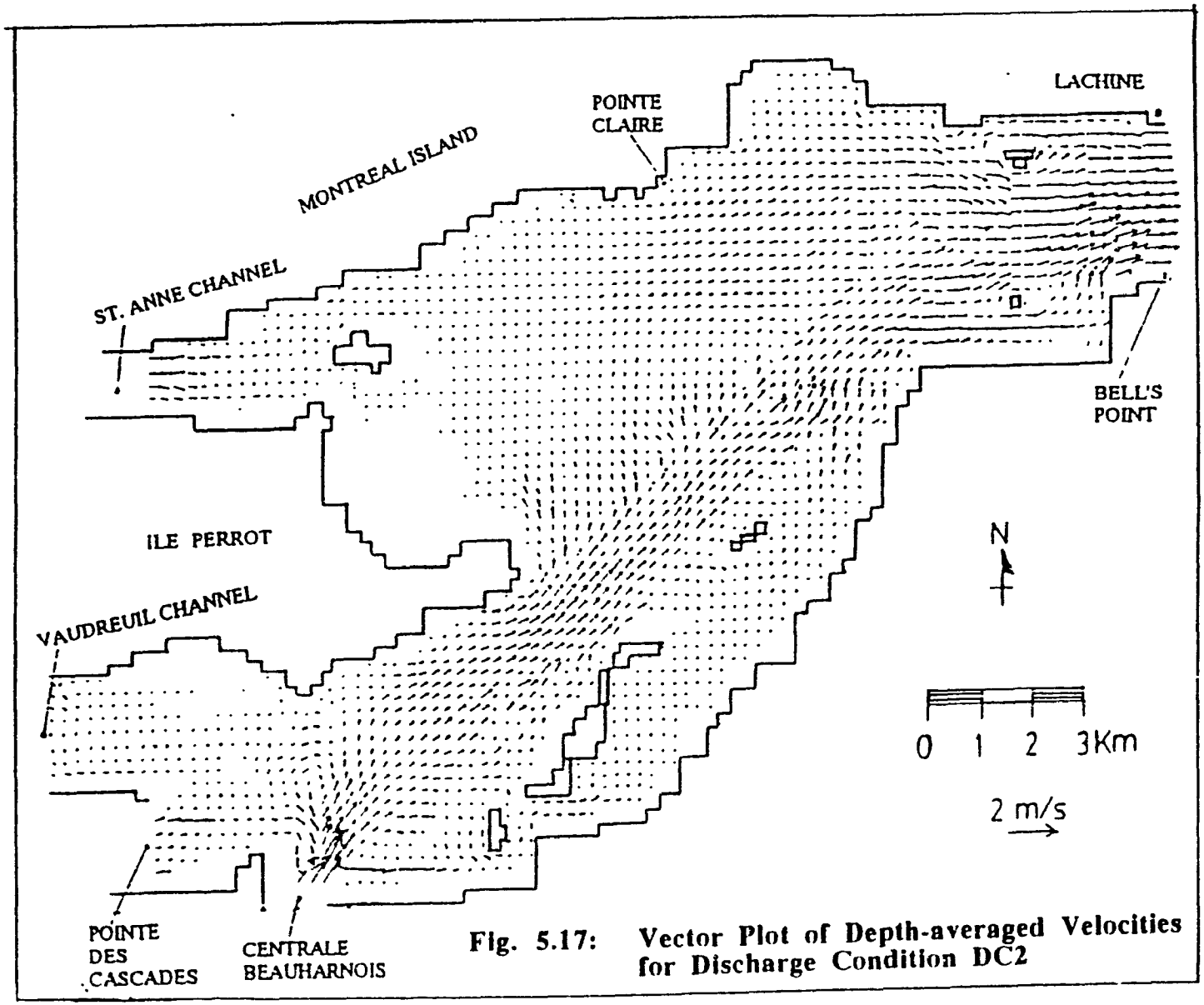

Fig. 5.17: Vector Plot of Depth-averaged Velocities for Discharge Condition DC2

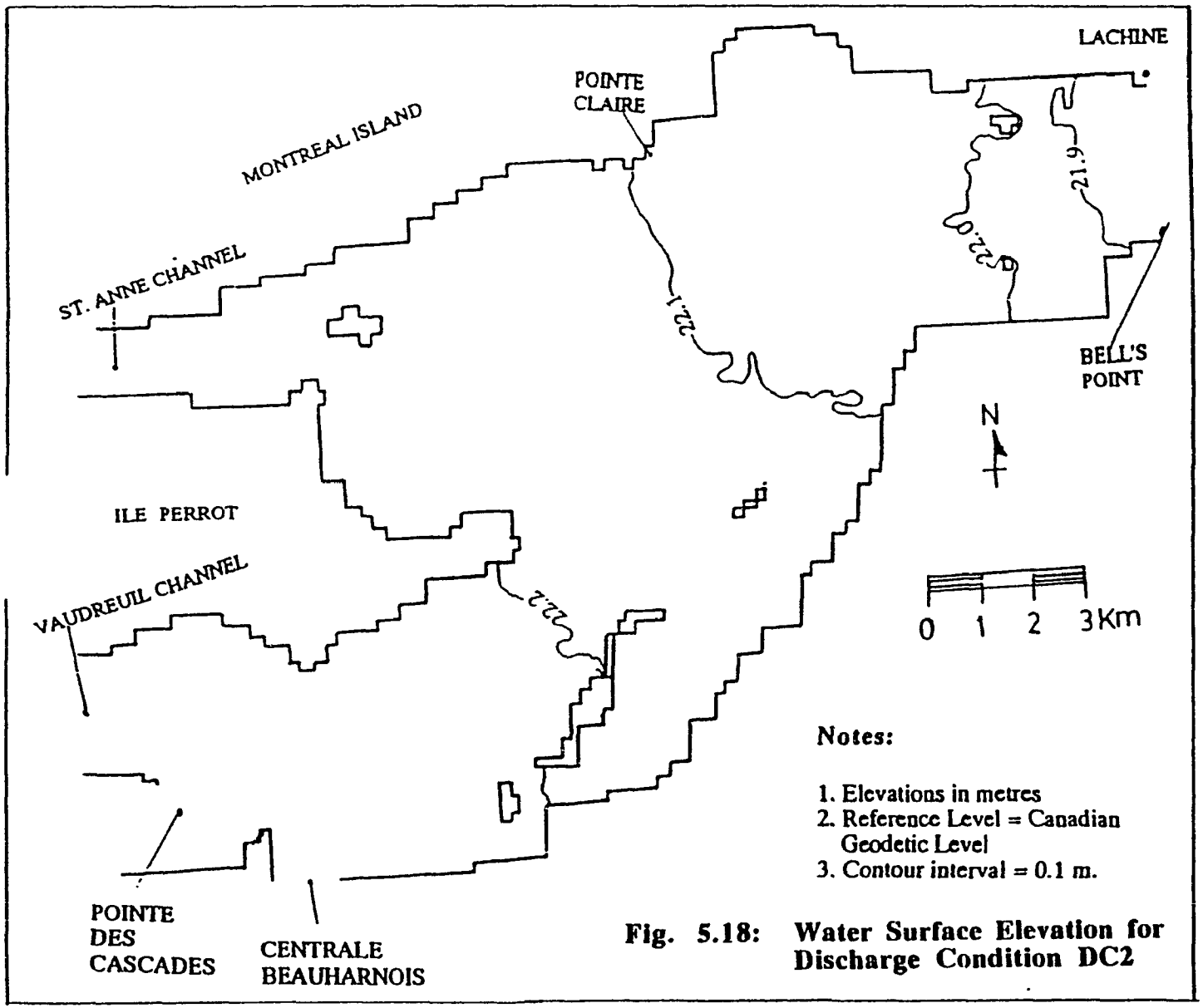

Fig. 5.18: Water Surface Elevation for Discharge Condition DC2

CHAPTER 6

SEDIMENT SIZE AND FLOW CORRELATIONS

6.1 GENERAL

The bed-surface sediment characteristics presented in section 4.3 of Chapter 4, and the flow variables obtained in Chapter 5 provide the primary inputs for investigation into the relationships between the sediment size and the flow parameters. The basic parameters describing the sediment are the median sediment size and its fall velocity ω_s. Those describing the flow are the shear velocity u_*, (which was seen in the previous chapter to be related to the turbulent kinetic energy), and the flow depth h. Other parameters required for this investigation are the particle density ρ_s, the kinematic fluid viscosity ν and the water density ρ. These were assumed to have constant values as follows: ρ_s = 2650 kg/m^3, ν = 10^{-6} m^2/s and ρ = 1000 kg/m^3. Another parameter of interest is the acceleration due to gravity g, which has been taken as 9.81 m/s^2.

From the 139 samples collected during the sediment survey, 115 were used in the investigation. The 24 samples that were excluded were those collected from stations which lay either outside the discretized computation domain, or within computational boundary cells. Points in the boundary cells were excluded because of localized errors in flow modelling that result from the replacement of curved

boundaries with a series of straight lines during space discretization. The proximity of the boundary cells to the shore also causes bank erosion effects to obscure those of hydraulic sorting. The stations that were excluded are marked in fig 4.5.

The sediment size/flow correlations were made using dimensionless plots. The dimensionless variables considered were those that are commonly used in sediment transport studies. The choice of these dimensionless variables is discussed in the next section, followed by the correlation plots in section 6.3. This chapter closes with a discussion of the observed correlations in section 6.4.

6.2 DIMENSIONLESS VARIABLES

6.2.1 Choice of Variables

Previous dimensional analysis by Yalin (1971) identified four basic independent dimensionless variables that describe the two-phase flow that characterizes the transport of cohesionless sediment by water. These can be taken as the dimensionless particle size D_*, the dimensionless boundary shear stress θ, the relative roughness e_r and the specific gravity s. They are given by the relationships:

$$D_* = \left| \frac{(s-1)\ gd^3}{\nu^2} \right|^{\frac{1}{3}} \qquad (2.12)$$

$$\theta = \frac{u_*^2}{(s-1)\,gd} \tag{6.1}$$

$$e_r = \frac{d}{h} \tag{6.2}$$

$$s = \frac{\rho_s}{\rho} \tag{6.3}$$

In the above expressions, d is a characteristic particle size. In this study, this size has been taken as the median size as was pointed earlier out in Chapter 4.

Of the four dimensionless variables, the specific gravity s, is considered the least significant dimensionless group. It only needs to be considered in the study of unsteady particle motion (Yalin 1971). This variable was not considered as an independent dimensionless group in this work mainly because there was no data on specific gravity of individual sediment particles. However, specific gravity still appears as part of the variables θ and D_*, where it has been set to a constant value as mentioned earlier.

Another dimensionless variable that was of considerable interest in this study is the ratio of the particle fall velocity to the shear velocity (ω_s/u_*). The dimensionless group ($\omega/\kappa\beta u_*$) appearing in the Rouse equation (equation 2.3), is usually referred to as the Rouse number Z_r. For a constant value of β, it is equivalent to (ω_s/u_*) multiplied by the reciprocal of Karman's constant κ, if the fall velocity in still water

ω_s is used instead of ω. In this work the ratio $\omega/u*$ will be referred to by the symbol Z_r* to distinguish it from the complete Rouse number. The ratio Z_r* was used in the study of hydraulic sorting by Middleton (1976). Further, it has been used as the criterion that determines the initiation of suspension of sediment particles by Bagnold, Engelund and van Rijn (van Rijn 1984). For this reason Z_r* is sometimes referred to as the suspension parameter.

According to Yalin (1971), Z_r* can be introduced as another dimensionless variable if either the dimensionless boundary shear stress (θ) or the dimensionless particle size ($D*$) is omitted. In this work, given the particular interest in spatial particle size distribution, $D*$ was retained but θ was dropped in favour of Z_r*.

6.2.2 Particle Fall Velocity

In order to compute Z_r*, the fall velocity should be known. The fall velocity for a particle of diameter d was computed using the following formulae (Van Rijn 1984 b)

$$\omega_s = \frac{1}{18}\frac{(s-1)gd^2}{\nu} \qquad d < 100\mu \tag{6.4a}$$

$$\omega_s = 10\frac{\nu}{d}\left\{\sqrt{1+\frac{0.01(s-1)gd^3}{\nu^2}} - 1\right\} \qquad 100\mu \le d \le 1mm \tag{6.4b}$$

$$\omega_s = 1.1\sqrt{(s-1)gd} \qquad d > 1mm \tag{6.4c}$$

These formulae are strictly valid for spherical particles falling in a quiescent fluid. Basically, their use in the case of coarse sediment whose size distribution has been determined by sieve analysis is an approximation. For fine sediments, the above formulae are more accurate in view of the methods used for determining the size distribution. Using the settling tube for example, the particle sizes are determined from their fall velocities using above formulae. Effects such as particle shape and specific gravity on the magnitude of the fall velocities are therefore implicit in the computed sizes.

6.2.3 Effects of Cohesive Forces

The analysis by Yalin (1971) was intended for cohesionless sediment. In the case of cohesive sediments, no similar analysis appears to have been carried out. This is due to the difficulty of quantifying the parameters that influence the magnitude of cohesive forces. However, if both entrainment from and deposition to the mixed (active) layer take place continuously, then the top sediment must be in a fairly loose state. In such a case, the effects of cohesion are likely to be minimal.

6.3 CORRELATIONS PLOTS

The data used for the correlation plots are tabulated in Table C2 of appendix C. These plots were made using the log-log scale as is traditional in sediment transport studies. This scale has two advantages. Firstly it depicts as straight lines the power type

relationships that are commonly encountered in sediment transport. Secondly, the scale allows better resolution of the of size ranges considered.

Three types of correlation plots were made. The plots for D_* and Z_{r*} are given in sub-section 6.3.1, those for D_* and e_r are given in sub-section 6.3.2 and those for Z_{r*} and e_r are given in sub-section 6.3.3.

6.3.1 Correlation Plots for Z_{r*} and D_*

For each of the two discharge conditions analyzed, a correlation plot was made for Z_{r*} against the dimensionless particle size (D_*). This is shown in fig 6.1 for the discharge condition DC1 and in fig 6.2 for DC2.

The general trend revealed in the plots is that Z_{r*} increases with dimensionless particle size (D_*). This shows that as the shear velocity or turbulence kinetic energy increases, the median particle size found on the bed surface decreases. It is particularly noteworthy that the fine grained particles do not show much scatter.

Although both plots show good correlation, that for DC2 is slightly better. The two plots do not differ significantly, indicating that the differences between the shear velocities induced by the two discharge conditions at the sediment sampling stations are not significant.

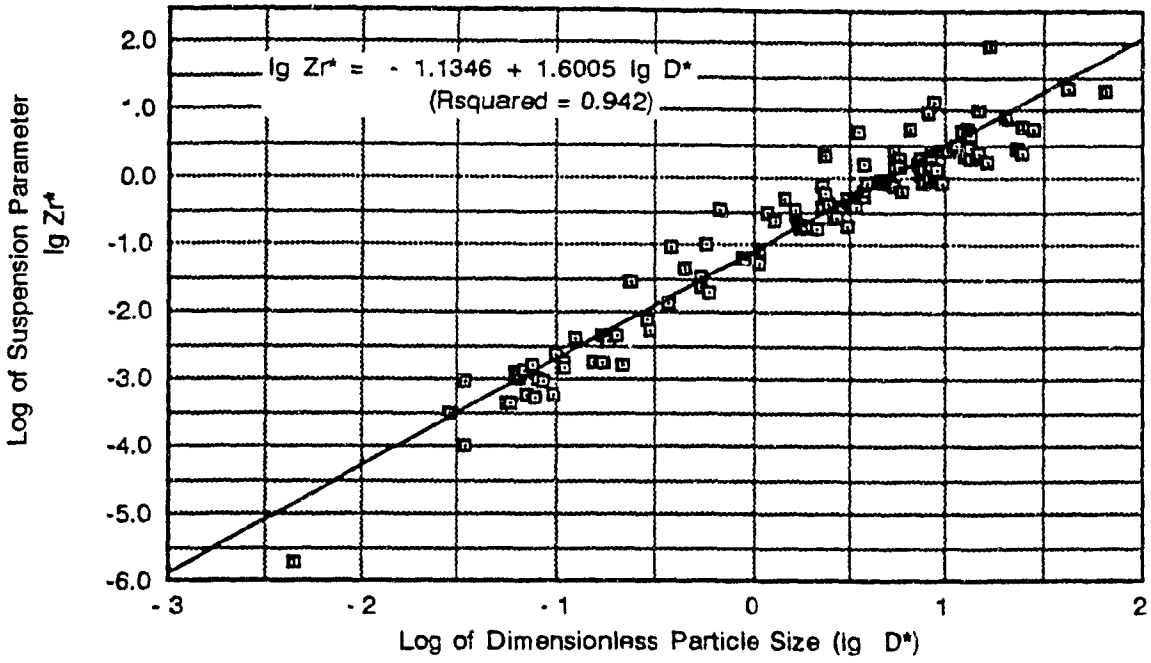

Fig 6.1: Plot of lg Zr* against lg D* for Discharge condition DC1

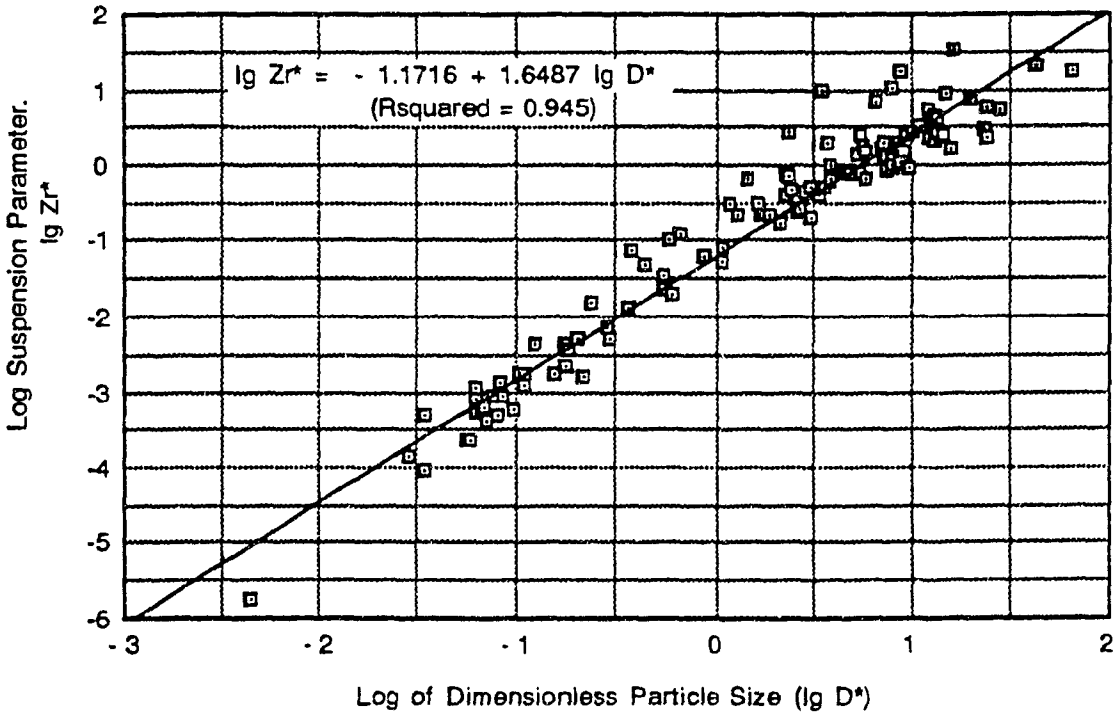

Fig 6.2: Plot of lg Zr* against lg D* for Discharge Condition DC2

The regression line from fig 6.2 for DC2 gives the following relationship

$$Z_{r*} = 0.067\ D_*^{1.65} \qquad (6.5)$$

with an r-squared value of 0.945. That for DC1 gives a constant of 0.07 instead of 0.067, an exponent of 1.6 instead of 1.65 and has an a slightly lower r-squared value of 0.942.

6.3.2 Correlation Plots for e_r and D_*

Figures 6.3 and 6.4 show the correlation plots between e_r and D_* for discharge conditions DC1 and DC2 respectively.

It is again observed that both discharge conditions give near similar results, and that condition DC2 still gives a slightly better correlation. Both plots show that the correlations between D_* and e_r are slightly weaker than those observed between D^* an Z_{r*}. The observed trend is for e_r to increase with D_* .

The equation of the regression line from fig 6.4 for DC2 is

$$e_r = 10^{-5.15}\ D_*^{1.04} \qquad (6.6)$$

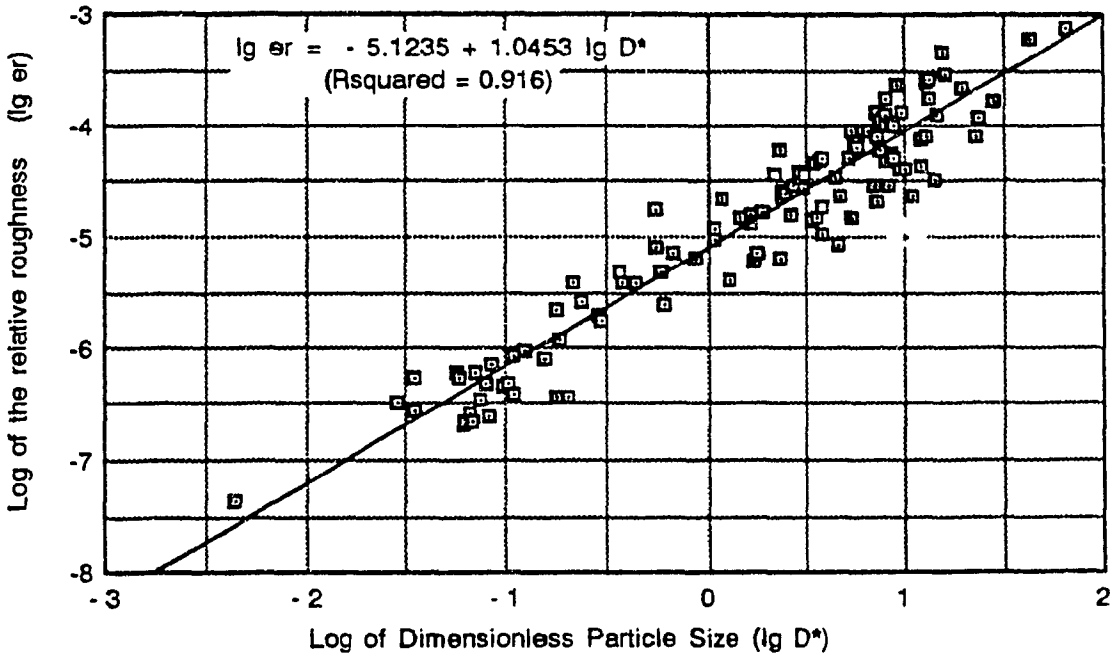

Fig 6.3: Plot of lg er against lg D* for Discharge condition DC1

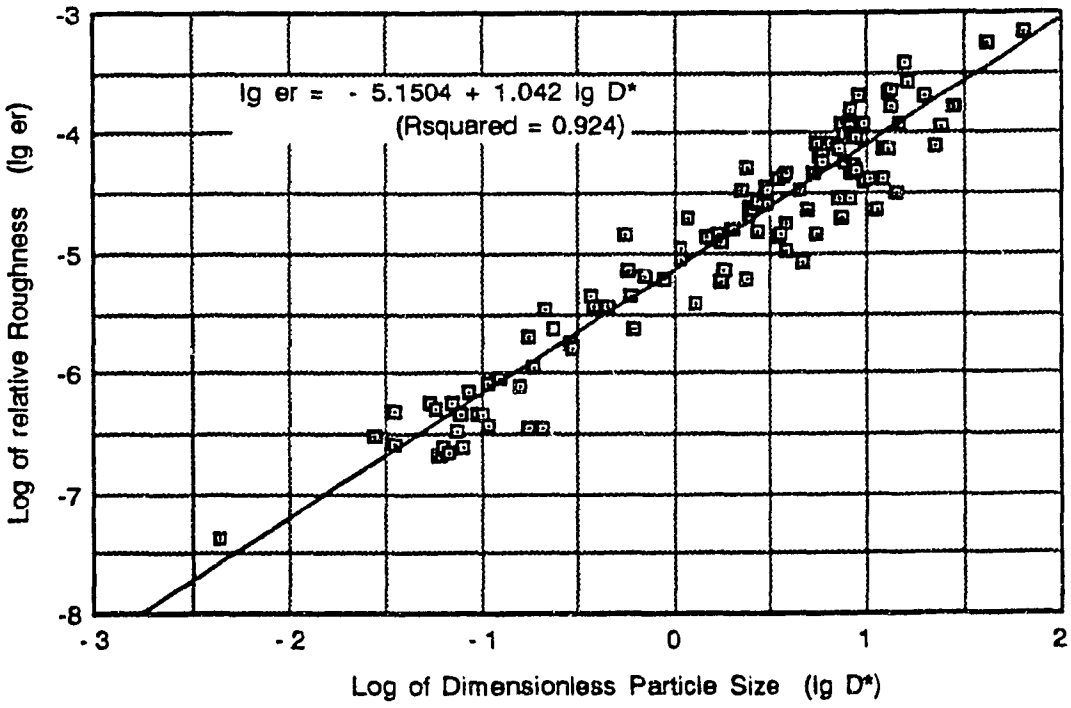

Fig 6.4: Plot of lg er against D* for Discharge Condition DC2

with an r-squared value of 0.924. That for DC1 gives a constant of $10^{-5.12}$ instead of $10^{-5.15}$, an exponent of 1.05 instead of 1.04 and has an r-squared value of 0.916.

6.3.3 Correlation Plot for Z_{r*} and e_r.

The correlation between Z_{r*} and e_r is plotted in figures 6.5 and 6.6 for discharge conditions DC1 and DC2 respectively.

These plots show slightly more scatter than those observed in the previous plots. Discharge condition DC2 still shows slightly better correlation. The observed trend is for e_r to increase with increasing Z_{r*}.

The equation of the regression line from fig 6.6 for DC2 is

$$e_r = 10^{-4.43} Z_r^{0.60} \qquad (6.7)$$

with an r-squared value of 0.886. That for DC1 gives a constant of $10^{-4.41}$ instead of $10^{-4.43}$, an exponent of 0.62 instead of 0.60 and has an r-squared value of 0.880.

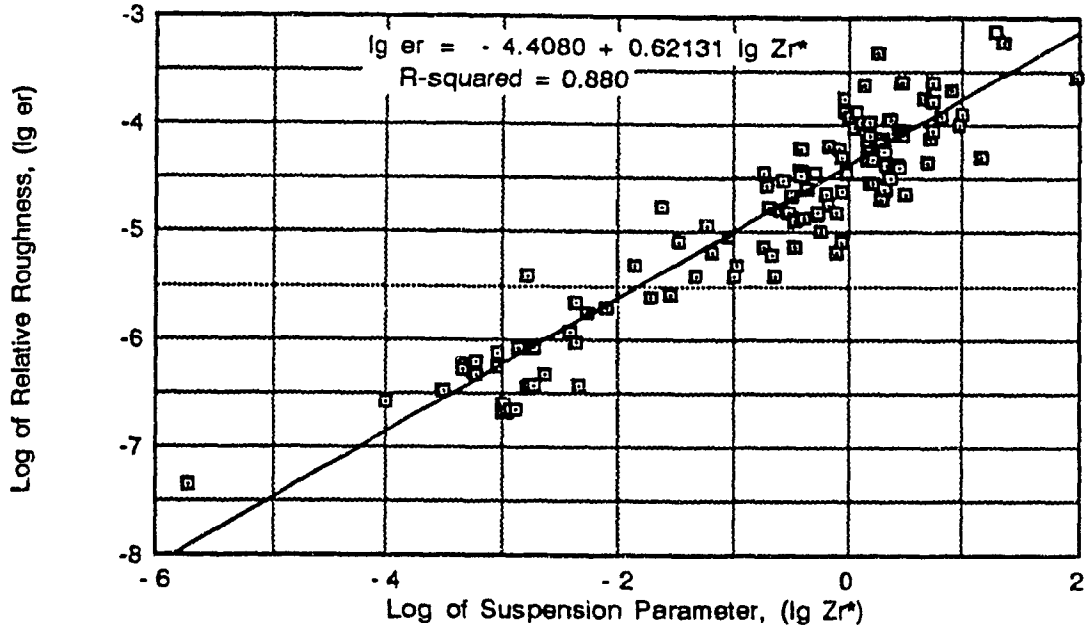

Fig 6.5: Plot of lg er against lg Zr* for Discharge Condition DC1

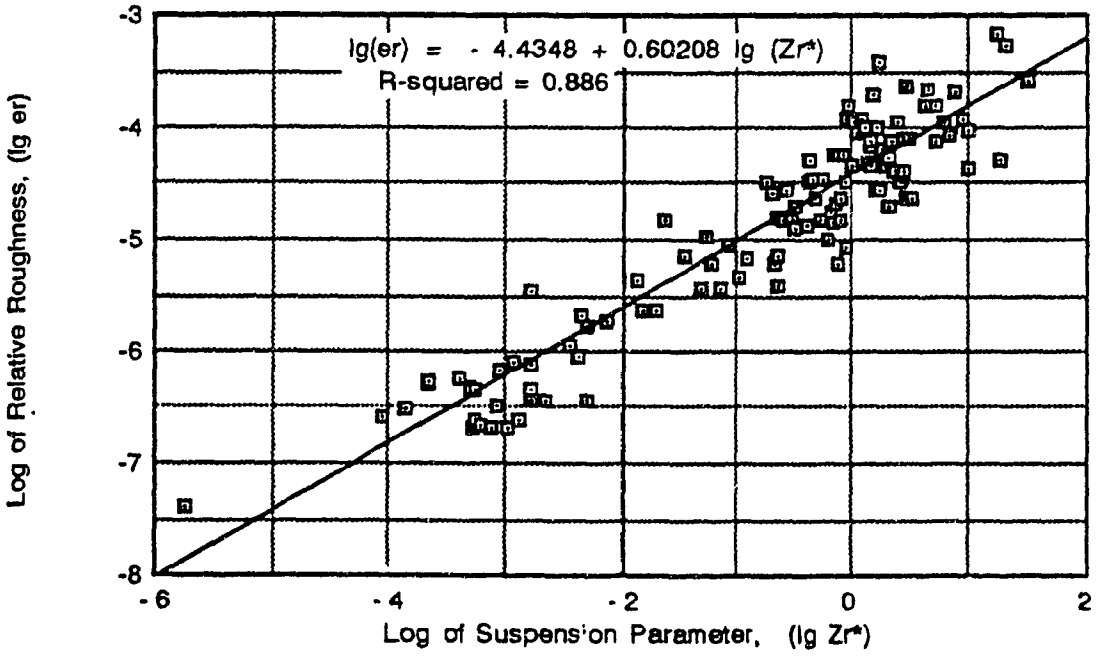

Fig 6.6: Plot of lg er against lg Zr* for Discharge Condition DC2

6.4 DISCUSSION ON OBSERVED CORRELATIONS

6.4.1 Global Effects of Hydraulic Sorting: Dynamic Equilibrium

From the plots presented in the previous section, it is clear that for bed-surface sediments, there is interdependence amongst the dimensionless variables D_*, Z_{r*} and e_r. Yet, from the point of view of dimensional analysis, these variables are supposed to be independent of each other. The interdependence is thought to result from gradual adjustment of all the flow and sediment parameters in the water body, so that a state of dynamic equilibrium prevails. This adjustment to and subsequent maintenance of the dynamic equilibrium is thought to be achieved through hydraulic sorting.

It is clear that arbitrary changes in any one of the variables that determine the equilibrium, such as depth changes during dredging operations, is very likely to upset this delicate equilibrium. This often results in unexpected and, in many cases, undesirable consequences.

There are two types of equilibrium in alluvial flows. The first one is the hydraulic sorting equilibrium, which prevails when the spatial variation of bed material sizes is compatible with the existing flow conditions. The second is the bed slope equilibrium, which prevails when the bed slopes no longer change with time. The two processes leading to these equilibrium conditions namely grain sorting and bed slope evolution have been shown to have two disparate time scales

(Deigaard 1980). Hydraulic sorting takes place much faster than bed evolution. After a quasi-equilibrium condition is established due to hydraulic sorting, bed slope evolution continues. However, the latter process is usually very slow. In a hypothetical case where the sediment and water discharge remain constant and the type of incoming bed material is also constant, bed slope equilibrium is achieved when the type of bed material is the same everywhere in the river system considered. The bed slope would also be the same throughout the river. From the observation that bed material size and slope vary spatially in most rivers, it may be argued that such equilibrium is never attained in real life. The use of the term dynamic equilibrium with regard to conditions in natural water bodies, therefore refers to the quasi-equilibrium set up through hydraulic sorting.

From a theoretical point of view, dynamic equilibrium can be set up by a corresponding 'equilibrium flow', defined as the flow that has established a bed configuration and slope consistent with the fluid, flow and bed material characteristics over the entire length of the channel (Simons and Senturk 1976). This definition is particularly appropriate to the type of flow in Lake St. Louis, where the discharge is regulated at a near-constant value. However, dynamic equilibrium also exists in the case of rivers with seasonal variations in discharges. In such cases the equilibrium is established over a sufficiently long averaging time. The response of the bed material composition to changing discharge is not proportional to the discharge. Higher discharges tend to be better correlated with the bed material type

due to their disproportionately greater influences. The correlations observed in this study confirms that the higher discharges are better correlated to the bed material type, although the differences in this case were insignificant due to flow regulation.

The study of the movement of fine sediments has always presented major difficulties because of their property of cohesion. It is therefore of major interest to note that the dimensionless variables used in this work appeared capable of describing the spatial distribution of both coarse as well as fine sediments. This may be taken as supportive of the earlier stated argument that cohesion is unlikely to be significant in active bed layer. Another possible explanation is that the presence of a large quantity of chemicals in the lake may have lowered the cohesion between the soil particles by altering their electro-chemical properties through surface adsorption.

Individual correlations are discussed in subsections 6.4.2 and 6.4.3.

6.4.2 Relation between Z_{r*} and $D*$

It can be seen from figures 6.1 and 6.2 that there is considerable overlap in the range $Zr^* = 0.31$ to 3.16 corresponding with $D* = 3.16$ to 10. This corresponds to the median size range $d_{50} = 0.125$ to 0.39 mm. This is near the size range into which most fluvial deposits belong, as was observed by Lane (1938). It was noted in Chapter 4 that the sediment size distribution was log-normal for the median

size in this range, and that it had the lowest standard deviation. In this size range, the particle fall velocity is of the same order of magnitude as the shear velocity, which is consistent with the analysis of Inman (1949).

Another area that shows some overlap corresponds to the range $D^* = 0.05$ to 0.1 or $d_{50} = 0.002$ to 0.004 mm. In Chapter 4, the sediment samples in this range were also found to have a log-normal distribution, but with a geometric standard deviation of about 5.

The existence of a strong correlation between Z_{r*} and D_* may be taken to signify the existence of the mixed or active bed layer referred to in section 6.2. Since both deposition and entrainment occur in this layer, it must be composed only of material that can be entrained by the flow. If this were not the case, then the bed would rapidly aggrade, thereby implying the lack of dynamic equilibrium. In the case of seasonal rivers, equilibrium may be achieved over a relatively long averaging time, with deposition and entrainment taking place during different seasons. In the case of Lake St Louis, both deposition and erosion are likely to take place simultaneously, due to the near constant discharge that results from flow regulation.

There are circumstances, however, where the existence of the mixed layer is not possible. These include rock beds, consolidated clay beds and armoured beds. In the first two cases, the flow attains a self cleansing capability, thereby preventing deposition. The equilibrium depth is then reached when the resistance to erosion offered by the

bed surface equals or exceeds the bed shear stress. Armoured beds are usually found in gravel bed rivers where the fine material is selectively entrained until the coarse material forms a protective or armour layer. The existence of an armoured bed would also imply the absence of deposition. In lake St Louis, a few stations were found to have rock beds and were not sampled. However, the majority of stations had relatively loose beds which could be sampled using ordinary bed sampling devices. It should also be remarked here that when deposition cannot occur in a lake, it is unlikely that the bed would be subject to extensive pollution as that observed in Lake St. Louis. The extent of pollution in the lake is documented in the report by Environment Canada (Champoux et al 1989).

If the material in the mixed layer can be entrained by suspension, then its size should be predictable using a suspension criteria. One of these criteria is that due to van Rijn (1984 b) and is given by the following equations:

$$\frac{\omega_s}{u_*} = \frac{D_*}{4} \; ; 1 < D_* \leq 10 \qquad (6.8a)$$

$$\frac{\omega_s}{u_*} = 2.5 \; ; D_* > 10 \qquad (6.8b)$$

Qualitatively, 6.8 a and b agree with the observed trend in figures 6.1 and 6.2, although the scatter in the region $D_* > 10$ is considerable.

A possible explanation for the observed trend, in which the smaller particles appear to require more energy per unit mass for their

suspension, may be found in the influence of near bed suspended sediment concentration. This concentration is a function of Z_r* (Lyn 1986), and increases with decreasing particle size. If it is assumed that suspended sediment dampens turbulence, then the explanation would be that the smaller sized sediments have less energy left for suspension because more is dampened out by the higher near-bed concentration. However, the effect of suspended sediment on fluid turbulence remains a controversial subject (Lyn 1986, Montes and Ippen 1973) and it is not known for certain whether turbulence dampening takes place. Nevertheless, it is plausible to assume that the presence of high concentration of suspended sediment in the near bed region would influence the suspension of bed-surface sediment. It would, for example, locally alter both the viscosity and density of the fluid. There would also be energy losses due to a large number of particle collisions. The effects of near bed concentration also seem to explain why Z_r* would remain near constant for large particle sizes as is given by van Rijn's suspension criteria. This is because the presence of large sized the bed surface particles is accompanied by lower near bed concentration. In the limit of very large particles, the near-bed suspension should be clear.

It is easy to perceive how the turbulence kinetic energy sets the lower limit of the particle size that can be deposited at a particular location. It does this merely by keeping in suspension all the particles lighter than a certain size. What is not so clear, is how the heavier particles are kept away from areas with low turbulence energy. If such particles were to be deposited in such areas, the bed

would certainly aggrade, since they would not be re-entrained by the flow. This would signify non-equilibrium conditions, since even for bed-slope equilibrium, the changes must take place slowly through mixing of grains of nearly equal sizes. It is also clear from the site data that the coarse sediments are generally not present in areas with low turbulence energy. This has also been observed in rivers, where both the energy slope and sediment size decrease in the downstream direction (Rana et al 1973). It would, therefore, appear logical to assume that the water-sediment flow system in a natural water body ensures that the path followed by a sediment particle is consistent with dynamic equilibrium requirements. Such a complex and delicate routing appears to be the work of hydraulic sorting.

6.4.3 Relation between e_r and Z_{r*} and between e_r and D_*

The explanation for correlations involving e_r are less straightforward than those described in the preceding sub-section. The reason for this is due to the complex nature of alluvial roughness. It is helpful to briefly review the factors influencing alluvial roughness before advancing interpretations of the observed correlations.

Though it is now well recognized that a strong interdependence exists between water discharge, alluvial roughness, flow depth and sediment discharge (Holly and Karim 1986, Kennedy 1983, Raudkivi 1990), the exact forms of these relationships are not yet known. The general trend is for high resistance and large water depths to occur with low water and sediment discharges. For high water discharges

the resistance may decrease, sometimes dramatically (Kennedy 1983). In contrast to flow over a fixed bed, that over mobile beds can have up to three combinations of depth and velocity for a given friction slope (Holly and Karim 1986, Raudkivi 1990).

The resistance to flow comes from skin friction, form drag and suspended sediment load. Skin friction is directly dependent on e_r for coarse sediment. It is less for mobile beds as compared to fixed beds with the same roughness. This is because the coarse sediment, unless armoured, moves as bed load thereby introducing a slip boundary. The dependence of frictional resistance on the bed load discharge is physically clear in such a case because the speed of the boundary is directly related to this discharge. The resistance due to form drag results from flow over bed forms, which are usually found in loose boundary flow with fine bed material. In the lower flow regime, the bed forms are ripples and dunes, whose sizes depend on the median particle diameter, the gradation of the particle size distribution, the flow depth and boundary shear stress (Simons and Richardson 1962). Suspended sediment load increases resistance indirectly by increasing the bulk density of the water sediment mixture and also through its influence on other properties of the fluid and flow.

The variation of the friction factor with the other quantities should be taken into account for accurate results when it is intended to model unsteady sediment transport of sediment by water (Correia 1992, Holly and Karim 1986). On the other hand, for modelling

steady or near-steady flow, particularly when dynamic equilibrium is known to prevail, it has been found that the use of Manning's formula gives reasonable results. Of the empirical friction formulae, it is perhaps the most widely used (Henderson 1966).

The applicability of a constant Manning or Chezy coefficient to natural flows over large areas may provide some explanation for the observed correlations between e_r and D_* and between e_r and Zr_*. Consider first the observed increase in er with D_*. As e_r increases, the skin friction increases as well. To maintain a near constant overall friction factor, the bed forms have to decrease in size. This is consistent with the experimental observation that bed form sizes decrease with increasing particle size. Similarly, as Z_{r*} increases, the resistance to flow decreases because there is less sediment in suspension, therefore if the overall resistance is to be the same, e_r must increase. The increase in overall frictional resistance with suspended sediment has been experimentally confirmed (Montes and Ippen 1973, Lyn 1986, 1991). The role of hydraulic sorting in the maintenance of dynamic equilibrium therefore appears to establish conditions whereby the overall resistance to flow is equal in all parts of the flow. An apparently more convincing argument would be that each particle of water follows the path of least resistance. Therefore, if one were to consider the water particles issuing from the same inlet, say Centrale Beauharnois, and subsequently re-converging at one outlet, say Lachine, then it seems plausible to reason that they have lost the same amount of energy. This would imply that they have encountered the same amount of total resistance per unit mass

irrespective of the path taken. An impediment to such an argument would be that diffusion always tries to redistribute the energy between the water particles by constantly mixing them. It would seem unrealistic in such a theoretical argument to neglect the effects of diffusion if frictional resistance is to be considered, since both are effects the same viscosity.

CHAPTER 7

SUMMARY, CONCLUSIONS AND RECOMMENDATIONS

7.1 SUMMARY

Hydraulic sorting of bed-surface sediments in a shallow regulated lake was studied. Both coarse and fine sediments were present in the bed of the lake considered. Analysis of sediment survey data showed that many of the samples with median sizes in the range 0.02-0.03 mm had log-normal particle size distributions in the 16^{th} to 84^{th} percentile range. These samples also had the lowest size spread with a geometric standard deviation of 1.4.

The flow in the lake was modelled using a finite difference model to solve the depth averaged flow equations. The suitability of this model for simulating the flow in the lake was assessed by comparing computational results with theory and the results of a physical model.

Independent dimensionless variables normally used in the study of cohesionless sediment transport were used to examine the interdependence of bed-surface sediment characteristics and flow parameters. It was found that strong interrelationships existed between all three dimensionless variables considered.

7.2 CONCLUSIONS

The results of this work show that the effect of hydraulic sorting is to create a strong interdependence between the flow parameters and sediment characteristics. In doing this, it attains and maintains a dynamic equilibrium condition. The proper understanding and appreciation of this equilibrium is important for planning engineering works that may upset it.

Analysis of the sediment data confirmed some previous research findings on particle size distributions. The lack of a strong correlation between particle size and median diameter may have been due to the different methods used in granulometric analysis of coarse and fine particles.

It appears from the observed correlations that cohesive forces need not be explicitly taken into consideration in the study of bed surface sediments with an active layer. However, the presence of a large amount of pollutants in the studied lake may have weakened these forces.

The methodology used in this work offers a convenient method of studying hydraulic sorting. The use of the modified MacCormack scheme to solve the depth-averaged flow equations and the k-ε model to compute the turbulent viscosity were found to give satisfactory results for the shallow-water two-dimensional flow that was considered.

7.3 RECOMMENDATIONS FOR FURTHER WORK

There is need to extend this work to other water bodies in order to investigate whether the correlations observed between the dimensionless variables are universal. Due to the slow processes of sorting, it is doubtful if such experiments can be economically conducted using a laboratory flume.

In the course of extension of this work, it would be preferable to carry out granulometric analysis using the same method for the entire size range present in a sediment sample. A method that determines the fall diameter eliminates the influence of particle shape and is therefore recommended. The resolution of the particle size should be such as to enable the determination of the 16^{th} percentile size. Particle specific gravity should also be determined.

List of References

Abbot, M.B. (1979). *Computational Hydraulics; Elements of the Theory of Free-Surface Flows.* Pitman, London

Abraham, G., van Os, A.G., and Verboom, G.K. (1981). "Mathematical Modeling of Flows and Transport of Conservative Substances: Requirements for Predictive ability." in *Transport Models for inland and Coastal Waters.* Proceedings of a Symposium on Predictive Ability, Ed. Fischer, H.B., Academic Press Inc., London.

Ariathurai, R. and Arulanandan, K. (1978). "Erosion Rates of Cohesive Soils." ASCE Journal of the Hydraulics Division, Vol. 104, No. HY2, pp 279-283.

Bagnold, R.A. (1954). "Experiments on the Gravity-Free Dispersion of Large Solid Spheres in a Newtonian Fluid under Shear." Proceedings of the Royal Society of London, Vol. A 225, pp 42-63.

Baldwin, B.S., MacCormack, R.W. and Deiwert, G.S. (1975). "Numerical Techniques for the Solution of the Compressible Navier-Stokes Equations and Implementation of Turbulence Models" AGARD -LS-73 on Computational Methods for Inviscid and Viscous Two- and Three- Dimensional Flow Fields, von Karman Institute, Rhode-Saint-Genese, Belgium, pp 2.1-2.24.

Boivin, R., Fau, J.P. and Hausser, R. (1982). "Projet Archipel de Montreal, Zone Sud-Est: Rapport d'Etape No. 1, Etalonnage et Conditions avant Management." Report No. LHL-851, Lassale Hydraulics Laboratory, Montreal (in French)

Bridge, J.S. (1981). "Hydraulic Interpretation of Grain-Size Distributions using a Physical Model for Bedload Transport." Journal of Sedimentary Petrology, Vol. 51, No. 4, pp 1109-1124.

Brush, L.M. Jr (1965). "Sediment Sorting in Alluvial Channels." in *Primary Sedimentary Structures and their Hydrodynamic Interpretations*. Ed. G.V. Middleton, Society of Economic Paleontologists and Mineralogists, Special Publication No. 12, pp 25-33.

Carballada, L. and Nguyen, D.L. (1982). "Projet Archipel de Montreal: Simulation Mathematique Bidimensionnale des Courants dans le Lac Saint Louis. Vol.2." Hydro-Quebec, Montreal.

Celik, I. and Rodi, W. (1991). "Suspended Sediment-Transport Capacity for Open Channel Flow." ASCE Journal of Hydraulic Engineering, Vol. 117, No. 2, pp 191-204.

Champoux, L. and Sloterdijk, H. (1988). "Etude de la Qualite des Sediments du Lac Saint-Louis (1984-1985): Rapport Technique No. 1, Geochimie et Contamination" Study Report. Environment Canada (in French).

Champoux, L., Sloterdijk, H., Couillard, Y., Jarry, V. and Ross, P. (1989). "Etude de la Qualite des Sediments du Lac Saint-Louis (1984-1985): Rapport Technique No. 2, Contamination et Toxicite des Elutriats." Study Report. Environment Canada (in French).

Chapman, R.S. (1982). "A Numerical Simulation of Two-Dimensional Separated Flow in a Symmetric Open-Channel Expansion using the Depth-Integrated Two-Equation (k-e) Turbulence Closure Model." Ph. D. Thesis, Virginia Polytechnic Institute and State University.

Chow, V.T. (1959). *Open-Channel Hydraulics*. McGraw-Hill Inc. N.Y.

Correia, L.R.P., Krishnappan, B.G. and Graf, W.H. (1992). "Fully Coupled Unsteady Mobile Boundary Flow Model." ASCE Journal of Hydraulic Engineering, Vol. 118, No. 3, pp 476-494.

Deigaard, R. (1980). "Longitudinal and Transverse Sorting of Grain Sizes in Alluvial Rivers." Series Paper No. 26, Institute of Hydrodynamics and Hydraulic Engineering, Technical University of Denmark.

Environment Canada (1986 a). "Quebec Surface Water Data 1985." IWD, Quebec Region, Water Quantity and Quality Branch, Longueuil, Canada.

Environment Canada (1986 b). "Montreal Area Hydraulic Stations Map." Inland Waters Directorate, Ottawa, Canada.

Ferguson, R.I., Prestegaard, K.L. and Ashworth, P.J. (1989). "Influence of Sand on Hydraulics and Gravel Transport in a Braided Gravel Bed River." Water Resources Research, Vol. 25, No.4, pp 635-643.

Finnie, J.I. and Jeppson, R.W. (1991). "Solving Turbulent Flows using Finite Elements." ASCE Journal of Hydraulic Engineering, Vol. 117, No. 11, pp 1513 -1530.

Fischer, H.B., List, E.J., Koh, R.C.Y. Imberger, J. and Brooks, N.H. (1979). *Mixing in Inland and Coastal Waters*. Academic Press Inc., London.

Flokstra, C. (1976). "Generation of Two-Dimensional Horizontal Secondary Currents." Research Report No. S163 Part II, Delft Hydraulics Laboratory.

Garcia, F.R. (1983). "Mathematical Modelling of Two-Dimensional Hydraulic Problems using a Fully-Dense Finite Difference Scheme." M.Sc. Thesis, University of Montreal.

Garcia, R. and Kahawita, R.A. (1986). "Numerical Solution of the St. Venant Equations with the McCormack Finite Difference Scheme." International Journal for Numerical Methods in Fluids, Vol. 6, pp 259-274.

Garcia-Navaro, P. and Saviron, J.M. (1992). "McCormack's Method for the Numerical Simulation of One-Dimensional Discontinuous Unsteady Open Channel Flow." IAHR Journal of Hydraulics Research, Vol. 30, No. 1, pp 95 106.

Garde, R.J. (1972). "Bed-Material Characteristics of Alluvial Streams." Sedimentary Geology, Vol. 7, pp 127-135.

Graf, W. H. (1984). *Hydraulics of Sediment Transport.* Water Resources Publications, Littleton, Colorado.

Henderson (1966). *Open Channel Flow.* Macmillan Publishing Co. Inc. N.Y.

Hirsch, Ch. (1990). *Numerical Computation of Internal and External flows, Vol. 2: Computational Methods for Inviscid and Viscous Flows.* John Wiley and Sons, N.Y.

Holly, F.M. Jr and Karim M.F. (1986). "Simulation of Missouri River Bed Degradation." ASCE Journal of Hydraulic Engineering, Vol 112, No.6, pp 497-517.

Inman D.L. (1949). "Sorting of Sediment in the Light of Fluid Mechanics." Journal of Sedimentary Petrology, Vol.19, No.2, pp.51-70.

Kamphius, J.W. and Hall, K.R. (1983). "Cohesive Material Erosion by Unidirectional Current." ASCE Journal of Hydraulic Engineering, Vol. 109, No. 1, pp 49-61.

Kennedy, J.F. (1983). "Reflections on Rivers Research and Rouse." ASCE Journal of Hydraulic Engineering, Vol. 109, No. 10, pp 1254-1270.

Kielland, P. (1985) "Rapport Final d'Operations: No. 80217, Lac Saint Louis." Report No. 5452-1985-1, Fisheries and Ocean Canada, Mont-Jolie, Quebec.(in French)

Kolmer, J.R. (1973). "A Wave Tank Analysis of the Beach Foreshore Grain Size Distribution." Journal of Sedimentary Petrology, Vol. 43, No.1, pp 200-204

Komar, P. D. (1987). "Selective Grain Entrainment by a Current from a Bed of Mixed Sizes: a Reanalysis." Journal of Sedimentary Petrology, Vol. 57, No.2, pp 203-211.

Lane, E.W. (1938). "Notes on the Formation of Sand." Hydrology Reports and Papers, Transactions of American Geophysical Union.

Lapidus, L. and Pinder, G.F. (1982). *Numerical Solution of Partial Differential Equations in Science and Engineering*. John Wiley and Sons, N.Y.

Lau, Y.L. and Krishnappan, B.G. (1984). "Sediment Transport under Ice Cover." Study Report No. 83-321, Hydraulics Division, NWRI, Canada Centre for Inland Waters, Burlington, Ontario.

Launder, B.E. and Spalding, D.B. (1974). "The Numerical Computation of Turbulent Flows." Computer Methods In Applied Mechanics and Engineering, Vol. 3, pp 269-289.

Little, W.C. and Mayer, P.G. (1976). "Stability of Channel Beds by Armouring" ASCE Journal of the Hydraulics Division Vol. 102, no. HY11, pp 1647-1661.

Lopez S., J.L. (1978). "Mathematical Modelling of Sediment Deposition in Reservoirs." Hydrology Paper No. 95, Colorado State University.

Lowright, R. , Williams, E.G and Dachille F. (1972). "An Analysis of Factors Controlling Deviations in Hydraulic Equivalence in some Modern Sands." Journal of Sedimentary Petrology Vol.42, No.3, pp 635-645.

Lyn, D.A. (1986). "Turbulence and Turbulent Transport in Sediment-Laden Open-Channel Flows." Report No. KH-R-49, W.M. Keck Laboratory of Hydraulics and Water Resources, California Institute of Technology.

Lyn, D.A. (1991). "Resistance in Flat-Bed Sediment-Laden Flows." ASCE Journal of Hydraulic Engineering, Vol. 117, No. 1, pp 94 -114.

MacCormack, R.W. (1969). "The Effect of Viscosity in Hypervelocity Impact Cratering." AIAA paper No. 69-354, AIAA Hypervelocity Conference, Cincinnati, Ohio, April 30 - May 2. pp1-6.

Mehta, A.J. and Partheniades E. (1975). " An Investigation of the Depositional Properties of Flocculated Fine Sediments" IAHR Journal of Hydraulics Research, Vol. 13, No. 4, PP 361-381.

Mehta, A.J., Hayter, E.J., Parker, W.R., Krone, R.B. and Teeter, A.M. (1989 a). "Cohesive Sediment Transport, Part 1: Process Description." ASCE Journal of Hydraulic Engineering, Vol. 115, No. 8, pp 1076-1093.

Mehta, A.J., McAnnaly, W.H., Hayter, E.J., Teeter, A.M. Schoellhamer, D., Heltzel, S.B. and Carey, W.P. (1989 b). "Cohesive Sediment Transport, Part 2: Application." ASCE Journal of Hydraulic Engineering, Vol. 115, No. 8, pp 1094-1112.

Meland, N. and Norrman, J.O. (1969). "Transport Velocities of Individual Size Fractions in Heterogeneous Bed Load." Geografiska Annaler, vol. 51A, No. 3, pp 127-144.

Middleton, G.V. (1976). "Hydraulic Interpretation of Sand Size Distributions." Journal of Geology, Vol. 84, pp 405-426

Montes, J.S. and Ippen, A.T. (1973). "Interaction of Two-dimensional Turbulent Flow with Suspended Particles." Report No. 164, Ralph M. Parsons Laboratory, Massachusetts Institute of Technology.

Parchure, T.M. and Mehta, A.J. (1985). "Erosion of Soft Cohesive Sediment Deposits." ASCE Journal of Hydraulic Engineering, Vol. 111, No. 10, pp 1308-1326.

Parker, G. (1990). "Surface-based Bedload Transport relation for gravel rivers." IAHR Journal of Hydraulic Research, Vol. 28, No. 4 pp 417-436

Patankar, S.V. (1980). *Numerical Heat Transfer and Fluid Flow.* Hemisphere Publishing Corpor on, N.Y.

Plouffe, R.P. (1987). "Two-Dimensional Modelling of Local Ice Cover Melting due to Thermal Effluent." M.Eng. Thesis, Concordia University, Montreal.

Rahuel, J.L., Holly, F.M., Chollet, J.P., Belleudy, P.J.; and Yang, G. (1989). "Modeling of Riverbed Evolution for Bedload Sediment Mixtures." ASCE Journal of Hydraulic Engineering, Vol. 115, No. 11, pp 1521 -1542.

Rana, S.A., Simons D.B., and Mahmood K., (1973). "Analysis of Sediment Sorting in Alluvial Channels." ASCE Journal of the Hydraulics Division, Vol. 99, No. HY11, pp 1967-1980.

Rastogi, A.K. and Rodi, W. (1978). "Predictions of Heat and Mass Transfer in Open Channels." ASCE Journal of the Hydraulics Division, Vol. 104, No. HY3, pp 397-419.

Raudkivi, A.J. (1990). *Loose Boundary Hydraulics*. 3rd Ed. Pergamon Press, N. Y.

Roache, P.J. (1976). *Computational Fluid Dynamics*. Hermosa Publishers, Albuquerque, N.M.

Rodi, W. (1984). "Turbulence Models and their Application in Hydraulics: a State of the Art Review." 2nd Ed. IAHR report

Rubey, W.W. (1933). "The Size-Distribution of Heavy Minerals within a Water-Laid Sandstone." Journal of Sedimentary Petrology, Vol. 3, No. 1, pp. 3-29.

Rukavina, N.A. (1986). "Lac St. Louis Bottom-Sediment Data." Interim Report. Hydraulics Division, NWRI, Canada Centre for Inland Waters, Burlington, Ontario.

Saade, R.G. (1990). "Numerical Modelling of Ice Cover Melting under Turbulent Flow Conditions." M.A.Sc. Thesis, Concordia University, Montreal.

Sarraf, S. and Saade, R.G. (1990). "Ice Cover Melting under Turbulent Flow Conditions." Proceedings of the ASME International Computers in Engineering Conference and Exposition, Boston Mass. 5-9 August, Vol.2, pp 313-316.

Schlichting, H. (1979). *Boundary Layer Theory*. Mc-Graw Hill Book Company, N.Y.

Sengupta, S. (1975). "Size-Sorting during Suspension Transportation - Lognormality and other Characteristics." Sedimentology, Vol. 22, pp 257-273.

Sengupta, S. (1979). "Grain-Size Distribution of Suspended Load in Relation to Bed Materials and Flow Velocity." Sedimentology, Vol. 26, pp 63-82

Simonin, O., Uittenbogaard, R.E., Baron, F. and Viollet, P.L. (1989). "Possibilities and Limitations to Simulate Turbulent Fluxes of Mass and Momentum, measured in a Steady, Stratified Mixing Layer." Proceedings of xxiii IAHR Congress, Ottawa Canada, 21-25 August, pp A55-A62.

Simons, D.B. and Senturk, F. (1976). *Sediment Transport Technology*. Water Resources Publications, Fort Collins, Colorado.

Simons, D.B., Richardson E.V. (1961). "Forms of Bed Roughness in Alluvial Channels." ASCE Journal of the Hydraulics Division, Vol.87, No HY3, pp 87-105.

Slingerland, R. (1984). "Role of Hydraulic Sorting in the Origin of Fluvial Placers." Journal of Sedimentary Petrology, Vol. 54, No. 1, pp 137 - 150

Steidtmann, J.R. (1982). "Size-Density Sorting of Sand Spheres during Deposition from Bedload Transport and Implications concerning Hydraulic Equivalence." Sedimentology, Vol. 29, pp 877-883

Stelczer, K. (1981). *Bedload Transport: Theory and Practice*. Water Resources Publication, Littleton, Colorado.

Stichling, W. (1974). "Sediment Loads in Canadian Rivers." Technical Bulletin No. 74, IWD, Water Resources Branch, Ottawa, Canada.

Thomas, W.A. and Prasuhn, A.L. (1977). "Mathematical Modelling of Scour and Deposition." ASCE Journal of the Hydraulics Division, Vol. 103, No. HY8 pp 851-863.

Thorn, M.F.C. and Parsons, J.G. (1980). "Erosion of Cohesive Sediments in Estuaries: an Engineering Guide." Third International

Symposium on Dredging Technology, Bordeaux, France 5-7 March. Published by BHRA.

van Niekerk, A., Vogel, K.R., Slingerland, R.L. and Bridge, J.S. (1992). "Routing of Heterogeneous Sediments over Movable Bed: Model Development." ASCE Journal of Hydraulic Engineering, Vol 118, No. 2, pp 246-262.

van Rijn, L.C. (1984 a). "Sediment Transport, Part I: Bedload Transport." ASCE Journal of Hydraulic Engineering, Vol. 110, No. 10, pp 1431-1456.

van Rijn, L.C. (1984 b). "Sediment Transport, Part II: Suspended Sediment Transport" ASCE Journal of Hydraulic Engineering, Vol. 110, No. 11, pp 1613-1641.

Vanoni, V.A. (1944). "Transportation of Suspended Sediment by Water" Transactions of the American Society of Civil Engineers, Paper No. 2267

Visher, G.S. (1969). "Grain Size Distributions and Depositional Processes." Journal of Sedimentary Petrology, Vol. 39, No. 3, pp.1074-1106.

Wilcock, P.R. and Southard J.B. (1988). "Experimental Study of Incipient Motion in Mixed-Size Sediment." Water Resources Research, Vol.24, No.7 pp. 1137-1151.

Symposium on Dredging Technology, Bordeaux, France 5-7 March. Published by BHRA.

van Niekerk, A., Vogel, K.R., Slingerland, R.L. and Bridge, J.S. (1992). "Routing of Heterogeneous Sediments over Movable Bed: Model Development." ASCE Journal of Hydraulic Engineering, Vol 118, No. 2, pp 246-262.

van Rijn, L.C. (1984 a). "Sediment Transport, Part I: Bedload Transport." ASCE Journal of Hydraulic Engineering, Vol. 110, No. 10, pp 1431-1456.

van Rijn, L C. (1984 b). "Sediment Transport, Part II: Suspended Sediment Transport" ASCE Journal of Hydraulic Engineering, Vol. 110, No. 11, pp 1613-1641.

Vanoni, V.A. (1944). "Transportation of Suspended Sediment by Water" Transactions of the American Society of Civil Engineers, Paper No. 2267

Visher, G.S. (1969). "Grain Size Distributions and Depositional Processes." Journal of Sedimentary Petrology, Vol. 39, No. 3, pp.1074-1106.

Wilcock, P.R. and Southard J.B. (1988). "Experimental Study of Incipient Motion in Mixed-Size Sediment." Water Resources Research, Vol.24, No.7 pp. 1137-1151.

Yalin, M.S. (1972). *Mechanics of Sediment Transport.* Pergamon Press, N.Y.

Yang, C.T. (1984). "Unit Stream Power Equation for Gravel." ASCE Journal of Hydraulic Engineering, Vol. 110, No. 12, pp 1783-1798.

Yang, C.T., Molinas A. and Song C.S.S (1988). "GSTARS - Generalized stream Tube Model for Alluvial River Simulation"in *Twelve Selected Computer Models developed in the United States.* Ed. Fau S. S., US Federal Energy Regulatory Committee, Washington.

Zhang, X.T. (1992). "Two-Dimensional Numerical Modeling of Ice-cover Leading Edge. " M.A.Sc. Thesis, Concordia University, Montreal

Zhang, X.T., Sarraf, S. and El-Jabi, N. (1991). "The Role of Heat Transfer Coefficient in Modelling Ice Cover Melting." Proceedings of The 1991 Annual Conference of the Canadian Society for Civil Engineers, Vancouver, B.C., 29-31, May. Vol. 4. pp 383-392.

APPENDIX A

Contents:

Table A: Lake St. Louis Bottom Sediment Data

Source: Rukavina (1986)

Notes: (1) Figures shown are cumulative percentages finer than corresponding sizes.

(2) Pre-fix SL shown against station number denotes Saint Louis

(3) Numbers shown for 16th, 50th and 84th are corresponding percentile sizes in Phi Units

TABLE A: LAC ST. LOUIS BOTTOM SEDIMENT SIZE DATA

SIZE	STATION						
(PHI)	SL001	SL002	SL003	SL004	SL005	SL006	SL007
-3.50	-	-	-	-	-	-	-
-3.00	-	-	-	-	-	-	-
-2.50	-	-	-	-	-	-	-
-2.00	-	-	-	-	-	-	
-1.50	-	-	-	-	-	-	
-1.00	-	-	-	-	-	-	-
-0.50	100.00	100.00	100.00	100.00	100.00	100.00	100.00
0.00	100.00	99.96	100.00	99.77	100.00	100.00	98.95
0.50	99.97	99.82	99.84	99.65	99.97	99.89	91.07
1.00	99.06	99.63	99.34	99.53	99.93	99.57	84.24
1.50	93.12	99.45	97.70	97.44	99.93	97.85	77.94
2.00	88.74	98.89	94.73	95.34	99.83	96.78	70.58
2.50	84.99	97.04	89.80	93.95	99.48	95.70	62.18
3.00	79.98	94.82	86.83	92.55	98.44	95.27	52.72
3.50	77.17	92.61	85.19	91.39	96.00	94.41	50.62
4.00	76.23	91.13	84.20	90.46	93.05	93.77	50.62
4.50	75.02	91.13	84.20	90.46	93.05	93.77	50.62
5.00	75.02	91.13	84.20	89.57	90.08	92.47	50.62
5.50	73.57	89.00	82.37	86.92	89.28	91.03	49.22
6.00	71.15	85.51	81.46	85.15	86.71	88.17	48.94
6.50	66.79	80.50	77.98	81.72	79.19	84.91	47.11
7.00	60.50	73.66	73.22	77.52	71.27	79.18	44.30
7.50	53.73	66.83	69.56	71.55	61.57	72.28	37.97
8.00	49.37	59.23	65.53	67.68	55.23	67.59	35.16
8.50	41.38	53.16	63.52	63.03	48.70	63.16	32.20
9.00	32.67	45.11	56.20	57.83	38.41	56.65	28.12
16TH	11.00	11.37	13.84	13.38	10.67	12.58	11.26
50TH	7.93	8.70	9.63	9.7	8.40	9.49	5.22
84TH	2.60	6.15	5.05	6.17	6.18	6.58	1.02

TABLE A (Cont'd)

SIZE	STATION						
(PHI)	SL008	SL009	SL010	SL011	SL012	SL013	SL014
-3.50	-	-	-	-	-	-	-
-3.00	-	-	-	-	-	-	-
-2.50	-	-	-	-	-	-	-
-2.00	-	-	-	-	-	-	-
-1.50	-	-	-	-	-	-	-
-1.00	-	-	-	100.00	100.00	-	-
-0.50	100.00	100.00	100.00	91.84	93.76	100.00	100.00
0.00	100.00	100.00	100.00	88.93	92.23	100.00	100.00
0.50	100.00	99.92	99.98	55.39	81.51	100.00	99.94
1.00	99.96	99.85	99.95	32.06	67.73	99.95	99.94
1.50	99.81	99.39	99.76	11.65	53.95	99.54	99.87
2.00	99.62	99.09	98.55	7.27	40.17	99.32	99.49
2.50	99.43	98.93	98.07	5.82	24.86	99.09	97.43
3.00	99.24	98.48	96.86	5.09	14.14	98.63	95.88
3.50	98.49	97.11	95.65	4.36	11.85	98.18	93.57
4.00	98.33	95.58	95.16	4.36	11.85	97.27	90.99
4.50	98.02	94.66	95.16	-	-	95.88	90.99
5.00	96.59	93.73	93.93	-	-	94.77	88.67
5.50	93.27	92.43	91.81	-	-	91.57	86.82
6.00	89.01	89.28	90.13	-	-	89.49	83.57
6.50	84.74	84.47	85.42	-	-	84.49	80.08
7.00	77.78	76.50	78.93	-	-	77.68	70.80
7.50	68.30	69.09	72.66	-	-	69.48	59.19
8.00	61.02	60.20	64.94	2.50	7.30	62.53	49.44
8.50	52.96	58.35	57.10	-	-	53.08	41.32
9.00	44.11	41.49	47.02	-	-	44.74	30.18
16TH	10.72	10.68	11.50	1.39	2.91	11.06	9.95
50TH	8.67	8.75	8.85	0.62	1.64	8.68	7.97
84TH	6.55	6.53	6.61	0.07	0.38	6.54	5.93

TABLE A (Cont'd)

SIZE	STATION						
(PHI)	SL015	SL016	SL017	SL018	SL019	SL020	SL021
-3.50	-	-	-	-	-	-	-
-3.00	-	-	-	-	-	-	-
-2.50	-	-	-	-	-	-	-
-2.00	-	-	-	-	-	-	-
-1.50	-	-	-	-	-	-	
-1.00	-	-	-	-	-	-	-
-0.50	-	100.00	100.00	100.00	100.00	100.00	100.00
0.00	-	100.00	100.00	100.00	99.30	99.98	99.93
0.50	-	100.00	99.91	99.32	97.91	99.91	99.87
1.00	-	100.00	99.81	93.17	96.51	99.55	99.73
1.50	-	99.85	99.53	81.56	91.63	99.01	99.34
2.00	-	99.09	99.25	46.72	86.05	97.31	98.01
2.50	-	97.58	98.13	22.82	85.36	93.04	97.67
3.00	-	96.97	97.20	19.40	79.08	86.53	97.34
3.50	100.00	95.46	96.08	18.03	70.71	80.91	97.08
4.00	43.20	93.95	95.33	17.35	37.24	76.42	96.01
4.50	43.20	93.33	95.05	17.35	36.79	74.42	96.01
5.00	43.20	91.97	93.77	16.68	35.96	70.72	94.81
5.50	40.66	88.14	91.50	15.52	33.97	65.30	91.38
6.00	34.31	86.28	89.38	14.65	31.78	60.74	88.81
6.50	26.68	81.34	82.85	13.30	29.41	54.32	83.84
7.00	20.33	74.54	77.74	10.80	26.20	49.76	76.12
7.50	13.98	68.11	68.38	8.48	22.92	43.20	69.61
8.00	12.71	61.81	60.86	7.33	20.48	39.21	61.72
8.50	-	55.13	50.65	5.69	17.34	32.36	54.69
9.00	-	46.23	43.?'	2.89	14.13	26.38	43.72
16TH	7.34	11.63	10.75	5.29	8.71	10.87	10.97
50TH	4.00	8.79	8.54	1.95	3.81	6.97	8.71
84TH	3.75	6.23	6.41	1.39	2.61	3.22	6.48

TABLE A (Cont'd)

SIZE (PHI)	STATION						
	SL022	SL024	SL025	SL026	SL027	SL028	SL029
-3.50	-	-	-	-	-	-	-
-3.00	-	-	-	-	-	-	-
-2.50	-	-	100.00	-	-	-	-
-2.00	-	-	96.62	-	-	-	-
-1.50	-	-	95.89	-	-	-	-
-1.00	-	-	93.61	-	-	-	-
-0.50	100.00	100.00	90.05	100.00	100.00	100.00	100.00
0.00	100.00	100.00	84.49	99.86	99.72	100.00	99.81
0.50	100.00	99.91	71.26	99.66	90.82	100.00	99.22
1.00	99.97	99.73	37.96	99.32	85.17	100.00	97.81
1.50	99.54	99.45	12.32	98.98	69.63	99.98	96.87
2.00	99.42	98.72	4.93	98.81	42.08	99.82	95.30
2.50	98.84	97.07	2.01	98.64	21.95	99.65	93.10
3.00	98.55	91.84	0.82	98.51	11.71	99.30	87.30
3.50	98.26	84.82	0.36	98.51	7.47	95.61	76.33
4.00	95.06	79.16	0.18	98.37	6.06	91.04	69.28
4.50	93.25	77.45	-	98.37	-	90.30	68.68
5.00	91.03	74.05	-	98.06	-	82.72	68.68
5.50	89.02	68.09	-	95.88	-	69.75	55.54
6.00	86.60	65.03	-	90.42	-	64.36	50.77
6.50	79.15	57.88	-	85.74	-	53.84	44.20
7.00	71.50	52.77	-	77.01	-	46.50	38.46
7.50	58.41	45.62	-	66.41	-	36.95	33.45
8.00	50.15	40.68	-	59.87	2.05	31.81	28.67
8.50	40.28	36.26	-	50.67	-	24.47	25.20
9.00	30.61	28.26	-	42 72	-	15.91	19.83
16TH	9.88	10.83	1.43	10.16	2.79	8.99	9.68
50TH	8.01	7.19	0.82	8.54	1.86	6.76	6.06
84TH	6.17	3.57	0.02	6.60	1.04	4.92	3.15

TABLE A (Cont'd)

SIZE	STATION						
(PHI)	SL030	SL031	SL032	SL033	SL034	SL035	SL036
-3.50	-	100.00	93.66	-	-	-	-
-3.00	-	85.61	89.14	-	-	-	-
-2.50	-	79.71	78.80	-	-	100.00	-
-2.00	-	76.09	73.57	-	-	99.58	-
-1.50	100.00	72.96	66.76	-	-	98.38	-
-1.00	99.97	71.15	62.81	-	-	97.04	-
-0.50	99.94	68.34	61.60	100.00	100.00	94.43	100.00
0.00	99.72	67.84	60.90	99.94	99.95	94.15	100.00
0.50	99.46	58.85	56.69	99.85	99.87	81.01	99.89
1.00	98.83	51.85	53.18	98.21	99.74	70.46	99.47
1.50	98.20	39.85	44.07	91.66	99.21	61.83	97.90
2.00	86.90	31.60	30.04	78.55	98.69	51.28	97.37
2.50	43.50	25.36	13.90	45.78	98.27	36.90	97.16
3.00	14.05	17.86	10.40	30.28	97.64	25.87	97.06
3.50	4.60	11.86	9.69	30.10	95.80	20.12	96.85
4.00	0.54	9.36	8.99	29.98	90.55	17.91	93.70
4.50	-	9.15	8.99	29.98	88.42	17.01	92.83
5.00	-	8.72	8.80	29.79	83.41	16.33	90.73
5.50	-	8.30	8.75	29.32	79.46	15.32	88.38
6.00	-	7.87	8.51	28.94	74.66	14.64	84.06
6.50	-	7.02	7.83	26.84	70.72	13.52	77.87
7.00	-	6.38	6.85	24.75	65.60	12.84	71.69
7.50	-	5.53	5.93	22.46	58.66	11.21	63.78
8.00	-	5.11	5.59	21.42	53.01	9.86	58.47
8.50	-	4.47	4.96	19.99	48.00	9.80	51.79
9.00	-	4.25	4.28	18.09	42.66	8.45	44.50
16TH	2.97	3.15	2.44	10.19	11.84	5.16	11.47
50TH	2.43	10.7	1.17	2.44	8.30	2.04	8.62
84TH	2.03	-2.86	-2.75	1.79	4.94	0.39	6.00

TABLE A (Cont'd)

SIZE	STATION						
(PHI)	SL037	SL038	SL039	SL040	SL041	SL042	SL043
-3.50	-	-	-	-	-	100.00	-
-3.00	-	-	-	-	-	94.91	-
-2.50	-	-	-	-	-	94.45	-
-2.00	-	-	-	100.00	-	93.88	-
-1.50	-	-	-	99.76	-	92.65	-
-1.00	-	-	-	99.64	-	91.93	-
-0.50	100.00	100.00	100.00	99.35	-	91.00	100.00
0.00	99.97	100.00	100.00	99.35	100.00	90.53	99.53
0.50	98.62	99.91	99.97	97.85	99.79	90.38	99.42
1.00	93.12	99.68	99.94	93.84	96.49	89.12	97.67
1.50	90.37	98.90	99.53	89.84	89.25	85.37	95.34
2.00	87.61	98.11	98.14	82.32	57.61	80.98	89.50
2.50	84.86	95.27	85.41	67.30	27.34	66.57	66.18
3.00	81.42	87.85	56.24	42.25	13.99	29.92	31.19
3.50	64.91	79.49	48.80	30.23	6.64	21.46	23.03
4.00	50.46	69.39	42.90	16.70	3.60	20.21	21.86
4.50	48.29	66.73	41.08	16.70	-	19.92	21.47
5.00	45.43	58.60	36.88	15.77	-	19.49	21.08
5.50	42.74	48.48	36.40	15.16	-	19.41	20.86
6.00	41.01	44.86	31.72	15.16	-	18.77	20.08
6.50	38.15	44.02	29.71	13.36	-	17.83	19.52
7.00	35.37	37.99	26.66	11.44	-	16.60	18.63
7.50	35.37	33.08	23.50	9.65	-	16.09	17.62
8.00	30.86	29.86	21.21	8.60	-	15.01	16.45
8.50	26.44	27.34	18.82	8.04	-	13.64	15.51
9.00	23.15	23.41	16.82	6.93	-	12.85	14.50
16TH	10.09	10.26	9.38	4.88	2.92	7.54	8.24
50TH	4.11	5.44	3.42	2.85	2.13	2.73	2.73
84TH	2.63	3.23	2.52	1.89	1.58	1.66	2.12

TABLE A (C ont'd)

SIZE	STATION						
(PHI)	SL044	SL045	SL047	SL048	SL049	SL050	SL051
-3.50	-	-	-	-	-	-	100.00
-3.00	-	-	-	-	-	-	96.44
-2.50	-	-	-	-	-	-	86.64
-2.00	-	-	-	100.00	-	-	84.97
-1.50	-	-	-	97.48	-	100.00	81.37
-1.00	-	-	-	96.56	-	98.37	80.04
-0.50	100.00	100.00	100.00	89.58	100.00	96.19	78.94
0.00	99.98	100.00	99.91	89.04	100.00	96.19	77.25
0.50	99.95	100.00	99.83	54.00	100.00	94.68	74.52
1.00	99.81	99.97	99.74	46.99	99.97	90.91	66.20
1.50	99.30	99.31	99.66	41.60	99.92	87.13	51.25
2.00	98.61	98.62	99.49	38.36	99.72	80.72	25.52
2.50	98.14	98.55	99.32	35.67	99.58	63.73	5.79
3.00	97.22	98.48	99.23	31.36	99.31	37.68	2.09
3.50	92.81	97.51	97.78	23.27	94.17	28.25	0.74
4.00	87.93	93.08	91.46	20.03	81.39	22.96	0.26
4.50	85.90	92.48	89.87	20.03	73.13	21.52	-
5.00	80.49	89.51	87.25	20.03	61.08	21.10	
5.50	75.76	84.99	83.73	19.73	52.82	19.23	
6.00	71.83	78.80	79.15	19.43	48.48	18.56	
6.50	66.02	72.01	73.62	18.21	44.42	17.62	
7.00	60.88	64.87	67.26	17.60	40.63	16.18	-
7.50	54.11	57.01	61.24	16.27	36.57	14.24	
8.00	48.43	50.94	55.67	15.12	33.18	13.05	-
8.50	44.91	45.11	49.99	13.36	30.07	11.18	
9.00	38.83	38.68	43.63	12.14	26.14	10.34	
16TH	11.23	10.70	11.65	7.62	10.98	7.05	7.24
50TH	7.86	8.08	8.50	0.79	5.83	2.76	1.53
84TH	4.68	5.58	5.46	0.07	3.90	1.72	1.87

TABLE A (Cont'd)

SIZE (PHI)	STATION						
	SL052	SL053	SL054	SL055	SL056	SL057	SL058
-3.50	-	-	-	-	-	-	-
-3.00	-	-	-	-	-	100.00	100.00
-2.50	-	100.00	100.00	-	100.00	92.51	87.02
-2.00	-	99.54	99.58	-	99.67	84.96	74.48
-1.50	-	99.00	99.86	-	98.51	71.46	54.37
-1.00	-	97.82	97.69	-	96.98	57.34	42.21
-0.50	100.00	95.59	96.68	100.00	95.29	44.25	37.15
0.00	100.00	95.59	96.68	99.80	95.29	43.57	36.81
0.50	100.00	85.20	92.07	99.60	92.98	29.28	32.79
1.00	100.00	77.05	86.31	99.21	70.70	24.17	30.95
1.50	99.48	62.22	82.86	97.04	53.80	17.70	29.44
2.00	98.96	34.04	80.55	96.05	26.15	12.26	26.25
2.50	98.61	13.28	78.54	94.07	13.09	8.86	21.06
3.00	94.11	7.35	69.61	92.10	9.25	6.64	17.71
3.50	66.38	5.50	48.30	91.70	7.71	6.47	17.21
4.00	42.81	5.13	38.51	89.72	6.94	6.47	17.04
4.50	38.26	-	35.72	89.72	-	6.47	17.04
5.00	31.88	-	31.09	89.72	-	6.47	17.04
5.50	30.06	-	28.30	89.72	-	5.86	15.88
6.00	28.24	-	26.45	89.72	-	5.86	15.02
6.50	24.59	-	25.05	87.20	-	5.24	13.57
7.00	21.86	-	20.41	83.17	-	4.32	11.55
7.50	16.40	-	19.07	78.63	-	3.08	9.82
8.00	14.57	3.84	16.70	74.60	3.40	1.85	8.37
8.50	12.75	-	14.85	69.56	-	1.85	6.35
9.00	9.11	-	13.45	63.51	-	0.62	4.62
16TH	7.61	2.43	8.19	13.50	2.39	1.66	5.45
50TH	3.85	1.72	3.46	10.12	1.57	-0.72	-1.32
84TH	3.18	0.57	1.33	6.90	0.70	-1.96	-2.38

TABLE A (Cont'd)

SIZE	STATION						
(PHI)	SL059	SL060	SL061	SL062	SL063	SL064	SL065
-3.50	-	-	-	-	-	-	-
-3.00	-	-	-	-	-	-	-
-2.50	-	-	-	-	-	100.00	-
-2.00	-	-	-	-	-	98.47	-
-1.50	-	-	-	-	-	97.95	-
-1.00	-	-	-	-	-	96.76	100.00
-0.50	100.00	100.00	100.00	100.00	100.00	95.42	99.96
0.00	100.00	99.52	100.00	99.97	100.00	95.42	98.20
0.50	99.97	99.05	99.96	99.76	99.81	89.36	94.72
1.00	99.86	95.24	99.93	98.18	98.87	80.61	87.89
1.50	99.72	90.48	99.45	92.72	97.73	71.18	79.87
2.00	99.56	80.96	97.79	84.84	95.28	55.69	67.69
2.50	99.48	78.58	95.22	66.03	86.78	32.80	27.84
3.00	99.20	77.15	81.96	30.25	72.42	25.39	4.56
3.50	96.87	76.20	40.37	19.93	54.29	24.38	0.60
4.00	90.08	42.87	28.59	16.29	43.71	24.05	0.07
4.50	88.74	42.07	-	-	39.48	23.53	
5.00	83.36	39.30	-	-	33.13	22.51	-
5.50	78.65	34.93	-	-	29.61	22.00	-
6.00	73.95	32.15	-	-	26.79	20.46	-
6.50	67.90	28.18	-	-	23.97	17.39	
7.00	61.17	25.40	-	-	20.44	15.35	
7.50	53.78	21.83	-	-	15.51	12.28	
8.00	48.40	18.26	7.95	5.11	12.69	10.23	
8.50	41.68	15.48	-	-	9.87	7.67	
9.00	34.96	12.70	-	-	6.34	4.60	
16TH	10.92	8.41	6.44	4.11	7.45	6.84	2.75
50TH	7.85	3.89	3.38	2.72	3.70	2.12	2.22
84TH	4.94	1.84	2.92	2.02	2.60	81	1.24

TABLE A (Cont'd)

SIZE (PHI)	STATION						
	SL066	SL067	SL070	SL071	SL072	SL073	SL074
-3.50	-	-	-	-	-	-	-
-3.00		-	-	-	-	-	-
-2.50	-	-	-	-	-	-	-
-2.00	-	-	-	-	-	-	-
-1.50	-	-	-	-	-	-	-
1.00		-	-	-	-	-	-
-0.50	100.00	100.00	100.00	-	100.00	100.00	100.00
0.00	99.95	100.00	99.45	-	100.00	100.00	100.00
0.50	99.63	99.20	98.07	-	99.91	99.88	99.93
1.00	99.30	95.22	95.58	-	99.72	99.54	99.82
1.50	97.75	86.18	93.37	-	98.88	98.15	97.85
2.00	94.01	75.55	90.34	-	98.69	96.30	94.28
2.50	91.51	65.98	86.47	-	98.50	93.21	80.68
3.00	88.51	55.88	84.13	-	98.13	75.31	55.29
3.50	76.03	42.59	83.44	100.00	94.58	38.89	33.46
4.00	55.06	33.02	82.88	99.15	84.67	29.01	19.87
4.50	46.23	27.33	82.88	99.15	79.50	25.60	17.43
5.00	33.76	19.36	82.74	97.08	69.80	20.05	14.67
5.50	27.01	15.94	82.00	91.58	59.46	17.07	12.84
6.00	23.89	13.66	81.11	84.69	54.94	15.36	12.23
6.50	20.78	11.39	79.78	77.81	49.77	14.51	10.39
7.00	18.70	9.11	78.01	69.54	45.89	12.80	9.78
7.50	15.06	6.26	74.91	61.28	40.07	11.09	7.95
8.00	13.50	3.98	74.02	53.71	34.90	9.39	7.03
8.50	10.91	2.28	71.80	48.20	31.67	8.11	6.11
9.00	8.31	1.14	69.14	37.87	26.50	5.55	4.28
16TH	7.37	5.49	21.95	10.63	10.63	5.81	4.76
50TH	4.29	3.22	13.22	8.34	6.48	3.35	3.12
84TH	3.18	1.60	3.09	6.05	4.06	2.76	2.38

TABLE A (Cont'd)

SIZE	STATION						
(PHI)	SL075	SL076	SL077	SL078	SL81	SL82	SL83
-3.50	-	100.00	-	-	-		-
-3.00	-	94.99	-	-	-	-	-
-2.50	100.00	87.60	-	-	-	-	
-2.00	98.77	77.76	100.00	-	-	-	
-1.50	96.45	66.40	99.81	-	-		
-1.00	94.76	59.59	99.66	-	-		
-0.50	93.72	54.20	98.92	100.00	100.00	100.00	100.00
0.00	93.61	50.60	97.94	99.95	100.00	99.70	100.00
0.50	87.68	46.20	94.80	99.22	99.95	95.50	99.95
1.00	76.62	37.45	84.63	95.61	99.87	94.00	99.75
1.50	60.53	26.78	58.95	92.25	98.97	92.79	98.51
2.00	41.42	16.42	18.11	85.53	98.46	91.89	97.52
2.50	25.33	9.17	2.46	77.26	98.20	90.69	96.53
3.00	12.26	2.00	0.33	66.40	96.91	89.94	96.04
3.50	6.23	0.33	0.08	45.73	92.29	89.19	95.05
4.00	5.22	0.04	0.02	32.03	87.15	88.14	90.09
4.50	-	-	-	25.00	84.38	88.14	88.32
5.00	-	-	-	16.79	78.15	86.20	80.38
5.50	-	-	-	13.67	70.55	83.78	72.43
6.00	-	-	-	13.28	63.63	81.36	66.24
6.50	-	-	-	11.72	56.71	78.46	60.06
7.00	-	-	-	10.15	48.41	73.61	55.64
7.50	-	-	-	7.81	42.19	69.25	47.70
8.00	2.18	-	-	7.42	36.66	64.41	41.51
8.50	-	-	-	6.64	32.51	60.05	36.21
9.00	-	-	-	5.86	24.90	54.72	28.26
16TH	2.86	2.03	2.07	5.13	9.94	13.76	10.37
50TH	1.78	.07	1.61	3.40	6.90	9.49	7.36
84TH	.67	-2.32	1.01	2.09	4.53	5.46	4.77

TABLE A (Cont'd)

SIZE (PHI)	STATION						
	SL084	SL085	SL086	SL087	SL088	SL089	SL090
-3.50	-	-	-	-	96.61	-	-
-3.00	-	-	-	-	86.18	-	-
-2.50	-	-	-	100.00	74.07	-	-
-2.00	-	-	100.00	97.83	66.97	-	-
-1.50	-	-	99.89	92.31	60.68	-	-
-1.00	-	-	99.81	86.44	55.96	-	-
-0.50	100.00	100.00	99.66	81.96	52.18	100.00	-
0.00	100.00	100.00	99.66	78.64	52.06	100.00	-
0.50	100.00	99.95	99.52	70.79	45.29	99.96	-
1.00	99.98	99.90	96.34	52.30	39.88	99.78	-
1.50	99.62	99.24	92.47	21.05	29.55	98.68	-
2.00	99.06	98.49	87.49	4.89	14.79	97.81	-
2.50	98.87	88.93	78.09	1.52	7.90	96.05	-
3.00	96.79	52.68	55.41	0.47	3.96	91.23	-
3.50	83.75	20.47	31.08	0.32	2.98	62.29	100.00
4.00	63.72	12.41	22.78	0.16	2.73	26.34	61.25
4.50	51.89	10.41	20.41	-	-	19.59	47.95
5.00	38.76	8.01	18.51	-	-	10.81	33.04
5.50	32.84	7.21	15.66	-	-	8.10	25.79
6.00	30.22	6.81	14.71	-	-	8.10	19.34
6.50	26.93	6.41	13.29	-	-	6.75	14.91
7.00	23.65	5.21	10.92	-	-	4.73	10.48
7.50	21.02	4.00	9.02	-	-	2.70	8.46
8.00	18.39	4.00	7.59	-	1.56	2.70	6.45
8.50	14.45	2.40	6.64	-	-	2.03	5.24
9.00	11.82	1.60	5.22	-	-	0.68	-
16TH	8.30	3.78	5.44	1.66	1.96	4.70	6.38
50TH	4.57	3.04	3.11	1.04	0.15	3.67	4.42
84TH	3.49	2.57	2.19	-0.73	-2.91	3.12	1.88

TABLE A (Cont'd)

SIZE	STATION						
(PHI)	SL091	SL092	SL093	SL094	SL095	SL096	SL097
-3.50	-	-	81.36	-	-	-	100.00
-3.00	-	-	81.36	100.00	-	-	98.77
-2.50	-	-	80.58	96.54	-	-	98.33
-2.00	-	-	78.80	91.86	-	-	98.33
-1.50	100.00	-	74.91	87.89	-	-	98.10
-1.00	-	-	70.56	81.99	-	-	97.23
-0.50	-	100.00	66.37	78.95	100.00	100.00	95.55
0.00	100.00	100.00	65.97	78.95	100.00	99.85	93.69
0.50	100.00	99.97	55.53	76.77	99.99	99.30	87.86
1.00	99.91	99.49	49.10	73.36	99.96	97.42	71.59
1.50	99.47	96.40	43.08	69.23	99.83	90.56	49.15
2.00	98.95	93.58	35.05	61.21	99.34	61.02	23.99
2.50	98.24	90.76	26.21	49.29	99.26	21.26	9.75
3.00	94.38	86.65	23.40	44.19	99.09	7.36	4.67
3.50	77.52	78.17	22.80	43.22	96.12	1.71	2.09
4.00	65.92	69.19	22.60	42.49	90.26	0.58	0.80
4.50	61.28	65.38	22.19	41.99	84.24	-	-
5.00	53.85	58.54	21.16	39.52	69.54	-	-
5.50	50.14	50.18	17.87	39.03	58.84	-	-
6.00	44.57	45.62	16.03	36.56	53.49	-	-
6.50	39.00	41.05	13.77	35.08	49.48	-	
7.00	32.50	34.97	11.92	32.61	44.13		
7.50	26.00	30.41	10.07	29.15	39.45		
8.00	20.43	25.85	8.42	26.68	34.77	-	
8.50	16.71	21.29	6.99	24.70	30.09	-	
9.00	12.07	15.21	5.75	20.75	24.74	-	
16TH	8.58	8.93	6.01	10.41	10.31	2.69	2.28
50TH	5.51	5.52	.93	2.47	6.43	2.14	1.48
84TH	3.31	3.16	-3.57	-1.17	4.51	1.61	.67

TABLE A (Cont'd)

SIZE (PHI)	STATION						
	SL098	SL099	SL100	SL101	SL102	SL103	SL104
-3.50	-	-	-	-	-	-	-
-3.00	-	-	-	-	-	-	-
-2.50	-	100.00	-	-	-	-	-
-2.00	100.00	99.68	100.00	-	-	100.00	100.00
-1.50	99.96	99.42	98.84	-	-	98.82	99.63
-1.00	99.90	99.20	98.75	-	-	95.95	99.29
-0.50	99.33	98.92	98.29	-	-	89.45	98.88
0.00	98.59	98.16	98.29	-	-	89.45	98.84
0.50	97.69	96.50	97.80	-	-	86.91	97.75
1.00	94.84	89.73	95.71	-	-	85.63	94.80
1.50	79.38	70.86	91.85	-	-	84.36	91.62
2.00	28.99	37.82	86.70	-	-	82.67	85.72
2.50	4.29	17.25	83.17	-	-	80.46	67.34
3.00	0.37	9.93	74.16	-	-	78.60	57.80
3.50	0.07	3.94	46.81	100.00	100.00	77.07	55.76
4.00	0.04	1.11	29.44	100.00	100.00	75.89	54.85
4.50	-	-	24.73	98.82	98.08	74.96	53.91
5.00	-	-	18.25	94.12	94.23	73.11	52.66
5.50	-	-	16.48	87.06	88.46	72.18	51.40
6.00	-	-	15.31	76.47	80.77	69.87	50.15
6.50	-	-	14.13	67.06	73.08	67.56	47.96
7.00	-	-	11.77	54.12	62.50	64.32	42.94
7.50	-	-	10.60	43.53	52.88	61.08	37.61
8.00	-	-	8.30	37.65	44.23	57.38	32.91
8.50	-	-	7.06	31.76	36.54	54.60	29.15
9.00	-	-	5.89	25.88	28.85	51.82	25.70
16TH	2.26	2.59	5.71	10.21	10.00	15.83	10.74
50TH	1.79	1.82	3.44	7.19	7.67	9.29	6.03
84TH	1.35	1.15	2.38	5.64	5.79	1.61	2.05

TABLE A (Cont'd)

SIZE	STATION						
(PHI)	SL105	SL106	SL107	SL108	SL109	SL110	SL111
-3.50	-	-	-	-	-	-	98.17
-3.00	-	-	-	-	-	-	98.17
-2.50	-	100.00	-	100.00	-	-	97.72
2.00	100.00	99.06	-	98.68	-	-	97.50
-1.50	99.81	96.08	-	97.87	-	-	96.69
-1.00	99.70	91.66	-	96.64	100.00	-	96.41
-0.50	99.44	86.18	100.00	93.69	99.87	100.00	95.66
0.00	99.44	85.82	100.00	88.07	99.57	100.00	94.75
0.50	97.90	70.12	99.90	75.27	98.73	99.97	93.44
1.00	90.22	62.56	99.61	48.27	92.90	99.92	90.11
1.50	81.76	51.23	99.21	18.74	63.38	99.00	82.32
2.00	64.09	42.73	98.69	6.49	14.80	98.00	64.55
2.50	36.42	36.11	98.16	3.49	1.04	95.84	40.85
3.00	25.66	31.15	96.85	1.43	0.08	88.01	18.67
3.50	23.74	24.78	87.41	0.61	0.03	71.36	6.72
4.00	22.59	20.06	65.39	0.21	-	61.04	1.08
4.50	22.35	18.49	52.07	-	-	58.38	-
5.00	21.13	16.61	37.54	-	-	53.08	-
5.50	20.65	15.35	30.88	-	-	49.10	-
6.00	20.16	14.73	27.85	-	-	45.78	-
6.50	18.70	13.16	26.64	-	-	42.46	-
7.00	17.73	11.59	26.03	-	-	38.48	-
7.50	16.27	9.71	21.19	-	-	33.84	
8.00	15.30	8.46	17.56	-	-	29.86	-
8.50	13.60	7.52	15.74	-	-	27.86	
9.00	12.15	6.27	12.71	-	-	25.21	-
16TH	7.64	5.24	8.43	1.61	1.99	10.89	3.11
50TH	2.25	1.57	4.57	.97	1.64	5.39	2.31
84TH	1.37	0.06	3.58	.16	1.15	3.12	1.39

TABLE A (Cont'd)

SIZE	STATION						
(PHI)	SL112	SL113	SL114	SL115	SL117	SL118	SL119
-3.50	-	-	81.02	-	-	-	-
-3.00	-	-	81.02	100.00	100.00	-	-
-2.50	-	-	79.26	94.79	98.40	-	100.00
-2.00	-	-	78.32	90.76	98.40	-	99.28
-1.50	-	-	77.05	80.41	98.31	-	98.67
-1.00	-	-	76.13	68.02	95.89	-	97.29
-0.50	100.00	100.00	75.42	58.07	92.24	100.00	93.87
0.00	100.00	100.00	75.42	57.72	92.24	100.00	89.09
0.50	99.95	99.99	74.05	47.02	82.82	99.84	79.98
1.00	99.89	99.76	68.10	43.57	73.98	99.67	60.98
1.50	99.56	99.04	63.07	38.04	61.03	99.18	43.52
2.00	99.13	98.55	55.75	30.44	43.36	98.36	13.24
2.50	98.80	98.31	42.49	21.46	21.58	97.70	2.33
3.00	98.47	98.07	23.28	13.18	15.10	94.91	0.46
3.50	96.61	96.87	15.96	11.45	12.74	78.65	0.14
4.00	89.08	89.39	15.51	10.76	12.15	60.25	0.04
4.50	81.36	84.43	15.51	10.76	12.15	55.39	-
5.00	66.51	79.46	14.61	10.56	11.25	47.62	-
5.50	55.82	75.74	13.72	10.15	11.25	42.27	-
6.00	51.07	72.63	13.42	9.54	10.80	38.87	-
6.50	45.73	70.15	12.23	8.93	9.90	35.47	-
7.00	40.38	63.94	11.03	8.12	8.55	32.07	-
7.50	35.63	58.35	8.95	7.11	7.65	27.69	-
8.00	30.88	52.15	8.05	5.89	6.75	25.27	-
8.50	26.13	47.18	6.86	5.68	5.85	22.84	-
9.00	21.97	40.97	5.07	4.87	4.95	18.95	-
16TH	9.99	11.73	3.50	2.83	2.93	9.69	1.95
50TH	6.10	8.22	2.22	.36	1.81	4.85	1.31
84TH	4.33	4.54	-3.58	-1.67	.44	3.34	.28

TABLE A (Cont'd)

SIZE	STATION						
(PHI)	SL120	SL121	SL122	SL123	SL124	SL125	SL126
-3.50	83.54	-	-	-	100.00	-	
-3.00	78.47	-	-	-	96.24	-	
-2.50	73.35	-	-	-	94.49	-	
-2.00	71.17	-	-	-	94.49	-	
-1.50	68.18	-	-	-	92.49	-	-
-1.00	66.64	-	-	-	90.16	-	
-0.50	64.81	100.00	100.00	-	86.57	100.00	100.00
0.00	62.65	100.00	100.00	-	81.35	100.00	99.66
0.50	59.36	99.97	99.92	-	71.67	100.00	99.49
1.00	48.93	99.87	98.87	-	45.67	99.97	98.99
1.50	33.68	99.49	96.22	-	22.45	98.72	94.59
2.00	21.03	98.47	94.71	-	7.55	98.21	82.41
2.50	13.08	97.35	93.19	-	1.55	97.96	64.15
3.00	5.26	93.12	90.92	-	0.24	97.45	58.74
3.50	2.27	71.46	84.87	100.00	0.04	94.38	50.63
4.00	1.14	45.46	73.53	100.00	-	90.55	42.51
4.50	-	37.26	72.06	98.20	-	90.55	40.55
5.00	-	26.83	71.57	91.62	-	85.95	38.59
5.50	-	22.36	68.13	86.23	-	80.57	35.97
6.00	-	20.87	63.23	81.44	-	76.74	35.32
6.50	-	18.63	57.35	74.25	-	69.83	32.70
7.00	-	16.02	51.96	67.07	-	63.69	28.78
7.50	-	14.16	44.12	58.08	-	55.25	24.85
8.00	-	11.92	38.23	51.50	-	50.65	21.58
8.50	-	11.92	32.35	43.71	-	44.51	18.97
9.00	-	8.94	25.49	37.13	-	36.83	14.39
16TH	2.32	7.01	10.13	10.66	1.72	11.01	8.82
50TH	.95	3.91	7.12	8.10	.92	8.05	3.54
84TH	-3.55	3.21	3.54	5.73	-.25	5.18	1.93

TABLE A (Cont'd)

SIZE (PHI)	STATION						
	SL127	SL128	SL129	SL130	SL132	SL133	SL134
-3.50	81.69	-	-	-	-	-	-
-3.00	79.57	-	-	-	-	-	-
-2.50	76.68	100.00	-	-	100.00	-	100.00
-2.00	72.94	99.12	-	-	98.77	-	99.39
-1.50	66.41	98.28	-	-	97.26	-	99.10
-1.00	61.72	97.48	-	100.00	96.28	100.00	98.97
-0.50	55.70	96.72	100.00	99.72	94.56	98.61	98.74
0.00	50.88	96.72	100.00	98.03	92.83	96.59	98.03
0.50	44.48	96.16	99.83	97.24	89.57	91.78	96.58
1.00	36.83	95.02	99.34	91.18	78.93	77.50	88.48
1.50	29.19	87.64	94.06	68.82	59.71	51.58	60.41
2.00	19.59	78.56	89.43	42.94	30.31	24.91	19.23
2.50	6.40	70.61	87.12	17.42	8.25	13.15	3.65
3.00	1.87	44.49	63.68	2.71	1.55	6.45	0.94
3.50	0.57	12.70	33.30	0.31	0.53	2.28	0.35
4.00	0.12	8.16	28.67	0.06	0.14	0.76	0.10
4.50	-	7.85	27.68	-	-	-	-
5.00	-	7.53	26.20	-	-	-	-
5.50	-	7.53	24.72	-	-	-	-
6.00	-	7.53	24.72	-	-	-	-
6.50	-	6.59	22.25	-	-	-	-
7.00	-	6.28	20.27	-	-	-	-
7.50	-	4.39	17.30	-	-	-	-
8.00	-	4.39	15.82	-	-	-	-
8.50	-	3.77	13.84	-	-	-	-
9.00	-	3.14	11.86	-	-	-	-
16TH	2.14	3.45	7.94	2.55	2.32	2.38	2.10
50TH	0.07	2.89	3.23	1.86	1.67	1.53	1.63
84TH	-4.06	1.70	2.57	1.16	0.76	0.77	1.08

TABLE.A (Cont'd)

SIZE (PHI)	STATION						
	SL135	SL136	SL137	SL138	SL139	SL140	SL141
-3.50	-	-	-	100.00	100.00	-	-
-3.00	-	-	-	95.96	92.85		-
-2.50	-	-	-	94.82	88.76	-	100.00
-2.00	-	-	-	92.62	82.53	100.00	99.71
-1.50	-	-	100.00	92.14	74.41	99.62	99.54
-1.00	-	-	99.74	92.14	65.88	99.62	98.80
-0.50	100.00	-	99.59	90.73	56.38	99.62	97.54
0.00	99.90	100.00	99.22	90.03	47.63	99.56	95.07
0.50	99.51	99.94	98.47	87.57	37.34	99.38	90.05
1.00	98.04	99.66	95.61	76.85	25.10	97.81	75.22
1.50	95.10	98.69	82.77	57.29	18.22	94.19	44.28
2.00	91.18	93.67	50.58	31.90	13.98	86.35	15.74
2.50	75.99	34.16	14.48	11.47	9.07	70.67	5.41
3.00	32.37	14.66	2.61	4.09	3.68	51.98	3.16
3.50	16.68	4.53	0.60	0.66	0.89	33.29	0.35
4.00	13.250	1.54	0.11	0.31	0.21	25.75	0.1
4.50	12.65	-	-	-	-	24.03	-
5.00	12.05	-	-	-	-	21.89	-
5.50	11.45	-	-	-	-	20.60	-
6.00	10.84	-	-	-	-	19.31	-
6.50	10.54	-	-	-	-	18.02	-
7.00	9.64	-	-	-	-	16.31	-
7.50	7.83	-	-	-	-	14.59	-
8.00	6.93	-	-	-	-	12.87	-
8.50	6.33	-	-	-	-	12.02	-
9.00	6.02	-	-	-	-	10.30	-
16TH	3.60	2.97	2.47	2.39	1.76	7.09	2.00
50TH	2.80	2.37	2.01	1.64	-0.14	3.05	1.41
84TH	2.24	2.08	1.45	0.67	-2.12	2.08	0.70

TABLE A (Cont'd)

SIZE	STATION						
(PHI)	SL142	SL145	SL146	SL147	SL148	SL150	
-3.50	-	-	93.60	-	-	-	
-3.00	100.00	-	86.72	-	-	-	
-2.50	99.12	-	80.77	100.00	-	100.00	
-2.00	97.35	-	72.88	99.73	-	99.89	
-1.50	94.38	-	67.43	99.10	-	98.73	
-1.00	84.19	-	63.62	98.21	100.00	98.31	
-0.50	80.48	100.00	60.59	96.92	98.36	97.46	
0.00	76.55	100.00	58.13	95.12	96.03	96.28	
0.50	71.65	100.00	53.81	92.94	92.29	93.06	
1.00	64.30	99.79	43.15	88.38	84.19	77.70	
1.50	55.84	98.75	27.07	79.76	64.99	42.85	
2.00	35.02	96.68	13.23	49.65	31.44	9.50	
2.50	11.86	90.45	5.41	11.43	9.12	2.06	
3.00	5.21	63.46	2.64	2.57	3.34	0.56	
3.50	2.05	38.55	1.55	0.55	1.53	0.14	
4.00	0.94	32.32	0.12	0.08	0.62	0.03	
4.50	-	32.32	-	-	-	-	
5.00	-	29.09	-	-	-	-	
5.50	-	27.47	-	-	-	-	
6.00	-	26.93	-	-	-	-	
6.50	-	24.78	-	-	-	-	
7.00	-	23.16	-	-	-	-	
7.50	-	19.39	-	-	-	-	
8.00	-	17.24	-	-	-	-	
8.50	-	15.08	-	-	-	-	
9.00	-	11.31	-	-	-		
16TH	2.41	8.79	1.98	2.44	2.35	1.90	
50TH	1.64	3.27	0.68	1.99	1.72	1.40	
84TH	-0.97	2.62	-2.77	1.25	1.01	0.79	

APPENDIX B

Contents

Table B: Lake St. Louis Water Temperature Data (Summer 1985)

Source: Champoux and Sloterdjik (1988)

Notes: (1) The following abbreviations are used in Table B:

Sta = Station

Surf = 0.1 m below surface

Bott = 1.0 m above bed

(2) Temperatures are shown in °C

TABLE B: LAKE ST. LOUIS WATER TEMPERATURE DATA; SUMMER(1985)

Stat	Surf	Bott.	Stat	Surf	Bott.	Stat	Surf	Bott.
1	18,0	16,6	30	18,0	18,7	59	19,0	17,0
2	18,0	18,0	31	15,5	15,5	60	17,0	16,5
3	17,5	17,0	32	15,5	15,5	61	17,5	17,5
4	18,5	18,0	33	16,0	16,0	62	17,0	16,5
5	17,0	17,0	34	16,0	15,5	63	16,5	16,5
6	18,6	18,6	35	17,0	17,0	64	17,0	17,0
7	17,6	17,	36	18,8	18,0	65	15,9	16,1
8	16,8	16,4	37	17,3	16,5	66	16,0	16,0
9	17,0	16,5	38	16,8	16,0	67	16,5	16,5
10	18,1	18,1	39	16,9	16,3	68	20,3	20,5
11	19,0	18,6	40	17,2	19,2	69	---	---
12	18,1	17,6	41	17,5	17,0	70	17,5	16,0
13	22,7	16,6	42	16,0	15,0	71	17,0	17,0
14	16,5	16,0	43	16,0	15,5	72	17,0	17,0
15	16,0	16,0	44	16,0	15,5	73	16,5	17,0
16	17,8	17,8	45	17,0	17,0	74	16,5	16,5
17	18,2	18,1	46	17,0	17,0	75	16,0	16,0
18	18,5	18,5	47	19,0	18,0	76	16,0	16,5
19	18,0	15,5	48	17,5	17,0	77	16,5	16,0
20	16,5	---	49	17,0	17,0	78	17,0	17,0
21	18,0	18,0	50	16,5	16,5	79	---	---
22	17,0	17,0	51	16,5	16,5	80	27,0	---
23	17,0	---	52	16,0	16,0	81	22,7	22,1
24	16,0	15,0	53	16,0	16,0	82	16,0	15,5
25	15,5	---	54	16,0	16,0	83	16,1	16,1
26	18,0	18,0	55	16,0	16,3	84	16,0	16,2
27	18,2	19,0	56	16,6	16,5	85	16,3	16,0
28	17,5	16,8	57	17,0	17,0	86	16,3	16,2
29	17,0	16,1	58	17,0	16,5	87	16,4	16,4

Table B:(Cont'd)

Stat	Surf	Bott.	Stat	Surf	Bott.	Stat	Surf	Bott.
88	16,4	16,3	117	17,0	17,0	147	17,0	16,8
89	21,2	22,2	118	17,2	17,5	148	16,1	16,0
90	23,0	21,6	119	16,5	16,5	149	20,9	19,3
91	21,6	21,1	120	17,0	17,5	150	20,0	20,1
92	21,2	21,2	121	18,0	17,8	151	21,6	22,3
93	16,0	16,0	122	18,0	18,8			
94	16,0	16,0	123	19,5	19,0			
95	16,2	16,0	124	17,4	17,2			
96	16,5	16,2	125	16,5	16,7			
97	16,5	16,5	126	16,7	16,5			
98	16,4	16,2	127	16,7	16,5			
99	16,4	16,3	128	16,9	17,0			
100	16,3	16,1	129	18,3	17,9			
101	20,9	20,9	130	18,5	18,5			
102	21,7	21,2	132	17,6	17,8			
103	17,9	17,9	133	16,5	16,7			
104	17,9	17,9	134	16,5	16,5			
105	16,7	16,3	135	16,5	16,5			
106	16,4	16,6	136	19,5	19,5			
107	17,3	17,3	137	21,2	21,6			
108	16,3	16,3	138	16,3	16,6			
109	16,3	16,3	139	16,2	16,2			
110	16,3	16,3	140	16,5	16,5			
111	16,3	16,3	141	19,0	19,0			
112	16,1	16,1	142	17,2	17,0			
113	16,7	16,5	143	20,4	20,1			
114	17,7	17,6	144	19,2	19,2			
115	17,0	17,0	145	20,6	19,6			
116	16,5	16,5	146	22,0	20,0			

APPENDIX C

CONTENTS:

TABLE C1: BASIC VARIABLES USED IN CORRELATION PLOTS

			DC.1		DC.2	
sta	d50 (mm/s)	ws (mm/s)	h (m)	u. (mm s)	h (m)	u. (mm s)
4	0.00112	0.001	3.468	3.805	3.734	7.963
5	0.00296	0.008	8.649	4.810	8.916	9.027
6	0.00138	0.002	2.553	1.911	2.818	3.466
7	0.02683	0.647	3.774	1.902	4.038	5.211
8	0.00246	0.005	11.393	4.531	11.659	6.938
10	0.00217	0.004	3.632	9.428	3.936	18.778
11	0.65067	88.402	2.248	0.944	2.513	2.729
12	0.32086	47.350	3.163	4.979	3.428	4.654
13	0.00244	0.005	11.393	5.428	11.659	4.847
14	0.00399	0.014	8.345	6.195	8.609	8.520
16	0.00226	0.005	4.242	10.204	4.544	20.628
18	0.25882	36.743	2.855	6.851	3.120	5.404
19	0.07130	4.571	9.862	25.105	10.127	20.614
20	0.00798	0.057	22.058	12.931	22.325	11.489
21	0.00239	0.005	11.252	4.610	11.549	9.723
24	0.00685	0.042	19.027	22.786	19.289	19.420
25	0.56644	79.713	17.482	34.926	17.752	32.070
26	0.00269	0.006	12.162	4.970	12.453	10.464
28	0.00923	0.077	3.626	2.818	3.915	5.020
29	0.01499	0.202	3.931	2.066	4.220	2.815
31	0.47632	69.287	6.220	14.041	6.482	13.288
32	0.44442	65.248	19.023	21.508	19.285	20.822
33	0.18428	22 726	22.068	27.172	22.331	25.856
34	0.00317	0.009	12.910	8.742	13.714	6.714
36	0.00254	0.006	10.028	5.475	10.318	10.182
37	0.05791	3.016	3.931	5.892	4.219	4.528
38	0.02304	0.477	4.846	4.449	5.134	4.735
39	0.09343	7.849	3.627	3.718	3.915	2.768

TABLE C1: (Cont'd)

			DC.1		DC.2	
sta	d50 (mm)	ws (mm/s)	h (m)	u. (mm/s)	h (m)	u. (mm/s)
40	0.13870	14.175	3.017	2.975	3.306	1.4375
41	0.22846	31.154	3.152	20.870	3.416	21.325
42	0.15073	16.368	14.434	28.897	14.698	27.802
43	0.15073	16.368	8.343	25.513	8.607	25.304
44	0.00430	0.017	11.391	9.303	11.656	9.731
47	0.00276	0.007	4.539	11.954	4.828	16.717
48	0.57834	80.996	4.539	8.055	4.828	8.929
49	0.01758	0.278	4.541	6.207	4.829	5.688
50	0.14762	15.796	3.017	9.538	3.305	8.080
51	0.34628	51.365	6.677	3.595	6.965	2.887
52	0.6935	4.325	11.375	20.370	11.640	19.988
53	0.30355	44.507	4.976	53.601	5.241	52.068
54	0.09087	7.426	14.432	9.734	14.696	9.694
56	0.33681	49.891	3.160	31.458	3.425	30.755
57	1.64718	179.614	2.703	8.089	2.990	8.814
58	2.49666	221.131	3.314	11.457	3.601	12.663
59	0.00433	0.017	5.145	11.871	5.432	13.698
60	0.06745	4.091	5.145	11.939	5.433	12.931
61	0.09605	8.297	4.234	13.612	4.522	11.869
62	0.15177	16.562	3.017	19.518	3.304	17.514
63	0.07695	5.324	4.602	26.627	4.872	23.776
64	0.23005	31.452	3.680	48.897	3.950	47.724
65	0.21464	28.543	14.400	36.848	14.666	35.585
66	0.05112	2.350	12.886	10.205	13.152	10.563
70	0.00017	0.00003	3.921	13.535	4.209	14.652
71	0.00309	0.009	6.361	15.451	6.648	16.769
72	0.01120	0.113	5.753	14.564	6.040	15.493
73	0.09807	8.649	3.930	20.755	4.217	18.894

TABLE C1: (Cont'd)

			DC.1		DC.2	
sta	d50 (mm)	ws (mm/s)	h (m)	u. (mm/s)	h (m)	u. (mm/s)
74	0.11502	10.119	3.331	27.073	3.616	24.324
75	0.29118	42.421	2.158	35.818	2.430	34.426
76	0.95264	114.122	8.270	50.062	8.539	48.659
77	0.32760	48.433	11.338	28.966	11.606	28.620
81	0.00837	0.063	2.180	38.774	2.447	38.595
82	0.00138	0.002	5.135	17.381	5.421	18.659
83	0.00609	0.033	7.574	18.425	7.861	19.708
84	0.04210	1.594	4.530	18.195	4.817	18.975
85	0.12158	11.201	3.319	22.540	3.606	21.123
86	0.11582	10.249	3.039	27.869	3.319	24.119
87	0.48633	70.513	11.606	32.104	11.876	31.049
88	0.90125	110.194	11.305	37.654	11.576	36.514
90	0.04671	1.962	2.144	6.299	2.419	6.406
91	0.02194	0.433	2.757	12.947	3.032	12.716
92	0.02179	0.427	1.237	18.068	1.511	17.965
93	0.52486	75.068	2.981	16.997	3.267	18.025
94	0.18049	21.998	5.122	23.548	5.407	25.072
95	0.01160	0.121	6.651	22.723	6.937	24.339
96	0.22688	30.858	3.300	15.614	3.586	17.492
97	0.35849	53.227	1.522	37.780	1.796	35.030
98	0.28917	42.077	14.335	21.943	14.607	21.298
99	0.28322	41.053	9.763	26.165	10.036	25.690
100	0.09214	7.635	1.539	20.504	1.812	18.448
101	0.00685	0.042	3.057	9.883	3.333	9.411
102	0.00491	0.022	5.192	5.110	5.468	5.007
105	0.21022	27.701	4.189	18.898	4.474	20.104
106	0.33681	49.891	6.027	23.469	6.312	24.836
107	0.04210	1.594	3.588	28.385	3.873	30.120

TABLE C1: (Cont'd)

			DC.1		DC.2	
sta	d50 (mm)	ws (mm/s)	h (m)	u. (mm/s)	h (m)	u. (mm/s)
108	0.51051	73.401	2.067	13.806	2.352	16.577
109	0.32086	47.350	1.823	51.391	2.095	51.480
110	0.02385	0.511	9.752	26.438	10.026	25.281
112	0.01458	0.191	3.048	14.002	3.324	14.417
113	0.00335	0.010	4.579	11.050	4.855	11.066
114	0.21464	28.543	2.352	10.487	2.636	10.957
115	0.77916	100.200	3.572	12.935	3.857	13.440
117	0.28519	41.393	3.576	26.428	3.860	27.823
118	0.03467	1.081	5.418	16.810	5.702	17.614
119	0.40332	59.723	9.681	23.221	9.965	22.109
120	0.51763	74.233	6.638	37.959	6.921	35.721
121	0.06652	3.979	4.241	13.461	4.517	13.317
122	0.00719	0.046	6.082	12.480	6.359	12.510
124	0.52851	75.486	2.037	25.944	2.322	27.457
125	0.00377	0.013	8.135	22.436	8.420	22.996
126	0.08597	6.646	2.345	36.356	2.629	37.624
127	0.95264	114.122	8.145	18.563	8.428	18.978
128	0.13490	13.500	9.669	35.041	9.952	35.033
129	0.10658	8.782	3.598	33.544	3.878	32.648
133	0.34628	51.365	3.542	45.303	3.828	45.539
134	0.32309	47.710	2.633	46.907	2.917	46.853
135	0.14359	15.058	9.650	28.432	9.934	29.005
136	0.19345	24.487	8.138	29.121	8.421	30.431
138	0.32086	47.350	6.583	31.939	6.868	32.810
139	1.10191	146.907	6.569	27.380	6.854	27.920
140	0.12074	11.060	4.429	55.953	4.714	55.708
141	0.37631	55.872	9.331	20.570	9.614	21.593
145	0.10366	8.337	6.548	32.898	6.832	34.135

TABLE C1: (Cont'd)

			DC.1		DC.2	
sta	d50 (mm)	ws (mm/s)	h (m)	u. (mm/s)	h (m)	u. (mm/s)
146	0.62417	85.761	1.349	46.498	1.634	49.769
148	0.30355	44.507	2.778	32.918	3.066	34.769
150	0.37893	56.254	2.854	62.864	3.142	62.069

TABLE C2: DIMENSIONLESS VARIABLES USED IN CORRELATION PLOTS

		DC.1		DC.2	
STAT	$D_* \times 10$	$Z_{**} \times 10^{}$	$e_* \times 10^{}$	$Z_{**} \times 10^{}$	$e_* \times 10^{}$
4	28.376	0.297	0.320	0.142	0.300
5	74.886	1.638	0.340	0.873	0.330
6	34.935	0.898	0.540	0.495	0.490
7	678.695	340.324	7.110	124.228	6.(40
8	62.104	1.196	0.220	0.782	0.210
10	54.820	0.448	0.600	0.225	0.550
11	16459.340	93618.412	289.500	32394.644	258.940
12	8116.372	9510.013	101.440	10173.507	93.600
13	61.675	0.985	0.210	1.103	0.210
14	100.889	2.309	0.480	1.679	0.460
16	57.148	0.450	0.530	0.222	0.500
18	6547.004	5363.130	90.650	6799.048	82.950
19	1803.544	182.087	7.230	221.750	7.040
20	201.777	4.425	0.360	4.980	0.360
21	60.406	1.112	0.210	0.527	0.210
24	173.239	1.851	0.360	2.172	0.360
25	14328.690	2282.368	32.400	2485.629	31.910
26	67.960	1.306	0.220	0.620	0.220
28	233.393	27.168	2.540	15.250	2.360
29	379.148	97.791	3.810	71.758	3.550
31	12048.940	4934.579	76.570	5237.828	73.480
32	11242.060	3033.687	23.360	3133.623	23.050
33	4661.631	836.376	8.350	878.941	8.250
34	80.261	1.036	0.250	1.348	0.240
36	64.294	1.061	0.250	0.571	0.250
37	1464.933	511.825	14.730	666.042	13.730
38	582.704	107.264	4.750	100.783	4.490
39	2363.353	2111.187	25.760	2835.396	23.860
40	3508.453	4765.423	45.970	9864.754	41.960

TABLE C2: (Cont'd)

41	5779.059	1492.787	72.490	1460.929	66.880
42	3812.758	566.416	10.440	588.712	10.250
43	3812.758	641.544	18.070	646.847	17.510
44	108.882	1.791	0.380	1.712	0.370
47	69.871	0.574	0.610	0.410	0.570
48	14629.770	10054.777	127.410	9071.103	119.790
49	444.679	44.770	3.870	48.852	3.640
50	3734.293	1656.181	48.940	1954.924	44.660
51	8759.418	14286.457	51.860	17790.922	49.720
52	1754.226	212.302	6.100	216.366	5.960
53	7678.555	830.354	61.000	854.800	57.920
54	2298.727	752.877	6.300	766.071	6.180
56	8519.891	1585.950	106.570	1622.199	98.340
57	41667.050	22204.847	609.480	23079.352	550.900
58	63155.430	19301.736	753.430	17462.175	693.270
59	109.639	1.423	0.840	1.233	0.800
60	1706.257	342.683	13.110	316.395	12.410
61	2429.795	609.552	22.690	699.059	21.240
62	3839.278	848.553	50.310	965.458	45.930
63	1946.436	199.958	16.720	223.930	15.790
64	5819.257	643.238	62.510	659.048	58.240
65	5429.558	774.611	14.910	802.117	14.640
66	1293.101	230.262	3.970	222.465	3.890
70	4.367	0.002	0.044	0.002	0.041
71	78.066	0.554	0.490	0.511	0.460
72	283.385	7.749	1.950	7.284	1.850
73	2480.851	416.738	24.950	457.789	23.260
74	2909.629	373.767	34.530	416.009	31.810
75	7365.763	1184.345	134.910	1232.239	119.840
76	24097.890	2279.624	115.190	2345.358	111.560
77	8286.913	1672.058	28.890	1692.310	28.230

TABLE C2: (Cont'd)

81	211.809	1.626	3.840	1.634	3.420
82	34.935	0.099	0.270	0.092	0.250
83	153.982	1.808	0.800	1.691	0.770
84	1064.986	87.603	9.290	84.001	8.740
85	3075.530	496.929	36.630	530.272	33.720
86	2929.867	367.754	38.120	424.938	34.900
87	12302.120	2196.422	41.900	2271.047	40.950
88	22797.990	2926.518	79.720	3017.824	77.860
90	1181.676	311.539	21.790	306.326	19.310
91	555.106	33.448	7.960	34.056	7.240
92	551.272	23.637	17.610	23.773	14.430
93	13276.790	4416.579	176.040	4164.687	160.650
94	4565.696	934.171	35.240	877.410	33.380
95	293.379	5.323	1.740	4.970	1.670
96	5739.141	1976.230	68.760	1764.098	63.270
97	9068.317	1408.879	235.610	1519.472	199.640
98	7314.884	1917.566	20.170	1975.609	19.800
99	7164.345	1568.992	29.010	1598.043	28.220
100	2330.816	372.353	59.860	413.841	50.860
101	173.239	4.268	2.240	4.482	2.050
102	124.208	4.243	0.950	4.330	0.900
105	5317.820	1465.837	50.180	1377.910	46.990
106	85.19.891	2125.804	55.880	2008.809	53.360
107	1064.986	56.208	11.730	52.919	10.870
108	12913.740	5321.638	247.040	4427.970	217.070
109	8116.372	911.787	176.030	919.777	153.140
110	603.253	19.344	2.450	20.229	2.380
112	368.781	13.650	4.780	13.257	4.390
113	84.837	0.915	0.730	0.914	0.690
114	5429.558	2721.688	91.270	2605.028	81.420
115	19709.710	7746.564	218.120	7455.249	207.000

TABLE C2: (Cont'd)

117	7214.178	1566262	79.760	1487.751	73.890
118	877.113	64.316	6.400	61.379	6.080
119	10202.390	2571.976	41.660	2701.273	40.480
120	13094.010	1955.598	77.980	2078.141	74.800
121	1682.766	295.620	15.690	298.821	14.730
122	181.852	3.724	1.180	3.715	1.130
124	13369.140	29090.600	259.500	27.49.261	227.640
125	95.446	0.571	0.460	0.557	0.450
126	2174.728	182.816	36.670	176.654	32.700
127	24097.890	6147.895	116.960	6013.354	113.030
128	3412.513	385.258	13.950	385.340	13.550
129	2696.027	261.814	29.620	269.002	27.480
133	8759.418	1133.803	97.760	1127.937	90.470
134	8172.825	1017.125	122.730	1018.287	110.760
135	3632.179	529.619	14.880	519.164	14.450
136	4893.393	840.853	23.770	804.659	22.970
138	8116.372	1482.514	48.740	1443.148	46.720
139	27873.740	5365.568	167.740	5261.657	160.780
140	3054.286	197.673	27.260	198.542	25.620
141	9519.164	2716.145	40.330	2587.542	39.140
145	2622.304	253.419	15.830	244.238	15.170
146	15788.860	1844.415	462.700	1723.172	382.020
148	7678.555	1352.061	109.270	1278.279	99.010
150	9585.375	894.841	132.750	906.310	120.610